GEOLOGY CLASS LIBRARY

GEOLOGY OF THE GOLDENVILLE FORMATION, TAYLOR HEAD, NOVA SCOTIA

by

Ian McKittrick Harris, M.Sc.

Thesis presented for the degree of Doctor of Philosophy of the University of Edinburgh in the Faculty of Science.

January 1971

	Page
PART II - SEDIMENTOLOGY	
CHAPTER 4 - PETROGRAPHY	30
General Statement	30
Rock Types	30
Slate	30
(a) Megascopic Characteristics	30
(b) Composition	31
Sandstone	34
(a) Megascopic Appearance	34
(b) Texture	34
(c) Matrix	38
(i) Definition	38
(ii) Origin	39
(d) Fabric	39
(e) Modal and Chemical Analyses	39
(f) Provenance	40
(g) Plagioclase	51
CHAPTER 5 - SEDIMENTARY STRUCTURES	52
General Features	52
Current Structures	52
Depositional Structures	52
(a) Graded Bedding	52
(b) Parallel Lamination	53
(c) Compound Stratification	53
(i) Description	53
(ii) Interpretation	53
(d) Amalgamated Bedding	60
(e) Mudflake Inclusions	60
(f) Ripple Cross-Lamination and Ripple-Mark	60
(i) Description	60
(ii) Interpretation of Paleocurrent Direction	71
Tool Moulds	74
Scour Moulds	95

Page

(a) Flute Moulds 95

(i) Sole Flutes and Associated Structures 95
(ii) Internal Flutes 95

(b) Channels 110

Primary Deformation Structures 110

Load Structures 110

(a) Description 110
(b) Interpretation 123

Primary Folds 128

(a) General Description 128
(b) Slurried Bedding 128

(i) Description 128
(ii) Interpretation 141

Slump Breccia and Pull-Apart Structures 141

Liquefaction and Biogenic Structures 148

Sand Mounds 148

(a) Description 148
(b) Origin 148
(c) Allied Structures 155

Sand Pipes 158

(a) Description 158
(b) Interpretation 165

Sheet Structures 165

(a) Description 165
(b) Interpretation 168

Sand Injection Dykes and Sills 171

Trace Fossils 171

(a) Description 171
(b) Interpretation 171
(c) Previous Accounts 178

R-Mode Association Analysis 178

Page

PART III - GEOLOGICAL HISTORY

CHAPTER 6 - BASIN ANALYSIS 181

Introduction 181

Interpretation Based on Regional Investigation 181

(a) Method and Results of Study 181
(b) Interpretation 182
(c) Limitations 182

Interpretations Based on Local Study 183

(a) Nature of Sedimentation 183
(b) Relationship of Fold Pattern to Sediment Distribution 184
(c) Limitations 185

Sedimentation Model Utilizing Both Regional and Local Findings 185

(a) Aspects of Turbidite Sedimentation in the Goldenville Formation 185
(b) Dispersal and Provenance 189

APPENDIX 1 - Diagrammatic Representation of Internal Strain 191

APPENDIX 2 - Vector Summation 195

APPENDIX 3 - Methods of Petrographic Examination 197

APPENDIX 4 - Mineralogy of the Sandstone of the Goldenville Formation 199

APPENDIX 5 - Previous Reports of Trace Fossils in the Meguma Group 209

APPENDIX 6 - A Summary Discussion of the Controversy on the Interrelationships of Slopes, Slumps, Turbidity Currents and Depositional Patterns in Flysch Basins 212

References 214

FIGURES

		Page
Fig. 1.	Distribution of the Meguma Group and intruded rocks. Inset map indicates relationship of the second-order Meguma Geosyncline to other major structural elements (the Avalon Platform and the second-order Acadian Geosyncline) in the Late Precambrian - Early Paleozoic Appalachian Geosyncline	3
Fig. 2.	Geological map of thesis area	(in pocket)
Fig. 3.	Hypothetical development of megacycles in a flysch sequence with an arrangement that might influence the distribution and orientation of later folds	20
Fig. 4.	Histograms of the distribution of the sedimentary lineations listed in the first row of Table 1	25
Fig. 5.	Representation of rotational strain	28
Fig. 6.	(A) Columnar sections of part of the Goldenville Formation (Sections 1 and 2 and intervening outcrop). (B) Columnar sections (Sections 3, 4, and 5). (C) Expanded graphic log of part of Section 3. (D) Table of statistics on vertical and lateral variations in bed thicknesses and sandstone-slate ratios.	(in pocket)
Fig. 7.	Current directions determined from measurements of ripple cross-lamination traces	73
Fig. 8.	Hypothetical model of sedimentation in the Meguma Geosyncline	188
Fig. 9.	Schematic representation of tectonically deformed sedimentary structures in rocks in the southeast limb of the Sober Island syncline	193

TABLES

	Page
Table 1 - Vector Summation of Orientation Data	22
Table 2 - Chemical composition (weight percent) of argillaceous rocks in the Goldenville Formation (analyses by X-ray fluorescence), compared with the chemical composition of argillaceous rocks in other areas.	35
Table 3 - Modal analyses (600 points per thin-section).	41
Table 4 - Chemical composition (weight percent) of sandstone (analyses by X-ray fluorescence).	42
Table 5 - Chemical composition (weight percent) of average sandstone in the Goldenville Formation compared with the chemical composition of sandstone in other areas.	43
Table 6 - R-mode Association Analysis of Sedimentary Structures in 231 Sedimentation Cycles (Sandstone bed plus overlying slate band).	180

PLATES*

		Page
Plate 1.	Thick sandstone bed with well developed planar shear-joints	15
Plate 2.	Representative slate band of interlayered silty, very fine sandstone, siltstone and mudstone (east shore of Carter Cove)	33
Plate 3.	Photomicrograph of an example of moderately well sorted sandstone	35
Plate 4.	Photomicrograph showing part of a grain of polycrystalline quartz with a grano-blastic-polygonal texture	45
Plate 5.	Photomicrograph showing rock fragment of polycrystalline quartz and epidote	47
Plate 6.	Photomicrograph showing plagioclase grain with zircon inclusions	50
Plate 7.	Parallel-laminated sandstone	55
Plate 8.	Photomicrograph showing laminae in sandstone of alternating coarse and fine material	57
Plate 9.	Photomicrograph shwoing a surface of erosion or interrupted deposition between two laminae of approximately comparable grain-size	59
Plate 10.	Compound bedding in sandstone	62
Plate 11.	Mudflake inclusions in fragment from sandstone bed	64
Plate 12.	Large mudflake inclusion in sandstone bed	66
Plate 13.	Ripple cross-lamination in sandstone gradational to sandy siltstone	68
Plate 14.	Transverse, slightly cresentic ripple-mark on upper bedding-surface in a sandstone fragment	70

* The locations of the rocks represented in the plates are given in Fig. 6, with the exception of the photomicrographs and those plates for which the location is indicated in the plate caption.

		Page
Plate 15.	Well developed groove moulds in three directions	76
Plate 16.	Prominent, spiralled groove moulds and prod moulds	78
Plate 17.	Groove moulds with small-scale spirals	80
Plate 18.	Groove moulds on slightly undulatory sole of sandstone bed	82
Plate 19.	Groove moulds and partly obliterated flute moulds (head of Mushaboom Harbour)	84
Plate 20.	Groove moulds, streaked-out flute moulds and shallow channel moulds	86
Plate 21.	Fine groove moulds on undulatory sole of sandstone bed (hammer length 35 cm.)	88
Plate 22.	Groove moulds on two intra-bed surfaces	90
Plate 23.	Internal groove moulds	92
Plate 24.	Groove moulds, incipient tension cracks and primary current lineation on intra-bed surface	94
Plate 25.	Conical, shallow flute moulds and longitudinal furrow moulds	97
Plate 26.	Longitudinal furrow moulds, flute moulds, and dimpled structures	99
Plate 27.	Longitudinal furrow moulds and shallow flute moulds	101
Plate 28.	Flute moulds with a variety of shapes (elongate-symmetrical, linguiform, slightly spiralled, cresentic, irregular)	103
Plate 29.	Anastomosing pattern of evenly distributed, elongate-symmetrical flute moulds	105
Plate 30.	Longitudinal furrow moulds and flute moulds laterally transitional to scaliform, non-oriented structures	107
Plate 31.	Reticulate scour moulds	109

		Page
Plate 32.	Flute marks on an intra-bed surface (hammer length 35 cm.)	112
Plate 33.	Cross-section exposure of channel mould. The outcrop consists mainly of sandstone in the upper half and slate in the lower half. The mould extends about 5 meters below the main part of the base of the sandstone bed in which it occurs (west shore of Wolf Island, 1 kilometer south west of thesis area)	114
Plate 34.	Longitudinal-section exposure of channel mould. The channel effects amalgamation with the underlying sandstone bed.	116
Plate 35.	Large load-ball at base of sandstone bed.	118
Plate 36.	Load mould at base of sandstone bed.	120
Plate 37.	Load structures at base of sandstone bed. Undeformed parallel lamination above load structures.	122
Plate 38.	Pseudonodules formed from thin beds of sandy siltstone overlying mudstone	125
Plate 39.	Pseudonodules of sandy siltstone developed in fine-grained sandstone	127
Plate 40.	Primary fold in laminated sandstone	130
Plate 41.	Primary folds in laminated sandstone	132
Plate 42.	Slump-deformed bed with primary folds throughout.	134
Plate 43.	Slump-deformed bed with primary contortion. Bed below and laminae above contortions are undeformed	136
Plate 44.	Slurried bedding, consisting of deformed laminae, detachment bodies and injection dykes of sandstone interspersed in argillaceous material. (south end of Phoenix Island; hammer length 35 cm.)	138

Page

Plate 45. Slurried bed beneath undeformed sandstone and above undeformed slate (hammer length 35 cm.) 140

Plate 46. Slide markings on upper bedding surface of sandstone bed. Slurried bedding (not shown in photograph) occurs immediately above the slide-marked surface. Transverse ripples with tectonically oversteepened crests on another bedding surface 143

Plate 47. Slump breccia, consisting of detached bodies of conglomeratic sandstone enclosed in an argillaceous (slate) matrix (south side of Outer Island) 145

Plate 48. Pull-apart structure represented by discontinuous sandstone bed below hammer (east side, Stony Island; hammer length 35 cm.) 147

Plate 49. Sand mounds on upper bedding-surface of sandstone bed. Radial grooves developed on some of the mounds. 150

Plate 50. Upper bedding-surface of sandstone bed with abundant sand mounds 152

Plate 51. Small sand mounds (? pit and mound structures) on upper bedding-surface of sandstone bed 154

Plate 52. Oval structures with radial, plate-like grooves about a central aperture. 157

Plate 53. Small protrusions at base of sandstone bed. Possibly developed as moulds in the apertures of vents in the underlying mud 160

Plate 54. Sand pipes in dip-section exposure of sandstone bed. Apparent tilting of the pipes towards the bedding is a tectonic effect 162

Plate 55. Sub-vertical sand pipes in slump-deformed bed 164

Plate 56. Sheet structures displayed in rock slab derived from sandstone bed. The structures occur as undulous, anastomosing and slightly raised ridges on the weathered (upper) parting surface, and as sinuous sub-parallel ridges with commonly branching terminations on the joint surface 167

		Page
Plate 57.	Sheet structures in sandstone occurring in layers separated by structureless sandstone	170
Plate 58.	Moulds of organic trails at base of sandstone bed	173
Plate 59.	Mould of winding, organic trail on base of sandstone bed	175
Plate 60.	Organic trails on sole of sandstone bed	177
Plate 61.	Photomicrograph showing flake of white mica and chlorite recrystallized from biotite(?) detrital particle (x 100).	203

ABSTRACT

This thesis describes and interprets the sedimentary features of the metasedimentary sandstone and slate of the Goldenville Formation (early Paleozoic flysch) in the vicinity of Taylor Head, Nova Scotia.

A number of exceptional sedimentary structures indicate that much of the Goldenville Sandstone was deposited as loosely packed, water-laden sand. The exceptional structures are (1) slurried beds, which are a unique slump feature, (2) pseudonodules of siltstone in sandstone, (3) abundant sand volcanoes (sand mounds) and vents (sand pipes), which were produced through liquefaction of the sediment, and (4) vertical sheet structures, produced by liquefaction or 'settling convection'. These structures are considered indicative of abnormally rapid deposition from turbidity currents.

The Goldenville Formation, although typical flysch in many respects, is in several respects atypical. Previous work indicates that sandstone in the Goldenville Formation has only small variation in average bed thickness, grain size, primary minerals and other attributes over 50,000 square kilometers of intermittent outcrop, and that distal equivalents appear to be absent. The Goldenville Formation is overlain conformably by the argillaceous Halifax Formation. This is inverse to the normal flysch succession. These large-scale peculiarities of the Goldenville Formation may have a relationship to the exceptional

sedimentary structures mentioned above.

The mean direction of linear current structures on sandstone soles coincides with the mean direction of slide markings associated with slurried bedding and other slump structures. This suggests the action of gravity impelled turbidity currents that moved down-slope with little or no deflection by indigenous ocean currents.

The mean orientation of transverse ripple-mark suggests the action of indigenous bottom currents, possibly geostrophic currents, generally at large angles to the main direction of turbidity current flow.

The mean direction of linear current structures on sandstone soles coincides almost perfectly with the regional strike of folds. This is attributed to an arrangement of sedimentary structures, particularly large-scale bedding features, which influenced the orientation and configuration of later folds. A regional change in the axial trend of folds (and a corresponding change in the paleocurrent trend) indicates horizontal rotation of folds from their initial positions.

The dispersal of the formation is longitudinal; evidence of lateral supply is lacking. The formation has a mixed provenance; acid or intermediate plutonic, metamorphic and sedimentary derivation is dominant.

The formation is interpreted as a prograding sequence of alternating turbidity current and indigenous, ocean-current

deposits which are possibly diachronous with the argillaceous sediments of the Halifax Formation and paralic deposits overlying the Halifax Formation.

ACKNOWLEDGEMENTS

The work of this thesis was carried out under the supervision of Dr. J.P.B. Lovell and Professor E.K. Walton, whose constructive advice and generous encouragement I gratefully acknowledge. Drs. R.F. Cheeney and M.R.W. Johnson gave freely of their advice on problems of structural geology.

Mr. M.A. Whyte kindly made available a computer program for vector summation analysis of orientation data, and another for 'R-mode' analysis of data on sedimentary structures. Mr. W.W. Boyd gave generously of his advice and assistance on refinements of the petrographic techniques described in the thesis.

The field work upon which this thesis is based was made possible by the Nova Scotia Research Foundation, who provided a monthly stipend during the two seasons spent in the field, and by Dr. P.E. Schenk, who defrayed field expenses through an operating grant from the National Research Council of Canada. Discussions in the field with Dr. Schenk were most helpful. Dr. B.R. Pelletier arranged for the provision of most of the equipment used in the field from the Canadian Department of Energy, Mines and Resources.

PART 1 - INTRODUCTION AND GEOLOGICAL FRAMEWORK

CHAPTER 1 - INTRODUCTION

Purpose of Study

The Goldenville Formation (Woodman 1904) is a sequence of intercalated sandstone and slate having the general characteristics of flysch as defined by Tercier (1947) and Sujkowski (1957). Although similar in many respects to other flysch sequences, the Goldenville Formation has sedimentary characteristics that are exceptional and possibly unique. The exceptional sedimentary characteristics are given emphasis in this thesis.

The formation constitutes the lower half, approximately, of a thick, eugeosynclinal succession which was deposited in the northeastern segment of the Appalachian Geosyncline. The succession accumulated during Lower Paleozoic time in a 'second-order' geosyncline, commonly referred to as the Meguma Geosyncline (e.g. Poole 1967). The Meguma Geosyncline was separated from the main part of the northeastern Appalachian Geosyncline (a 'second-order' geosyncline which previous workers have described as the Acadian Geosyncline) by a positive area (the Avalon Platform) (Kay and Colbert 1965; Poole 1967) (Fig. 1, inset map). The platform contributed little, if any, sediment to the Meguma Geosyncline; hence the great volume of sediment represented by the present rocks (Fig. 1) must have been derived from the general direction of the present continental margin. Contributions to the knowledge of the Meguma geosynclinal rocks, as provided in this

Fig. 1. Distribution of the Meguma Group and intruded rocks. Inset map indicates relationship of the second-order Meguma Geosyncline to other major structural elements (the Avalon Platform and the second-order Acadian Geosyncline) in the Late Precambrian - Early Paleozoic Appalachian Geosyncline.

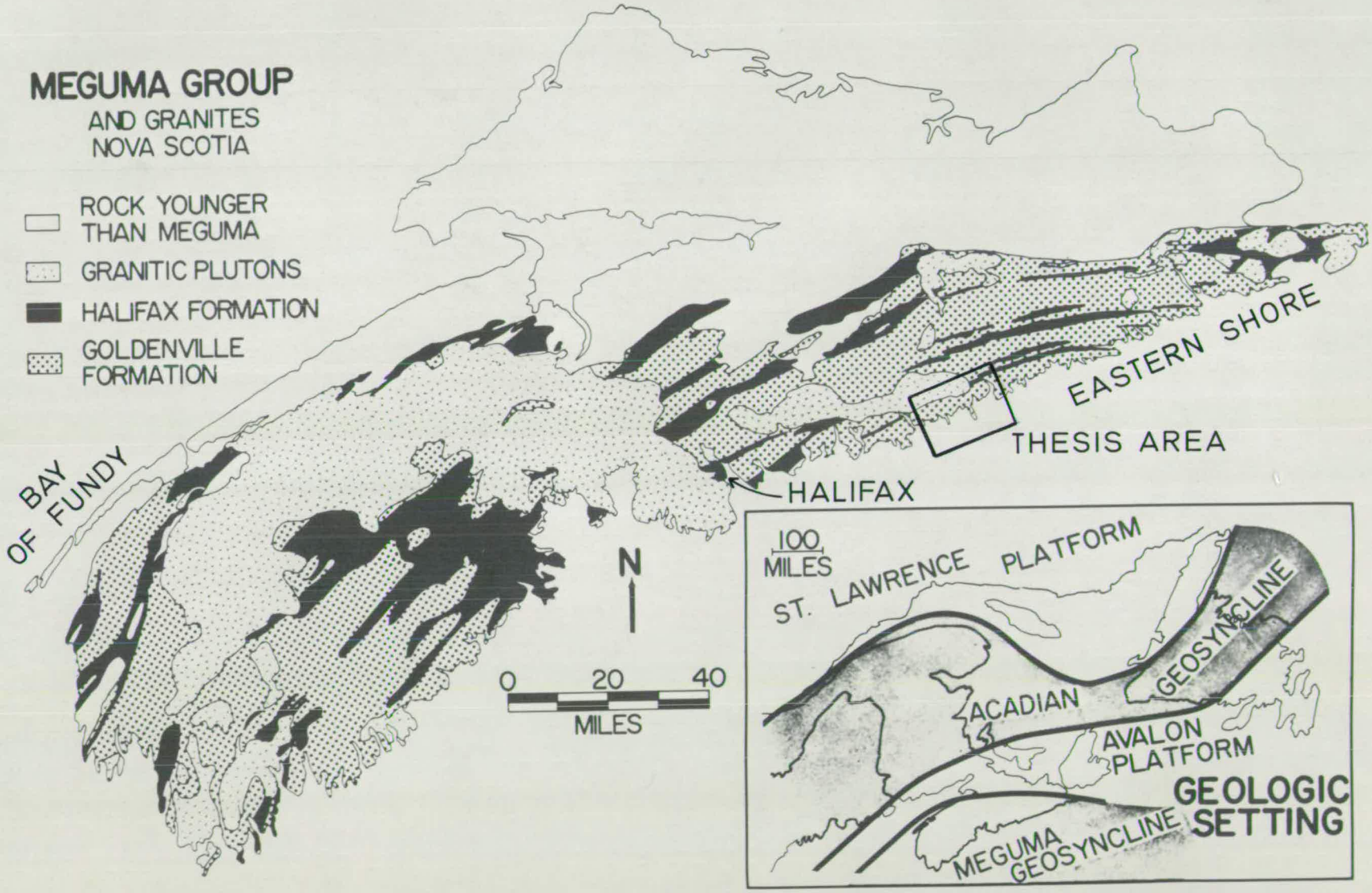
MEGUMA GROUP
AND GRANITES
NOVA SCOTIA
ROCK YOUNGER THAN MEGUMA
GRANITIC PLUTONS
HALIFAX FORMATION
GOLDENVILLE FORMATION
BAY OF FUNDY
EASTERN SHORE
THESIS AREA
HALIFAX
N
0 20 40
MILES
100 MILES
ST. LAWRENCE PLATFORM
GEOSYNCLINE
ACADIAN
AVALON PLATFORM
MEGUMA GEOSYNCLINE
GEOLOGIC SETTING

thesis, may ultimately prove significant to an understanding of the evolution and relation to global tectonics of the Appalachian Geosyncline.

The purpose of the thesis is to describe the general geology of the Goldenville Formation in a selected area, with emphasis on the sedimentary properties that contribute directly to an understanding of the sedimentological history of the formation. On this basis, tentative interpretations of the history of sedimentation in the Meguma Geosyncline are briefly considered.

Previous Work

Previous workers have suggested a number of possible environments of deposition for the Goldenville Formation and overlying Halifax Formation (the latter formation named by Ami 1900; the two formations constitute the Meguma Group, named by Woodman 1904, and modified by Stevenson 1959). Most agree with a marine, geosynclinal (presumably eugeosynclinal) setting. Woodman (1904) believed that the sea was moderately shallow and occasionally turbulent during deposition of the Goldenville Formation, but that either water depth increased or the source area lowered to accommodate deposition of the shaly Halifax Formation. Conversely, Taylor (1967) suggested that initially the water depth was great but lessened due to infilling by northwestward-moving turbidity currents, so that the sea became muddy and shallow. Phinney (1961) briefly examined a small area and concluded that the entire Meguma was deposited by northeastward-moving turbidity currents. Other

writers suggest a climatic control for the Meguma. Malcolm (1929) invoked a combination of heavy precipitation alternating with short periods of drought, changes in shore-current velocity and direction, and variations in subsidence rates. Douglas, et al. (1938) equated graded sedimentation units with varves, presumably glacial. Crosby (1962) also hypothesized seasonal fluctuations. Crosby (1962) and Campbell (1966) have provided comprehensive summary accounts of the work previous to their papers.

Schenk (1970) and his students (Campbell 1966; Campbell and Schenk 1967) were the first to undertake systematic sedimentological studies of the Meguma Group. Campbell (1966) made a preliminary survey of a 6000 square kilometer coastal area which includes the present thesis area. He concluded that turbidity currents flowing from the south-southwest deposited the Goldenville Formation in a well-defined, northeastward plunging, deep-sea trough. Schenk (1970) proposed that the sediments of the Meguma Group were moved into the area by turbidity currents, chiefly, but were completely reworked by contour-following bottom currents that flowed from the south-southwest. Schenk based his conclusions on moving average and trend surface analyses of sedimentological data from selected outcrops nearest to intersection points of a five kilometer grid placed over the entire Meguma region. His methods and conclusions are discussed further in a later section. The present study was undertaken in collaboration with Schenk (Harris and Schenk 1968).

Field Methods and Thesis Area

Detailed sedimentological investigation was carried out at well-exposed sections at the localities labelled Sections 1, 2, 3, 4 and 5 in Fig. 2 (in pocket). This included bed-by-bed description of megascopic sedimentary properties at each section. The detailed work was supported by general observations and mapping throughout the area outlined in Fig. 2, and by reconnaissance observations in adjacent areas.

The thesis area is approximately 65 miles (105 kilometers) by road northeast of Halifax, and occurs on the stretch of coast known locally as the Eastern Shore (Fig. 1). This area was chosen for study because (1) the grade of metamorphism is low relative to the Meguma region as a whole, (2) the exposures on the outer islands and headlands are exceptionally good, and (3) the sections are roughly aligned parallel to the prevailing strike (with the exception of Section 1).

The thesis area is topographically low-lying, poorly drained, densely forested, and thinly inhabited, typical of most of the Meguma region. Most of the area landwards of the outer islands and headlands is drift-covered, but locally rocks are well exposed at cliff faces and in stream beds.

Structure of Thesis

The thesis is presented in three parts. Part 1 (Introduction and Geological Framework) is divided into three sections; (1) an introduction, of which this sub-section is a part, (2) a general description of the rocks of the Meguma Geosyncline,

and (3) a discussion of structural relationships in the thesis area together with a consideration of possible tectonic effects on sedimentary orientation data. Part 1 provides the geological setting for Part 2 (Sedimentology) and Part 3 (Geological History). Part 2 deals with the petrography and sedimentary structures. Those petrographic features which contribute most to an understanding of the sedimentary provenance and geological environment are described in the text; details of the petrography are relegated to appendices. In the section on sedimentary structures emphasis is given to features which characterize recurring conditions of deposition or foundering in the Goldenville Formation, and, in the case of distinctive or exceptional structures, interpretations are presented. Sedimentary structures that are generally widespread in flysch sequences and not particularly distinctive of the Goldenville Formation are accorded relatively brief description. Part 3 is an account of the geological history of the Goldenville Formation, based on the apparent environment of deposition, dispersal and regional distribution of the formation. The thesis concludes with tentative interpretations of overall deposition in the Meguma Geosyncline.

CHAPTER 2 - REGIONAL GEOLOGY

Meguma Group

(a) Lithology

The lower part of the Meguma Group (the Goldenville Formation) consists of intercalated sandstone and slate in proportions characteristic of sandy flysch (Dzulynski and Walton 1965). The upper part (the Halifax Formation) consists of generally thin-bedded dark slate and siltstone with minor interbeds of sandstone. In some localities the contact between the two formations is abrupt and in other localities transitional, but it is everywhere conformable. The transitional zone, where present, involves a gradual upwards decrease in the sand/slate ratio in the upper 1000 metres or less of the Goldenville Formation (Taylor 1967, 1969). Excluding the transitional zone, the lithologies of the two formations are approximately consistent throughout the outcrop region.

(b) Age

The Meguma Group is generally considered to be Lower Paleozoic in age but a lack of fossils renders its precise age problematical. Crosby (1962) and earlier workers found Early Ordovician (Tremadocian) graptolites (Dictyonema flabelliforme (Eichwald)) in the Halifax Formation at a number of localities near the Bay of Fundy. W.H. Poole and P.E. Schenk (personal communication, 1970) found a poorly preserved graptolite in uppermost Goldenville or lowermost Halifax rocks near Tangier, in the present

thesis area. This specimen has been identified as probably Didymograptus or Monograptus; therefore either a Canadian (Arenigian) or Silurian age is possible, with the former being more likely.

(c) Thickness

The thickness of the group is unknown, as the base is nowhere exposed. Faribault (1914) and Taylor (1967) reported slightly over 6000 meters of the Goldenville Formation in southwestern N.S. Faribault (1909) and Crosby (1962) reported a thickness of approximately 4000 meters for the Halifax Formation in the western part of the region, whereas Taylor (1967) found Halifax strata to range in thickness from 500 to 1650 meters at the southern end of the province. The group therefore is at least 7000 meters thick and is probably more than 10,000 meters thick in some areas.

(d) Structure

The rocks of the group were folded into an arcuate fold belt (Fig. 1) during the Devonian Acadian orogeny. The Ordovician Taconian orogeny, which affected the rocks throughout much of the Acadian Geosyncline to the northwest, apparently had relatively little influence on the rocks of the Meguma Group (Poole 1967). Subsequent to the main episode of folding, the Meguma was intruded by granite to quartz-diorite plutons that generally cut across folds without changing their trends (Poole et al., 1964). On the basis of gravity measurements, Garland (1953) suggested that the

present exposures of igneous rocks (Fig. 1) are the surface expression of a slab-like plutonic mass underlying the entire Meguma fold belt. On the basis of K/Ar and Sr/Rb age determinations, intrusion occurred mainly during the Devonian, and possibly also during the Mississippian (Fairbairn et al., 1960).

The major folds are generally persistent features up to 160 kilometers (100 miles) in length and up to 16 kilometers (10 miles) in width. The folds are asymmetric to isoclinal, generally with steeply inclined axial planes and gently plunging axes. A marked regional cleavage parallels the northeast trend of the folds. At outcrops, joint-fractures are characteristically well developed and complex in arrangement. Northwest-trending faults offset the folds, with horizontal separations (generally left-lateral) of up to one mile. Small faults with normal or reverse movements are numerous but have relatively little influence on the regional structure. Dextral movements may have been extensive along fractures parallel to the regional foliation (Fyson 1966). Fyson described two sets of cross-folds which are associated with the general fracture pattern and which partly post-date the intrusion of the plutons.

(e) Metamorphism

The largest part of the Meguma Group rocks is in the greenschist facies of regional metamorphism (Turner and Verhoogen 1960). Rocks of the almandine-amphibolite facies occur in the northern part of the region (Taylor and Schiller 1966). Contact-metamorphism assemblages occur in aureoles 2/5 kilometer (¼ mile)

to 2 kilometers (1¼ mile) wide about the granitic intrusions. Contact metamorphism is not evident in the area of almandine-amphibolite regional metamorphism, apparently because the temperatures and pressures of the regional metamorphism were at least as high as those accompanying the emplacement of the granitic plutons (Taylor and Schiller 1966).

(f) Overlying Rocks

Sedimentary and volcanic rocks of (?)Ordovician, Silurian and Devonian age occur in conformable sequence with the rocks of the Meguma Group. These rocks crop out in the cores of synclines in the western part of the Meguma orogen. They were deposited in shallow marine conditions, chiefly (Smitheringale 1960; Crosby 1962; Taylor 1965). They represent the last, paralic phase of deposition in the Meguma Geosyncline prior to major orogeny. Following the Acadian orogeny, the folded and intruded rocks of the Meguma Geosyncline were deeply eroded prior to onlap of Carboniferous sediments from the northwest.

CHAPTER 3 - STRUCTURAL GEOLOGY

Folds

Large, nearly upright folds with an average strike of 70° are continuous across the thesis area (Fig. 2, in pocket). In the northwest, a granite intrusion intersects the folds with little disruption of the trends. The sections at which principal sedimentological investigation was carried out lie on the southeast limb of the Sober Island syncline (Fig. 2). The Sober Island syncline has an inter-limb angle of roughly 75 degrees, which, according to Fleuty (1964), is an open fold (inter-limb angle $> 70°$) but nearly a close fold ($30° <$ inter-limb angle $< 70°$). The major anticlines and syncline to the northwest of the Sober Island syncline are close and tight folds. The fold axes are nearly horizontal; the axis of the Sober Island syncline, for example, plunges at about six degrees toward the northwest. Gentle to tight subsidiary folds occur in the hinge zones of the major folds. Black slate of the Halifax Formation is preserved in the core of the Liscomb Harbour syncline. The Sober Island and Liscomb Harbour synclines were so named by Faribault (1896, 1897).

Fractures

(a) Cleavage and Joints

Slaty cleavage is well developed in the fine-grained rocks. It tends to obscure sedimentary structures, except in the southwestern part of the area and adjacent to the granite intrusion where metamorphism has healed the cleavage fractures or prevented their development.

At and near the hinge zone of folds, sandstone beds commonly have fractures and bedding-surface mullions approximately parallel with cleavage fractures in the interlayered slate. In some instances, cleavage-aligned fractures in sandstones are the sites of tensional separations. On the limbs of folds, cleavage fractures in slate are generally not penetrative into sandstone.

Planar shear-joints are well developed approximately normal to the bedding, both parallel and at large angles to the tectonic strike (Plate 1). Minor shear-joints are abundant.

(b) Faults

Large-scale fractures, where exposed, invariably exhibit some degree of fault displacement, generally less than several tens of meters. Strike-slip faults, both left-lateral and right-lateral, predominate. The majority of these are steeply inclined linear features that lie between 20 and 40 degress, approximately, on either side of an imaginary plane normal to the fold axes. Faults with normal and reverse displacements are limited mainly to the hinge zones of folds, and generally lie parallel or sub-parallel to the axial planes.

Deformed Sedimentary Structures

Tectonically deformed sedimentary structures indicate that appreciable internal strain occurred during the folding of the rocks. On the limbs of folds, protruberances on the bottom-surfaces of sandstone beds, such as flute casts and channels, are markedly oversteepened in the down-dip direction, whereas upper-surface protruberances,

Plate 1. Thick sandstone bed with well developed planar shear-joints.

notably sand mounds (sand volcanoes, Dzulynski and Walton 1965, and biogenic sand piles), are oversteepened in the up-dip direction. Ripple cross-laminations with an up-dip current sense are markedly oversteepened in that direction, and those with a down-dip current sense are correspondingly flattened. In plan view, the sand mounds are elliptical in outline; presumably they were originally circular structures.

The deformed sedimentary structures and pressure fringes around pyrite and magnetite crystals (Spry 1969) indicate that maximum shortening by internal strain occurred approximately normal to the axial planes of folds, that maximum extension occurred approximately parallel to the axial planes and normal to the fold axes, and that minor extension occurred parallel to the fold axes (Appendix 1).

Relative Rotation of Sedimentary, Bedding-Plane Lineations

The sand mound ellipses have a short axis/long axis ratio of about 0.67. The long axes are approximately parallel to the cleavage-bedding intersection lineation (cleavage trace). This indicates relative bedding-plane shortening normal to the cleavage trace. Sedimentary bedding-plane lineations therefore must have experienced rotation towards the cleavage trace during deformation, with the exception of those lineations that are normal or parallel to the cleavage trace.

The observed angles between the cleavage trace and sedimentary bedding-plane lineations oblique to the cleavage trace

are less than the original (pre-tectonic) angles. Utilizing the observation that the short axes of the sand mound ellipses are 0·67 times the long axes, the original angles may be calculated by the expression

$$\tan\beta = \frac{\tan\beta_o}{0{\cdot}67}$$

where β_o is the observed angle between a linear structure and the cleavage trace, and β is the original angle. This expression is employed in the determination of original (pre-tectonic) distributions and mean dispersions of sedimentary lineations (see below).

Horizontal Rotation of Folds (An Interpretation)

The mean direction of linear sole markings in the Goldenville Formation is approximately parallel to the regional fold trend. This situation prevails throughout the Meguma region (Schenk 1970). The folds and mean paleocurrent trend together describe an arc that involves a change in direction of between 70 and 80 degrees (Fig. 1).

Many folded flysch sequences, perhaps the majority, have axial paleocurrent trends. Directional changes in regional paleocurrent trends are commonly associated with changes in the direction of the tectonic axes (e.g. Dzulynski et al., 1959; ten Haaf 1959; Wood and Smith 1958a; Enos 1969). The marked parallelism of tectonic and paleocurrent trends has been ascribed to tectonic controls which determined the shape and prevailing slope of the

basin during deposition. Be that as it may, the correlation of paleocurrent trends with arcuate or sinuous regional fold patterns suggests that the paleocurrent trends are commonly associated with a pattern of sediment-distribution that influences the nature and direction of later folds.

Large-scale channels, elongate sand bodies and other sedimentary features aligned parallel to the prevailing paleocurrent trend may have combined to impart a preferred sedimentary "grain" along which initial folds developed. Fig. 3 illustrates the possible effects of laterally differential compaction in controlling the development of large-scale lensoid megacycles. Such a distribution of sediment may have tended to impart a preferred orientation to later folds.

According to this view, folds may initially develop oblique to the direction of maximum principal tectonic stress. In such situations, the folds would tend to rotate into a position approximately at right angles to the direction of principal compression, or into a stable position determined by the tectonic framework of the region. The initial position of the axis of maximum principal stress is probably important in determining whether or not an initial fold pattern will develop along a depositional trend.

Applying these remarks to the Goldenville Formation, the parallelism of the mean paleocurrent direction with the folds is attributed to an original distribution of sediments that controlled

Fig. 3. Hypothetical development of megacycles in a flysch sequence with an arrangement that might influence the distribution and orientation of later folds.

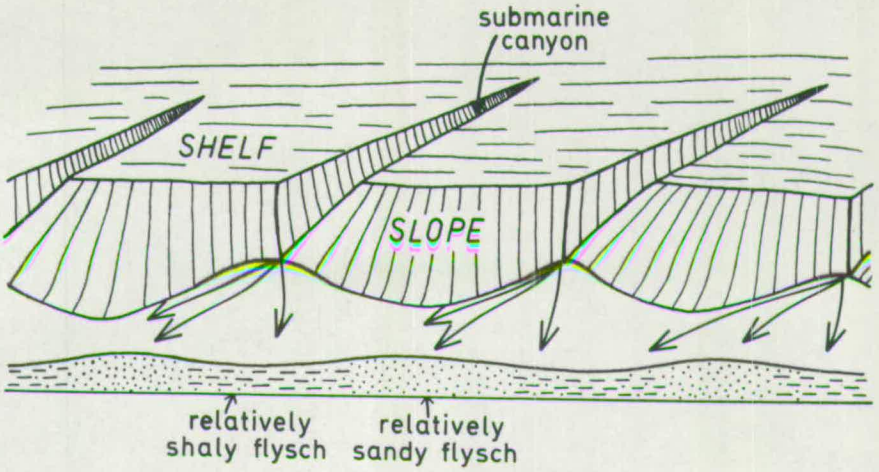

A. Development of submarine fan-complex with relatively sandy flysch deposited in front of canyon mouths and relatively shaly flysch in between.

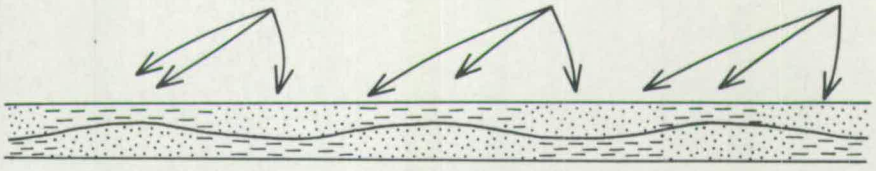

B. Greater compaction of shaly flysch than sandy flysch in A induces deflection of currents debouching from canyons causing a temporary change-about of the shaly flysch/sandy flysch deposition pattern.

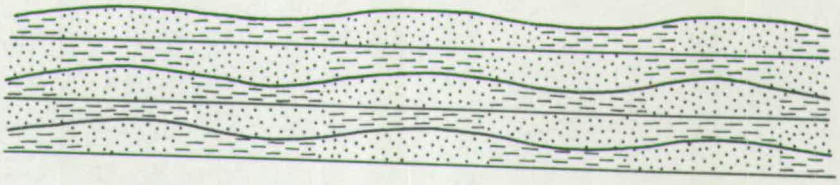

C. Continued deposition with repetitions of the pattern of megacycles developed in A and B.

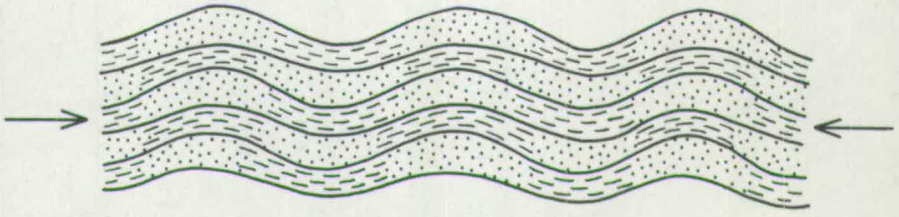

D. At onset of tectonism, folds develop with a distribution and orientation controlled by the distribution of the sedimentary megacycles. Arrows indicate direction of principal tectonic stress.

the initial fold pattern. The early-formed folds are presumed to have experienced horizontal rotation in adjusting to a position of maximum tectonic stability. The present arcuate distribution of folds suggests that rotation may have been either (1) anticlockwise in the southwestern part of the Meguma region and clockwise in the northeast, or (2) clockwise throughout the region, with greatest rotation in the northeast and least in the southwest, or (3) anti-clockwise throughout the region, with greatest rotation in the southwest and least in the northeast.

A comprehensive investigation of the regional structure is a prerequisite to assessing the validity of the interpretation of structural relationships presented above. At present, the regional structure is not sufficiently well understood for this purpose.

Orientation Data Analysis in Relation to Tectonic Effects

(a) Vector analysis

Vector summation analysis of orientation data (Krumbein 1939; Pincus 1953; Curray 1956; Potter and Pettijohn 1963; Batschelet 1965) is given in Table 1. This analysis applies to primary, bedding-surface structures that indicate a line of paleocurrent or paleoslide movement but not necessarily a direction or sense of movement. A description of the terms and the method of calculation employed is given in Appendix 2. The mean vector azimuth (Table 1, column 3) is calculated from the azimuth orientations of the sedimentary lineations, as determined by the

TABLE 1 - VECTOR SUMMATION OF ORIENTATION DATA

Nature of data	Number of Observations	Mean Vector Azimuth (degrees)	Vector Magnitude (r_c)	Mean Angular Deviation (s)
Linear sole markings (total)	650	71.2	0.67(0.55)	23.3(27.2)
Linear sole markings at Section 1	123	72.4	0.77(0.68)	19.7(22.9)
Linear sole markings at Section 2	144	68.9	0.64(0.52)	24.4(28.0)
Linear sole markings at Section 3	199	68.3	0.66(0.53)	23.7(27.8)
Linear sole markings at Sections 4 and 5 and at the southern end of Phoenix Island	161	75.9	0.65(0.53)	24.0(27.8)
Linear sole markings in beds containing mudstone inclusions greater than one meter in length	65	68.3	0.65(0.54)	24.2(27.4)
Transverse ripple crests (total)*	34	84.5	0.71(0.57)	21.9(26.6)
Slide lineations (total)	147	72.0	0.57(0.45)	26.7(30.1)
Slide lineations at Section 1 and at outcrop between Sections 1 and 2	56	76.1	0.62(0.51)	25.2(28.6)
Slide lineations at Sections 2,3,4 and 5 and at the southern end of Phoenix Island	91	68.9	0.54(0.41)	27.6(30.9)

* The orientation of ripple crests, taken with data on ripple cross-laminae (see below), indicate flow towards the north (354.5°).

method outlined by Ramsay (1961). This method involves an imaginary 'unrolling' of the folds about the fold axes, and, except when the fold axes are horizontal, further 'untilting' of the beds into a horizontal position.

Two values for the vector magnitude and the mean angular deviation are presented for each set of linear structures listed in Table 1. The unbracketed figures (Table 1, columns 4 and 5) are dispersion values for the present (observed) distribution of sedimentary lineations, whereas the bracketed figures approximate the dispersion of the original (pre-tectonic) distribution. The former were calculated directly from field measurements; the latter were determined from the same measurements, corrected for the effects of internal strain by the expression given above ($\tan\beta = \tan\beta_o/0{\cdot}67$). Histograms of the distributions of sedimentary lineations represented in the first row of Table 1 are illustrated in Fig. 4. Fig. 4A represents the present distribution of sedimentary lineations, and Fig. 4B the original distribution.

Sole markings that denote the sense of paleocurrent movement (e.g. flute casts, ruffled groove casts, longitudinal furrows with cuspate cross-bars) indicate, in every observed case, paleocurrent directions within 90 degrees on either side of the prevailing east-northeasterly paleocurrent trend in the thesis area. It may be assumed, therefore, that the bracketed figures in columns 4 and 5 of Table 1 provide a good approximation of the means and dispersions of the

Fig. 4. Histograms of the distribution of the sedimentary lineations listed in the first row of Table 1. A. Present (observed) distribution. B. Original distribution determined by adjusting each observed lineation direction (azimuth) relative to the tectonic axis (70°) by the expression $\tan\beta = \tan\beta_o/0{\cdot}67$, where β_o is the present angle between the tectonic axis and a sedimentary, bedding-surface lineation, and β is the adjusted angle. Degrees azimuth are indicated at the base of each histogram. The numbers above histogram columns represent the number of lineations represented in each case.

270
136
114
35
35
20
16
12
10
Mean Vector Azimuth
160(340)
0(360)
20
40
60
71.20
80
100
120
140
160
A

210
148
105
51
44
31
22
20
19
Mean Vector Azimuth
160(340)
0(360)
20
40
60
72.25
80
100
120
140
160
B

direction of movement as well as the line of movement of the paleocurrents that formed the structures.

(b) Original Orientation of Sedimentary Lineations

Vector analysis gives the mean dispersion of the sedimentary lineations and their distribution relative to one another, but it does not necessarily indicate the original true position of the lineations. This point is illustrated by the following example: Suppose that the diagrams in Fig. 5 represent plan views of the Goldenville sedimentary sequence before and after tectonic deformation, and that deformation involved rotational strain as indicated. Let mm' represent a fold axis that has been rotated 26 degrees from its original position in A to its present position in B. An imaginary ellipse in B, deformed from an imaginary circle in A, has a short axis/long axis ratio of 0·36. This is approximately equivalent to the trace in the plane of minimum and intermediate principal strains of a typical bedding-surface sand mound in the southeast limb of the Sober Island syncline (Appendix 1). The lineations represented by pp', nn' and qq' have been rotated from their original positions by approximately 52 degrees, 26 degrees and 0 degrees respectively. If the original distribution of pp', nn' and qq' relative to mm' in A is calculated from the present distribution in B by a modification of the expression given above (i.e. $\tan\beta = \tan\beta_o/0{\cdot}36$), then pp', nn' and qq' are returned to their original orientations relative to mm'. All the lineations are now 26 degrees from their

Fig. 5. Representation of rotational strain. Diagrams and notations are explained in the text.

A

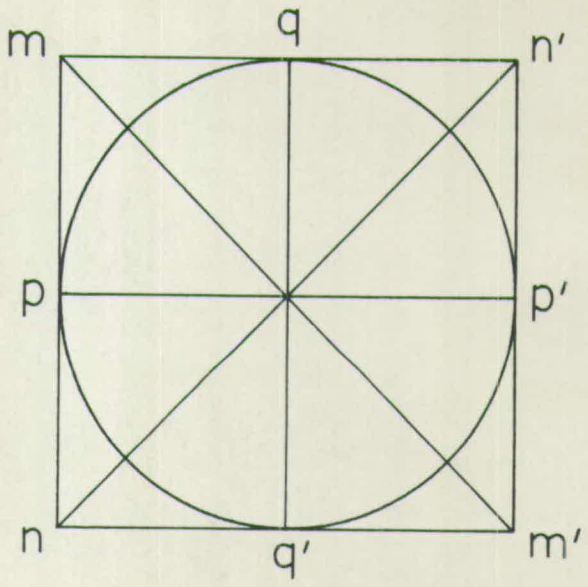

B

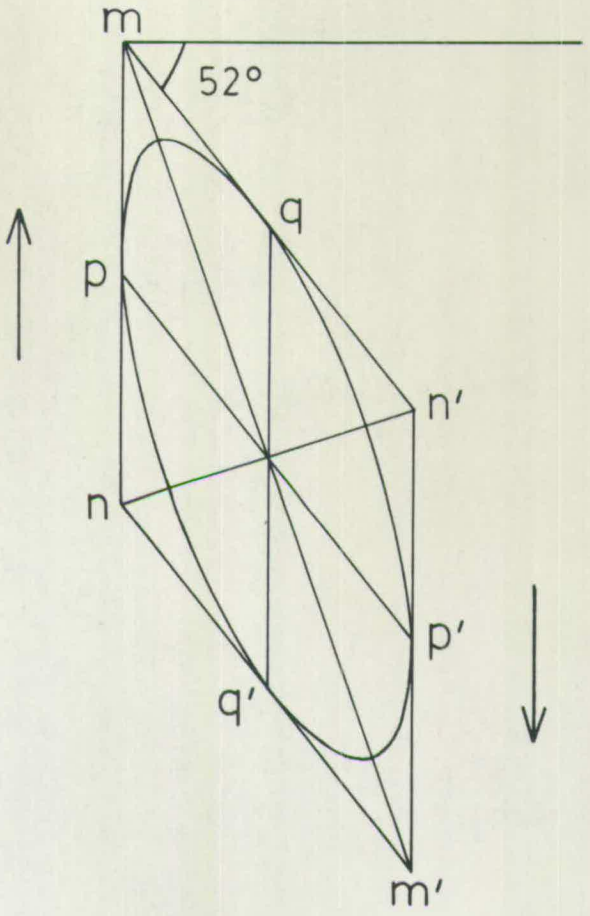

original position in A. The calculation, therefore, gives the original relative distribution, but not the original positions of the lineations.

The original position of sedimentary lineations in folded rocks can be determined precisely only through a detailed knowledge of the structural geology and sedimentation pattern. In the present case, this knowledge is not complete and the original orientation of the sedimentary lineations is, therefore, unknown. Consequently, the dispersal and source of the Meguma sediments can be only broadly estimated (see below).

PART II - SEDIMENTOLOGY

CHAPTER 4 - PETROGRAPHY

General Statement

The methods of petrographic examination upon which much of this chapter is based are given in Appendix 3. A discussion of the mineralogical composition of the sandstone in the thesis area is presented in Appendix 4.

The rocks of the Goldenville Formation are metasediments, and as such contain a large proportion of secondary (metamorphic and diagenetic) components. Widespread development of pyrite, epidote, magnetite and sodic plagioclase is attributable mainly to diagenesis. The presence of secondary biotite in most of the rocks and an abundance of secondary chlorite in all of them indicate regional metamorphism. Contact metamorphism adjacent to the granite intrusion in the western part of the area is recognized by the development of peletic hornfels containing cordierite and garnet porphyroblasts set in a fine-grained micaceous matrix.

Potassic and calcic feldspars, amphiboles and pyroxenes are absent. If initially present, these minerals have contributed, in the course of their disintegration, to the development of the secondary minerals.

Rock Types

Slate

(a) Megascopic Characteristics

Argillaceous rocks without megascopically visible laminations are herein regarded as mudstone; laminated argillaceous rocks are either siltstone or sandy siltstone. The three are referred to

collectively as slate. Mudstone, siltstone and sandy siltstone are commonly intimately interlayered within bands, herein referred to as slate bands, between sandstone beds.

In most of the thesis area, the mudstone is medium grey-green, and the siltstone and sandy siltstone are lighter shades of the same colour. In parts of the area where metamorphism is relatively highly developed, the mudstone is dark grey and the siltstone and sandy siltstone are light grey. In the latter rocks, silty and sandy laminations stand our clearly against the dark background of the mudstone (Plate 2).

(b) Composition

The slate consists primarily of fine-grained chlorite, white mica, quartz and feldspar, with porphyroblasts of chlorite and biotite, up to 6 mm. in maximum diameter, dispersed throughout. Biotite porphyroblasts are absent in the rocks at some localities and abundant in the rocks at other localities. The chlorite and mica crystals, both large and small, impart to the rock a prominent slaty cleavage.

Silt-sized particles of quartz and feldspar are abundant in the mudstone and predominent in the siltstone and sandy siltstone. Because quartz and feldspar, like chlorite and mica, may be products of diagenetic and metamorphic development, the extent to which the present grains represent detrital particles of originally comparable size and composition is problematical.

Authigenic pyrite is widespread. It tends to occur as large

Plate 2. Representative slate band of interlayered silty, very fine sandstone, siltstone and mudstone (east shore of Carter Cove).

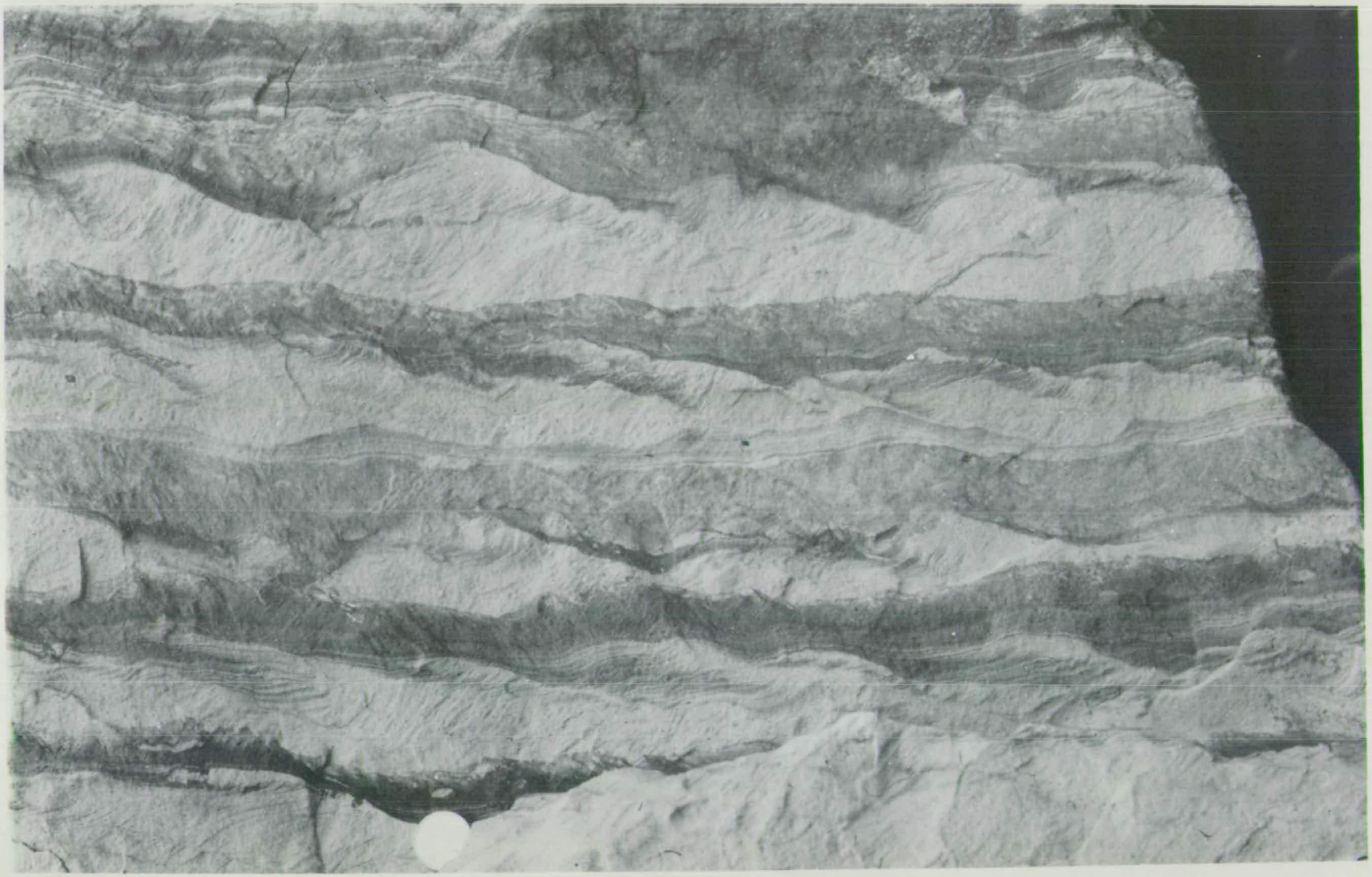

crystals; at one locality, a pyrite cube 6 cm. along an edge was observed. The pyrite crystals are bounded by relatively large pressure fringes infilled with quartz and chlorite.

The chemical compositions of 3 samples of mudstone and 1 sample of siltstone from the thesis area are compared with the chemical compositions of similar rocks in other areas in Table 2.

Sandstone

(a) Megascopic Appearance

The sandstone contains a chlorite-rich matrix that imparts a medium to light grey-green colour to the rock. A general abundance of quartz grains imparts a 'quartzitic' appearance, particularly on weathered surfaces. The relative proportion of quartz grains (see below) is not sufficient, however, to warrant the name 'quartzite' given to the diagnostic Goldenville rock by early writers (Dawson 1850; Woodman 1904; Faribault 1913).

(b) Texture

The sandstone in the thesis area consists mainly of poorly sorted framework grains with varying proportions of interstitial matrix. The minimum proportion of matrix observed in thin-sections is approximately 20 percent, whereas the maximum amount is represented in specimens which are close to sandy siltstone in composition. Beds with more than 45 percent matrix are uncommon. Some of the sandstone is moderately well sorted (Plate 3). The well sorted sandstone generally occurs in the upper portion of beds and tends to contain minimal amounts of interstitial matrix.

TABLE 2 - Chemical composition (weight percent) of argillaceous rocks in the Goldenville Formation (analyses by X-ray fluorescence), compared with the chemical composition of argillaceous rocks in other areas: A, B and C, mudstone, Goldenville Formation; D, average of A, B and C; E, siltstone, Goldenville Formation; F, average of shale and siltstone accompanying greywackes in the Franciscan, California (Bailey et al., 1964); G, average of 78 shales (Clarke, 1924); average of 36 slates (Eckel 1904). The locations of the Goldenville samples are indicated in Fig. 6.

	A	B	C	D	E	F	G	H
SiO_2	57·4	58·1	59·9	58·5	65·4	63·2	58·5	60·6
Al_2O_3	18·7	19·8	18·2	18·9	14·1	15·7	15·6	17·3
ΣFe as Fe_2O_3	8·0	6·6	6·6	7·1	7·0	6·5	6·8	5·6
MgO	3·2	2·5	2·6	2·8	2·8	3·0	2·4	2·6
TiO_2	0·8	0·9	0·7	0·8	0·7	0·7	0·7	0·7
Na_2O	2·1	2·3	2·1	2·1	3·1	2·1	1·3	1·2
K_2O	4·1	4·4	4·3	4·3	2·4	2·4	3·3	3·7
CaO	0·7	1·1	0·6	0·8	1·4	1·5	3·0	1·5

Plate 3. Photo micrograph of an example of sandstone with much better sorting than is normally the case with sandstone in the Goldenville Formation (x 55).

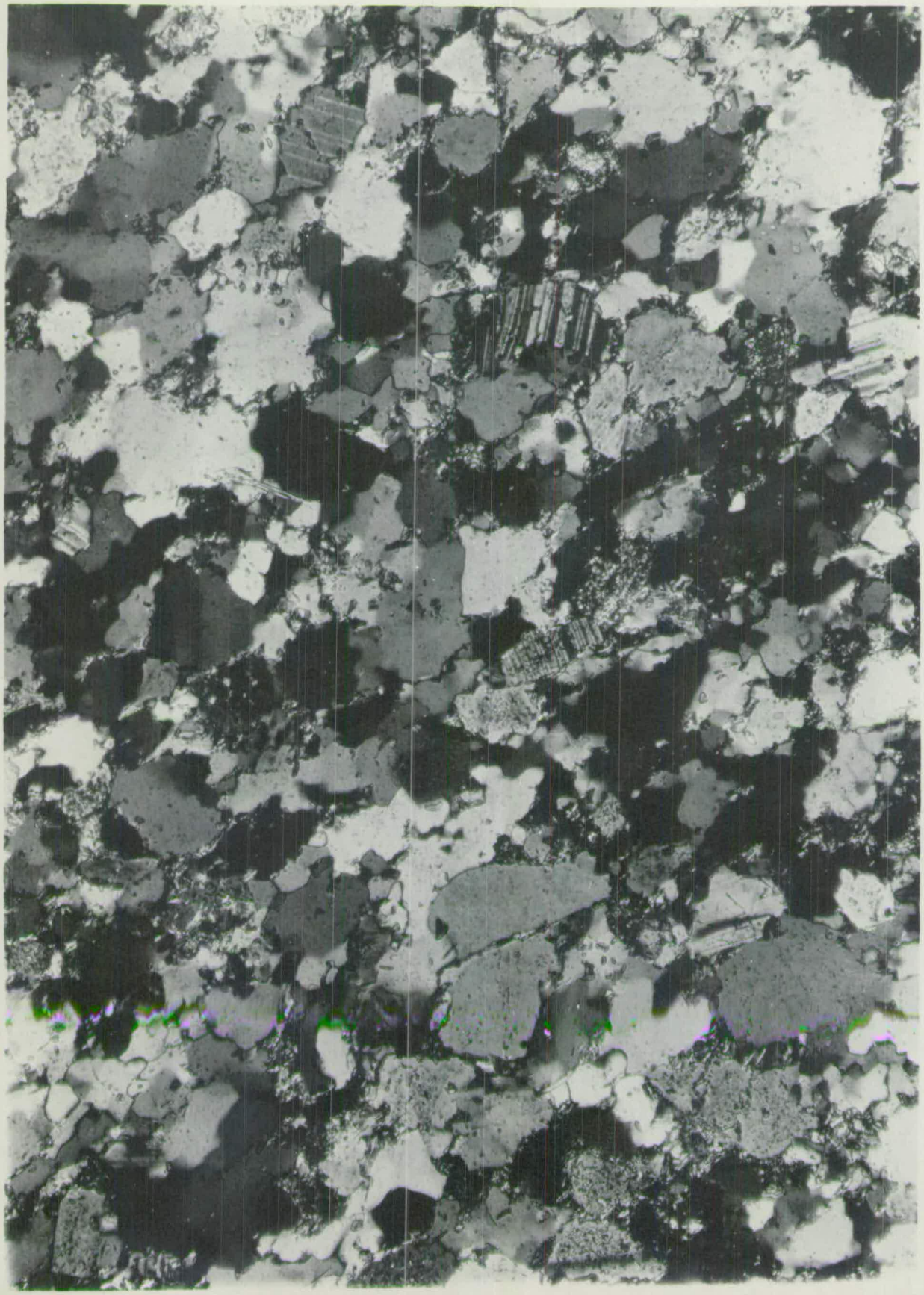

In the average sandstone bed, the average size of the framework grains is about 0·2 mm., and the maximum size is about 1 mm. The average grain size in sandstone beds rarely exceeds 0·7 mm., and the maximum grain size rarely exceeds 5 mm.

The shape and roundness of the framework components is commonly difficult to determine due to overgrowths and other modifications to the grain margins. In approximate shape, the framework components vary from equidimensional to elongate (maximum length/width ratio of 7). The roundness varies from well-rounded to angular.

The sandstone is everywhere highly indurated. Interstitial voids that may have existed originally have disappeared due to the development of secondary minerals and to the readjustment of the framework components through pressure solution and reprecipitation on grain margins.

(c) Matrix

(i) Definition

The upper size limit of matrix particles in sandstone is commonly defined at around 0·02 or 0·03 mm. (Pettijohn 1943; Dott 1964). This size designation cannot be applied precisely in the present case because of diagenetic and metamorphic replacement and enlargement of the original matrix components. For present purposes, the matrix is regarded as all quartz and feldspar grains finer than 0·05 mm., and secondary chlorite and mica grains of all sizes except that which occurs as replacement bodies in

recognizable detrital grains. Heavy minerals, irrespective of size, are not included in the matrix.

(ii) Origin

The matrix is probably derived partly from the alteration of unstable framework grains (Cummins 1962; Brenchley 1969) and partly from the alteration of lutum transported and deposited with the sand grains (Kuenen 1966; Audley-Charles 1967). In the present case, beds having equivalent grain size and framework composition, from the same locality or from different localities, commonly have marked differences in the proportion of matrix present. In such cases, relatively small amounts of matrix suggest a chiefly secondary derivation, whereas large amounts of matrix suggest partial derivation from lutum deposited as part of the original sediment.

(d) Fabric

In many specimens, a sedimentary fabric is preserved in the orientation of the long axes of framework grains, parallel both to the bedding plane and to the paleocurrent lineation. A tectonic fabric is superimposed on the sedimentary fabric. Matrix chlorite and mica impart a distinct axial plane foliation. A proportion of the framework grains are generally weakly aligned in this plane.

(e) Modal and Chemical Analyses

Modal and chemical analyses define the composition of the sandstone. Definition of the sandstone according to published classifications is avoided, because such classifications are presently controversial and consequently equivocal (Klein 1963; McBride 1963; Dickinson 1970).

Modal analyses of 5 representative thin-sections of the sandstone are presented in Table 3. The chemical compositions of 11 samples of the sandstone are listed in Table 4, and the average of these is compared in Table 5 with average chemical analyses of various sandstone types (taken from Pettijohn 1957, 1963; Bailey et al., 1964).

(f) Provenance

The following characteristics of the framework grains (Appendix 4) suggest derivation from metamorphic source rocks:
(1) A number of quartz grains have deformation lamellae possibly indicative of high-grade regional metamorphism (Fairbairn 1949)
(2) Grains of polycrystalline quartz having a granoblastic-polygonal texture (Plate 4) indicative of medium- to high-grade metamorphism (Spry 1969) are numerous.
(3) Rock fragments of schist and/or phyllite are present (although not abundant).
(4) Grains of the epidote group minerals, probably derived chiefly from calc-silicate metamorphic rocks, are ubiquitous.
Epidote group minerals occurring in rock fragments are commonly associated with polycrystalline quartz (Plate 5).
(5) Some grains of epidote and (?)staurolite contain quartz inclusions that have a metamorphic fabric-alignment.

Needle-like (?)rutile inclusions in many quartz grains possibly indicate plutonic source rocks (Mackie 1896). Large, angular grains of zircon and large zircon inclusions in plagioclase

TABLE 3 - Modal analyses: (600 points per thin-section) A, B, C and D, poorly sorted sandstone; E, moderately well sorted sandstone (same rock as Plate 3); F, average of A to E inclusive. The sample locations are indicated in Fig. 6.

	A	B	C	D	E	F
Quartz	51·7	57·7	42·6	44·4	55·5	50·4
Matrix	34·4	20·7	38·8	39·1	21·5	30·9
Plagioclase	8·6	12·0	9·6	10·7	15·9	11·4
Heavy Minerals - Non-opaque	3·2	4·9	3·9	2·8	2·9	3·5
Opaque	-	1·2	0·2	-	0·2	0·3
Detrital Mica	-	0·4	1·3	1·2	0·2	0·6
Calcite	-	-	2·0	-	0·2	0·4
Rock Fragments*	2·1	3·1	1·6	1·8	3·0	2·3

* excludes polycrystalline quartz (included with quartz)

TABLE 4. - Chemical composition (weight percent) of sandstone (analyses by X-ray fluorescence): A, sample of sandstone with moderately well sorted framework grains; B to K inclusive, samples of typical, poorly sorted sandstone. The sample locations are indicated in Fig. 6.

	A	B	C	D	E	F	G	H	I	J	K
SiO_2	76·0	74·5	76·8	75·3	72·5	71·6	72·5	73·1	70·3	70·0	64·8
Al_2O_3	10·0	10·7	10·0	9·8	12·5	12·4	12·1	11·0	13·3	12·6	12·7
ΣFe as Fe_2O_3	3·0	4·2	3·3	4·6	4·0	4·6	4·5	5·1	4·6	6·0	7·8
MgO	1·1	1·9	1·1	1·9	1·6	1·7	1·7	1·8	1·9	2·3	3·0
TiO_2	0·5	0·5	0·6	0·6	0·5	0·7	0·6	0·5	0·6	0·5	1·7
Na_2O	3·1	2·9	3·7	2·9	3·2	3·2	3·1	3·2	2·8	2·8	1·9
K_2O	1·6	1·4	1·2	1·1	1·8	1·7	1·6	1·3	2·6	1·5	1·6
CaO	0·9	0·9	1·1	0·8	0·9	1·1	0·9	0·8	0·9	1·3	2·5

TABLE 5 - Chemical composition (weight percent) of average sandstone in the Goldenville Formation compared with the chemical composition of sandstone in other areas: A, average of 11 samples of Goldenville sandstone listed in Table 4; B, average of 21 Franciscan graywackes (Bailey et al., 1964); C, average of 23 graywackes (Pettijohn 1957); D, average of 17 Harz mountain graywackes (Mattiat 1960); E,'average graywacke' (Pettijohn 1963); F, average lithic sandstone (subgraywacke)(Pettijohn 1963); G, average arkose (Pettijohn 1963); H, Carboniferous, coal-measure sandstone (subgraywacke ?) (Cayeux 1929).

	A	B	C	D	E	F	G	H
SiO_2	72·5	67·5	64·7	69·7	66·7	66·1	77·1	74·5
Al_2O_3	11·6	13·5	14·8	14·3	13·5	8·1	8·7	10·8
Fe_2O_3	4·7	4·5	5·8	4·5	5·5	5·3	2·3	4·6
MgO	1·8	2·2	2·2	1·8	2·2	2·4	0·5	1·3
TiO_2	0·6	0·5	0·5	0·5	0·6	0·3	0·3	0·5
Na_2O	3·1	3·6	3·1	3·1	2·9	0·9	1·5	1·1
K_2O	1·6	1·7	1·9	1·4	2·0	1·3	2·8	1·5
CaO	1·1	2·4	3·1	1·3	2·5	6·2	2·7	0·4

Plate 4. Photomicrograph showing part of a grain of polycrystalline quartz with a granoblastic-polygonal texture (x 110).

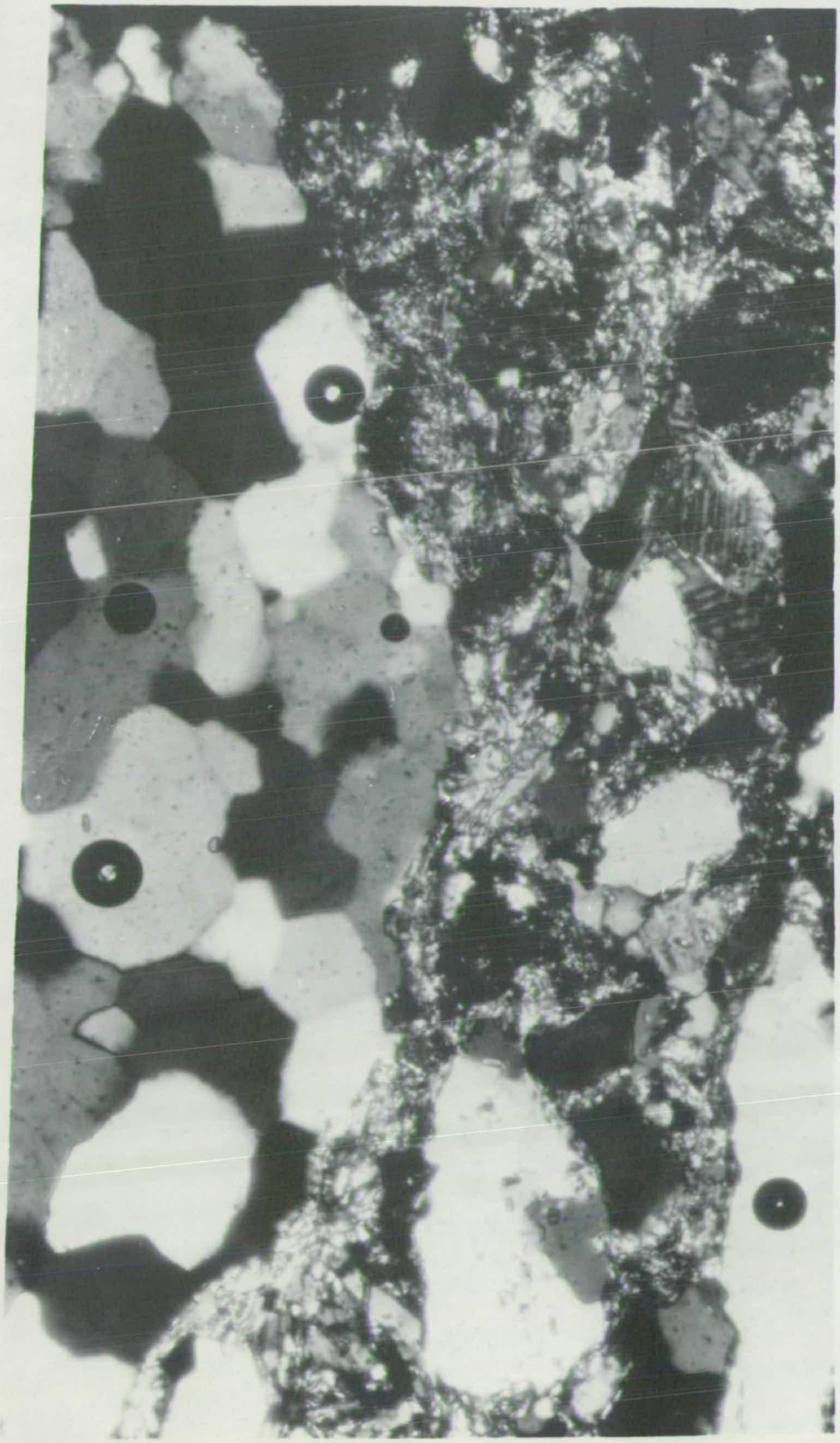

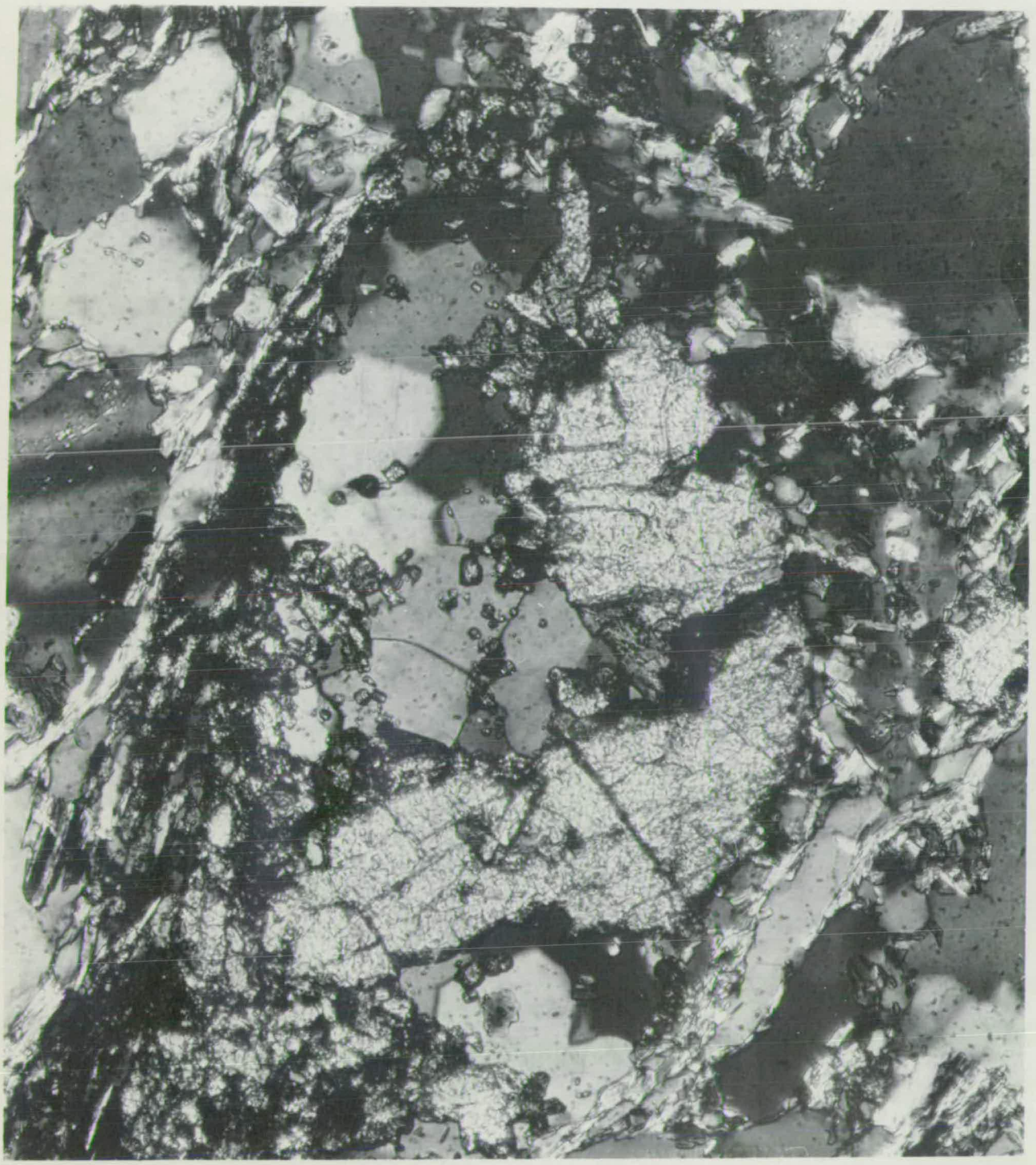

grains (Plate 6) also suggest plutonic rocks in the source area.

A high proportion of angular grains of the epidote group minerals, zircon and sphene, as well as quartz and feldspar, suggest a derivation from freshly exposed crystalline rocks. Well rounded grains of the same mineral species, on the other hand, suggest sedimentary reworking of part of the source material.

Nearly all grains of apatite and tourmaline are well rounded (excluding overgrowths), and these presumably also represent sedimentary reworking. Rarely, tourmaline grains have a 'layered' aspect, whereby one or several 'layers' surround a 'core', the whole enclosed in normal overgrowths. The core, layers and overgrowths are distinguished by slight differences in colour. The layers may be remnant overgrowths from previous sedimentation cycles.

According to Dickinson's (1970) compositional criteria for salient provenance types, the Goldenville sandstone has a chiefly plutonic (mainly granitic) and 'tectonic' (mainly sedimentary and metasedimentary) derivation.

The relatively high iron and magnesium content of the Goldenville sandstone and similar sandstones (Table 4) may be explained by a partial volcanic provenance (Middleton 1960). Volcanic-derived particles recognized in the present rocks are limited to rare volcanic rock fragments. Other grains of volcanic derivation, if initially present, must have been removed by disintegration and reconstituted as secondary minerals. Ubiquitous secondary magnetite and pyrite in the sandstone suggests that this may have been the case.

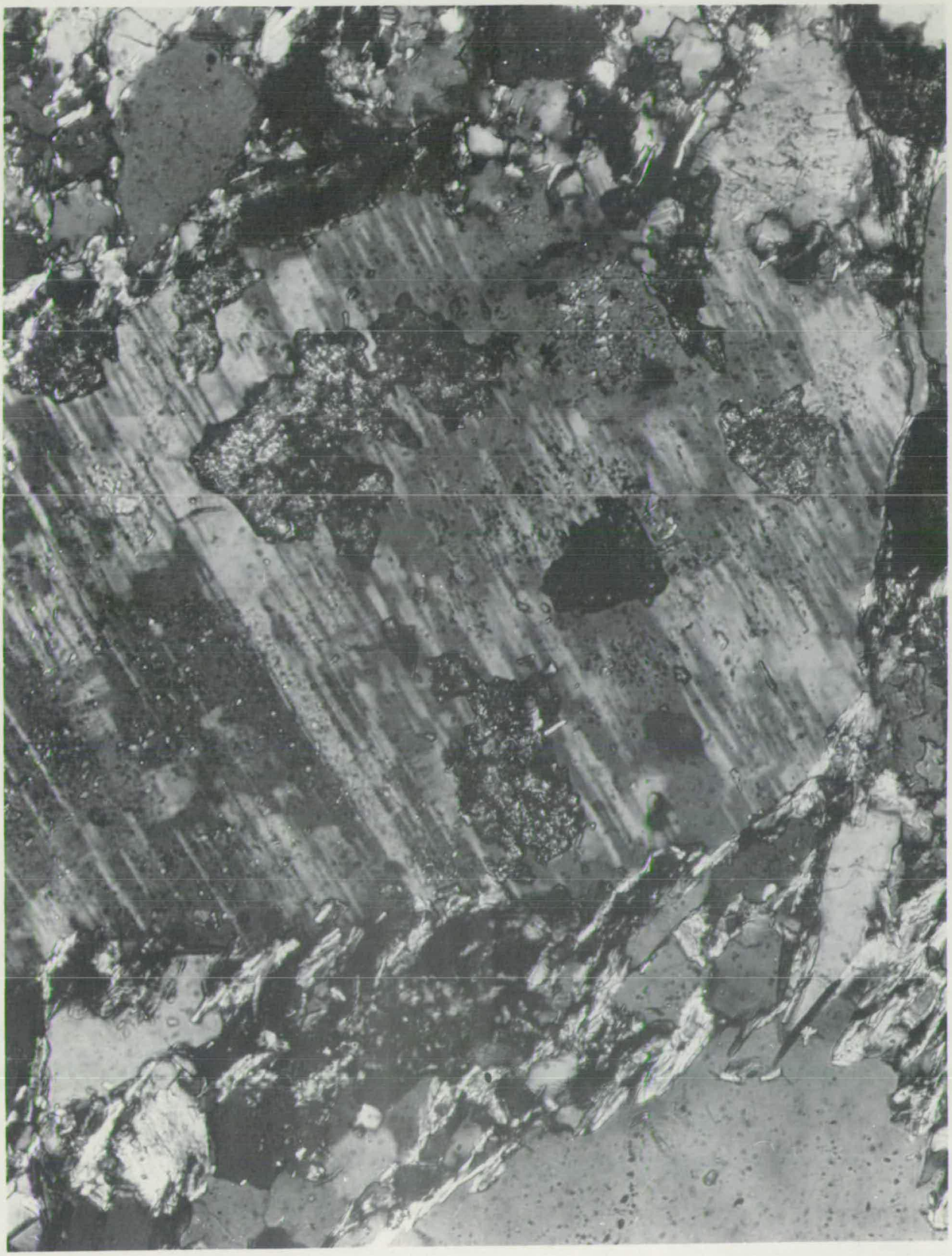

Grains of zircon, sphene and rutile commonly have pronounced marginal embayments that reflect chemical corrosion and replacement during diagenesis. Less resistant minerals that were unstable in the geochemical environment that prevailed during burial may have been completely removed, as inferred above in the case of volcanic-derived particles. In view of the apparent provenance of the sandstone, potassic feldspars, garnet, amphibole and pyroxene are examples of mineral species that may have been present in the original sediment although absent in the present rocks.

(g) Plagioclase

The composition of plagioclase grains in the sandstone is that of calcic albite/sodic oligoclase, with very little variation (Appendices 3 and 4). Plagioclase compositions are typically albitic in sandstones which are mineralogically and chemically comparable in other respects to the sandstone of the Goldenville Formation. The origin of the albite/oligoclase is uncertain (Pettijohn 1963). A partial volcanic (spilitic) provenance, combined with rapid erosion and little chemical weathering is a possible explanation (Middleton 1960). Albitization during burial, involving soda metasomatism, is another possibility. Whatever the origin, albitic plagioclase and the relatively high content of Na_2O it represents are characteristics of the graywacke-type sandstones which the Goldenville sandstone mineralogically and chemically resembles.

EX BIBL UNIV. EDINBURGEN

CHAPTER 5 - SEDIMENTARY STRUCTURES

General Features

The succession of alternating sandstone beds and slate bands represented in Sections 1 to 5 inclusive is depicted in Fig. 6 (in pocket). A table of statistics on the vertical and lateral variations in bed thicknesses and sandstone/slate ratios is included (Fig. 6D). Both the sandstone beds and slate bands in Sections 1 to 5 have a log normal distribution of thicknesses (cf. Bokman 1953; Pettijohn 1957; McBride 1962).

At outcrops, the majority of beds are approximately constant in thickness along strike. A large minority of beds, on the other hand, are variable in thickness over distances of a few meters.

Sandstone beds reach a maximum thickness of 50 meters in the thesis area. These beds, when traced along strike, appear either to be discontinuous or to become segregated into a number of thinner beds over a distance of several kilometers.

Current Structures

Depositional Structures

(a) Graded Bedding

The beds of the Goldenville Formation characteristically display delayed grading (Walton 1956) with poor separation (Dzulynski and Walton 1965; Walton 1967). Interrupted grading (Kuenen 1953) is common. Continuous grading (Ksiazkiewicz 1954) is prevalent in sandy siltstone and siltstone beds that generally occur interlayered with mudstone in slate bands. Mudstone beds

above graded divisions are generally less than 10 cm. in thickness.

(b) Parallel Lamination

Megascopically visible, parallel laminae occur in slightly less than half of the sandstone beds. They are most common near the base of the beds but also occur at other horizons. Some beds are laminated throughout their thickness (Plate 7). The laminae comprise alternating thin layers of varying grain size (Plate 8) or layers of more or less uniform grain size bounded by parting planes or incipient parting planes which represent surfaces of interrupted deposition and possibly erosion (Plate 9). The parting surfaces, when exposed, commonly display current-sculptured lineations.

Thin parallel laminae occur abundantly in slate bands, particularly above graded divisions.

(c) Compound Stratification

(i) Description

A majority of sandstone beds, particularly those exceeding a meter in thickness, exhibit compound (multiple) layering. Each layer is bounded above and below by parting surfaces or incipient parting surfaces, or by the bottom or top of the bed. Exposed parting surfaces commonly display current markings.

(ii) Interpretation

The layers in a given bed developed either as a consequence of a succession of separate sedimentation events generally involving

Plate 7. Parallel-laminated sandstone.

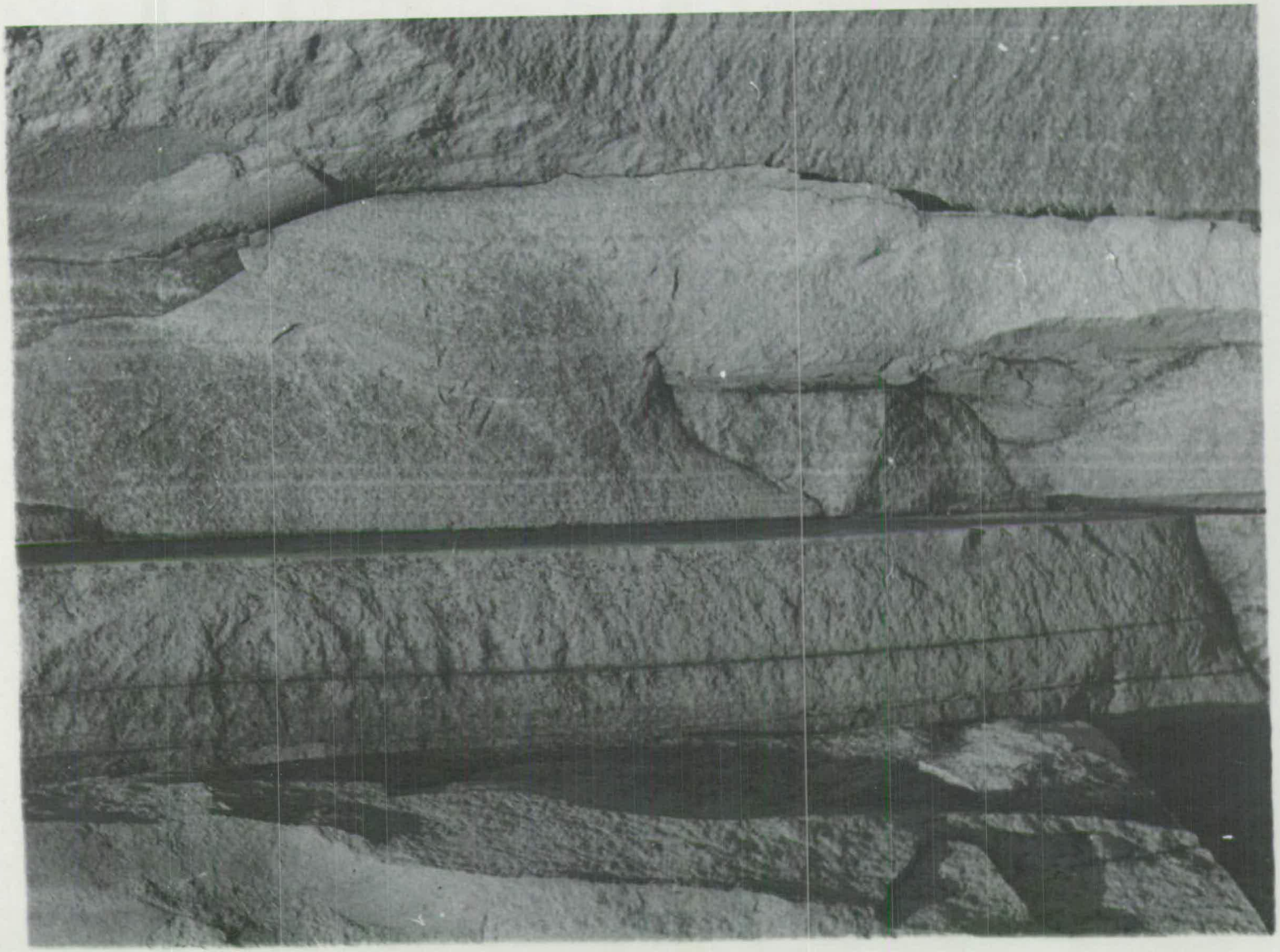

Plate 8. Photomicrograph showing laminae in sandstone formed by alternating layers of coarse and fine arenaceous material (x 12).

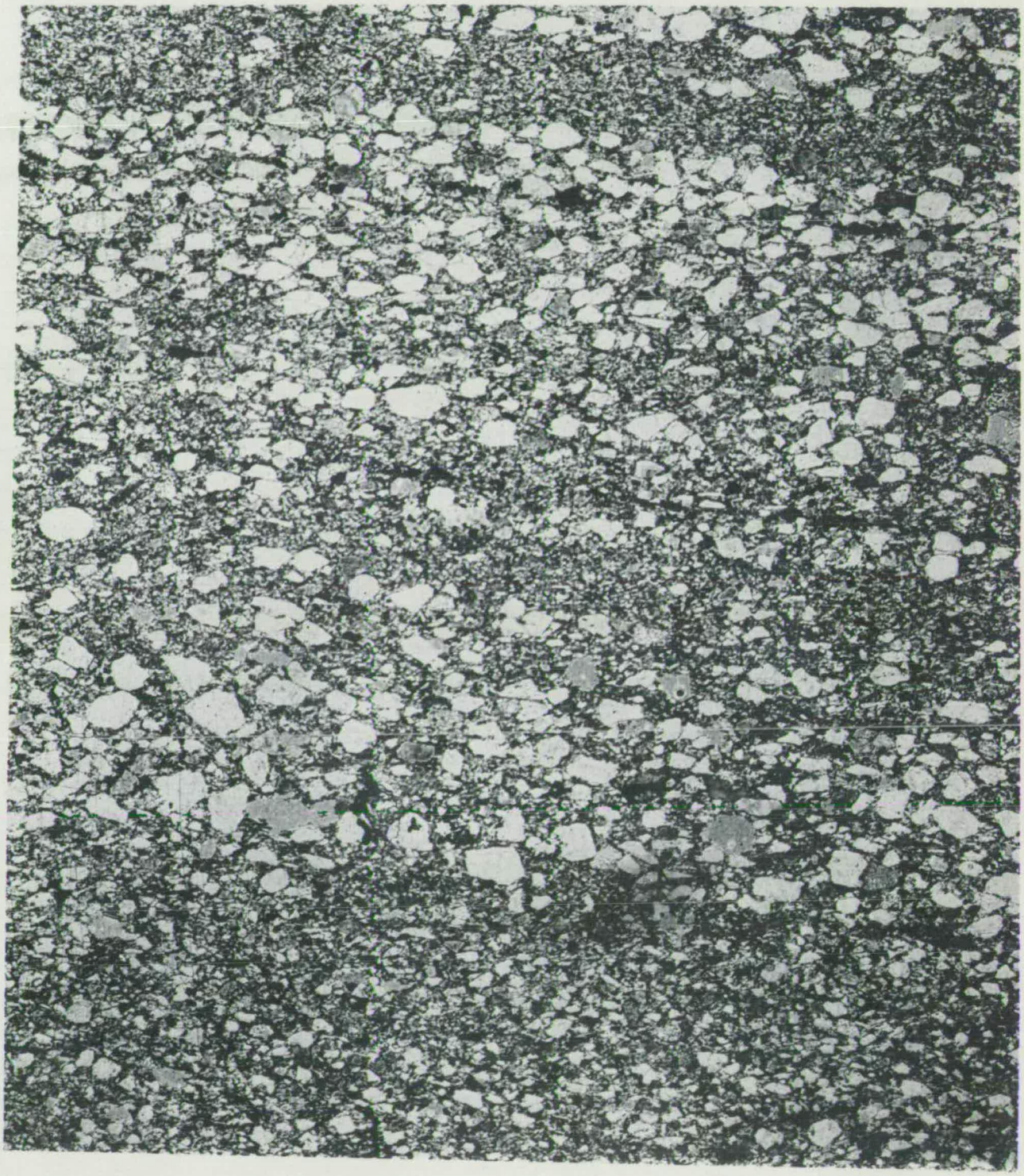

Plate 9. Photomicrograph showing a surface of erosion or interrupted deposition (dark line in central part of picture). The surface separates two laminae, both of which are not fully visible in the picture (x 8).

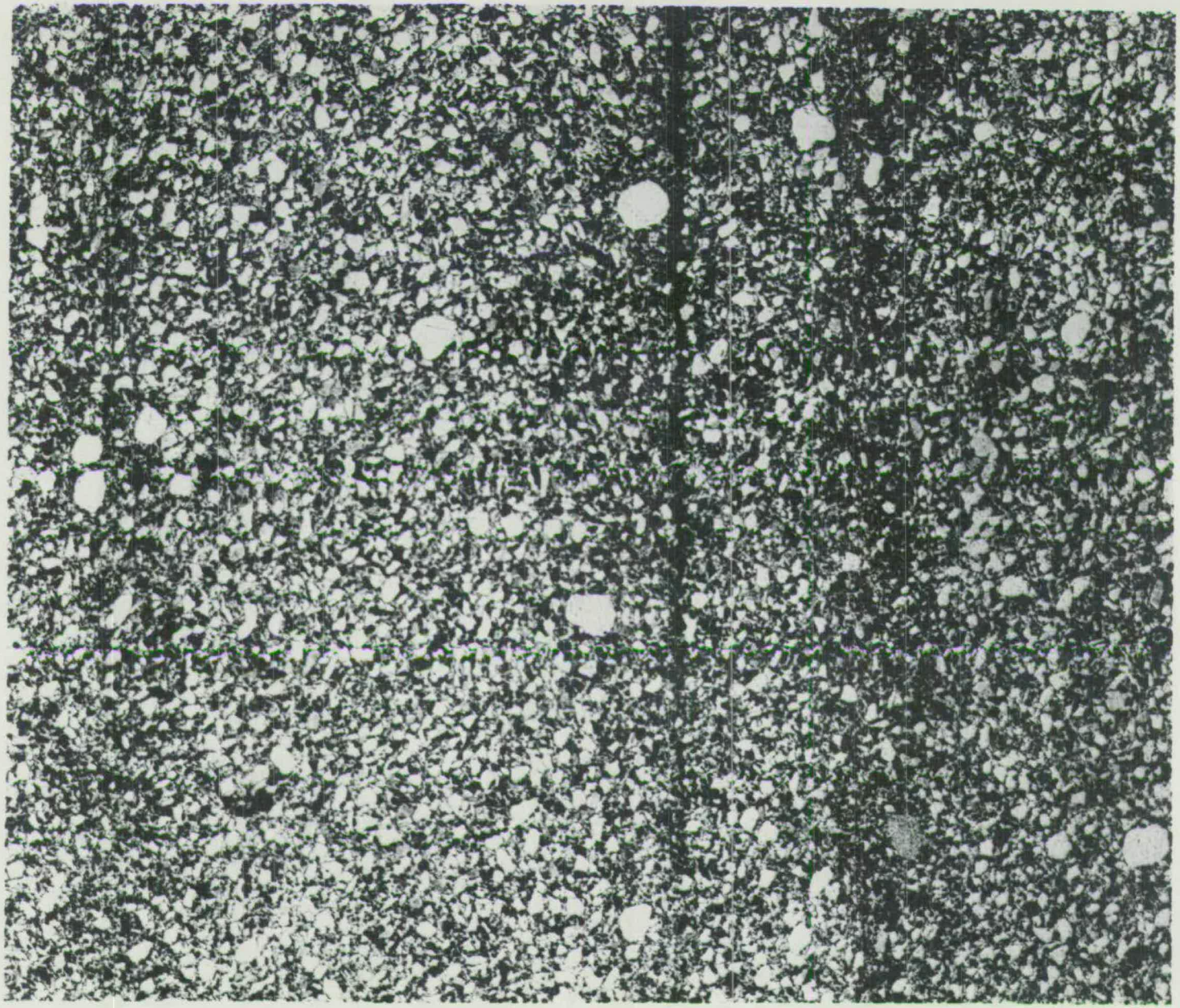

partial erosion of a layer below prior to deposition or a layer above, or as a consequence of pulsations of deposition during a single episode of sedimentation. Thick layers bounded by parting surfaces with well developed current markings probably belong in the former category, whereas thin layers with rather weakly developed bounding surfaces (Plate 10) may belong in the latter category.

(d) Amalgamated Bedding

Amalgamated bedding, both straight and curved (Lovell 1969), is present. Amalgamated bedding may laterally develop into compound stratification.

(e) Mudflake Inclusions

Megascopic fragments of mudstone, siltstone and argillaceous sandstone, here referred to collectively as mudflake inclusions, occur in about 50 percent of the sandstone beds. They are generally elongate fragments several cm. or tens of cm. in length (Plate 11), but many exceed one meter in length (e.g., Plate 12).

(f) Ripple Cross-Lamination and Ripple-Mark

(i) Description

Ripple cross-lamination, commonly in the form of 'ripple-drift bedding' (Sorby 1908)(Plate 13), is very widespread.

Ripple-mark is well displayed at the top of some sandstone beds (Plate 14), due to the preferential weathering and erosion of overlying slate. Transverse ripples are most common. Cresentic

Plate 10. Compound stratification in a sandstone bed. Knife blade marks base of bed.

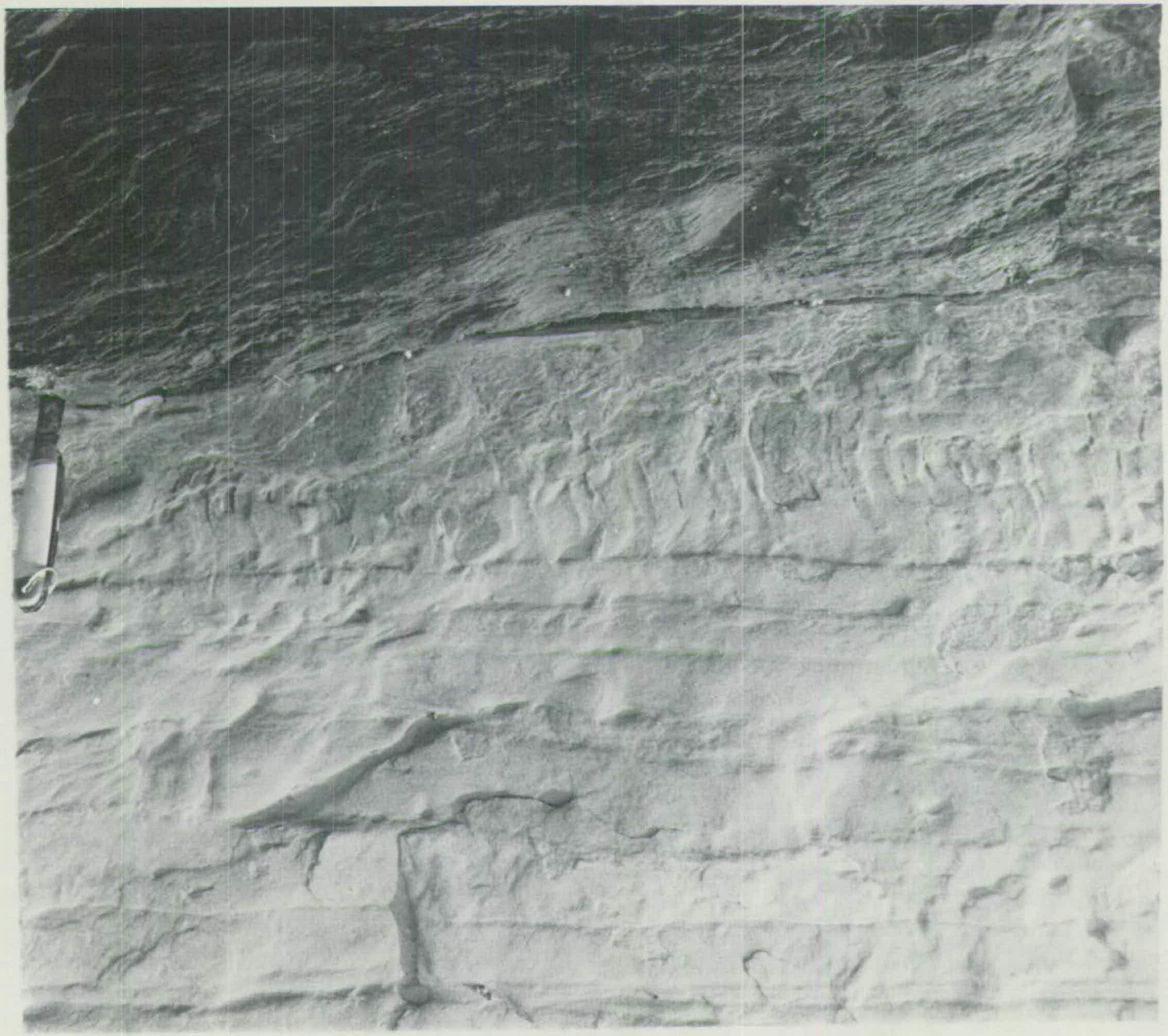

Plate 13. Ripple-drift cross-lamination in sandstone gradational to sandy siltstone. Parallel lamination beneath the cross-lamination. Arrows indicate an incipient parting surface which corresponds to the exposed surface illustrated in Plate 14.

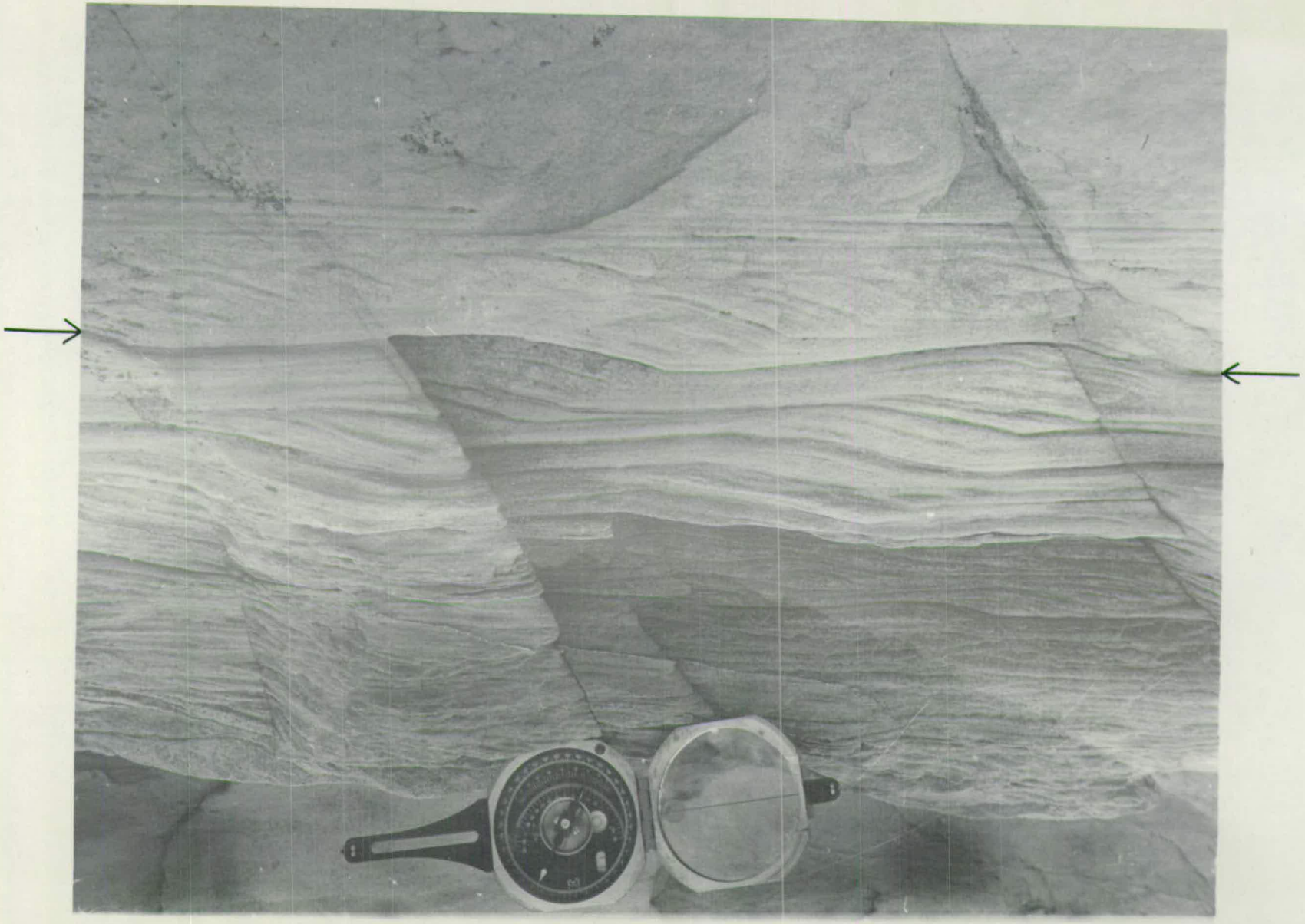

Plate 14. Transverse, slightly cresentic ripple-mark on upper bedding-surface in a sandstone fragment (the bedding-surface indicated in Plate 13).

ripples (Dzulynski and Walton 1965, p. 175) are next in abundance, and appear generally to grade upwards through increasingly fine sediment to transverse ripples. Longitudinal ripples (van Straaten 1951; Kelling 1958) are rarely present.

(ii) Interpretation of Paleocurrent Direction

Data on random measurements of traces of ripple cross-laminae (dip direction of foreset laminae) on exposed surfaces are presented and compared in Fig. 7 with the mean direction of ripples exposed on the upper bedding-surfaces of sandstone beds (see Table 1). The traces of ripple cross-laminae suggest a mean paleocurrent direction toward the northeast, approximately parallel to the tectonic strike. This, in turn, is parallel to the mean paleocurrent direction indicated by current markings at the base of sandstone beds (see above). A line of mean paleocurrent movement at a large angle to this direction is indicated by the ripples.

A difference in paleocurrent directions indicated by ripples and sole markings is common in nature (e.g. Prentice 1956; Craig and Walton 1962; Kelling 1964; Hsu 1964). The difference between the ripple paleocurrent direction and the direction indicated by ripple cross-laminae as well as by sole markings is unusual, except that the indicated direction of ripple cross-laminae may be more apparent than real. Ripple cross-laminae tend to be well exposed on cleavage surfaces relative to surfaces at large angles to the cleavage. This introduces a bias into a random

Fig. 7. Current directions determined from measurements of ripple cross-lamination traces on exposed surfaces. Numbers indicate the total for each of the 45 degree class intervals. The mean direction of ripple mark (direction parallel to ripple crests) and the regional tectonic strike are indicated.

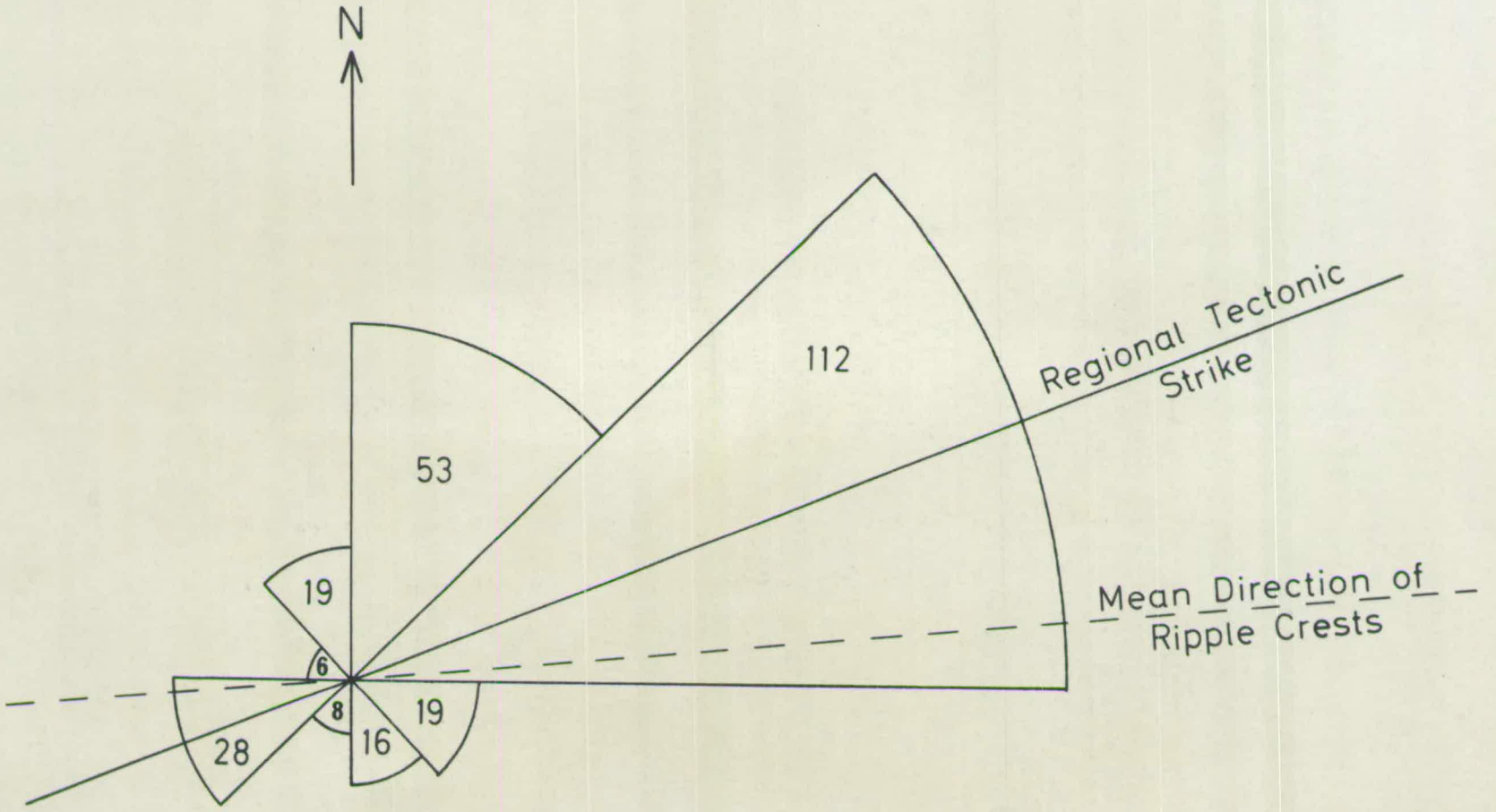
N
112
53
19
6
8
28
16
19
Regional Tectonic Strike
Mean Direction of Ripple Crests

measurement of cross-laminae traces on exposed surfaces, tending to favour a paleocurrent direction parallel to the cleavage. In view of this, the ripples may be a truer representation of the prevailing paleocurrent line of movement that affected most of the sediment of fine grain-size than are the ripple cross-laminae. The fact that ripple cross-laminae indicate a predominant paleocurrent trend towards the northeast rather than towards the southwest is significant, however, as laminae in both directions are equally well exposed on cleavage surfaces.

In conclusion, the ripples and ripple cross-laminae are attributed to paleocurrents that generally moved from south to north, approximately, at large angles to the mean direction of paleocurrents that formed the sole markings at the base of sandstone beds.

Tool Moulds

Groove moulds occur on the under-surfaces of 85 percent of the sandstone beds. Examples are illustrated in Plates 15 to 21 inclusive. Grooves are commonly associated with current-smoothed moulds (small channels) and flute moulds (Plates 19, 20). Exceptional grooves have a twisted or spiralled aspect (Plates 16, 17). Some end abruptly in prod-like terminations (Plate 16).

Intra-bed surfaces with groove markings (Einsele 1963, Hubert et al. 1966) are fairly common (Plates 22, 23 and 24). The internal grooves typically occur in association with scour depressions (internal flutes and channels) (Plate 22) and incipient tensional

Plate 16. Prominent groove moulds, spiralled in right-centre part of picture, and terminated in a prod mould on the left near the hammer-head.

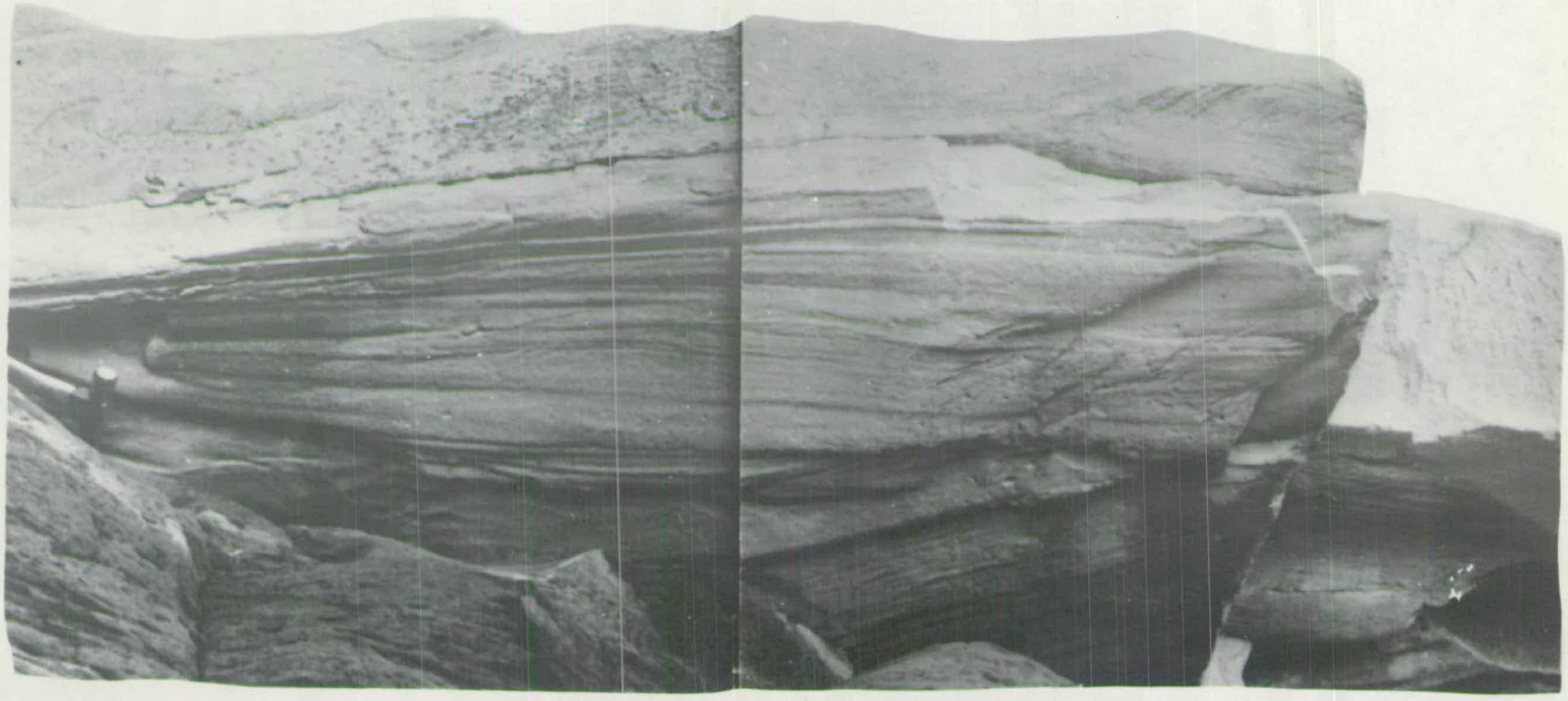

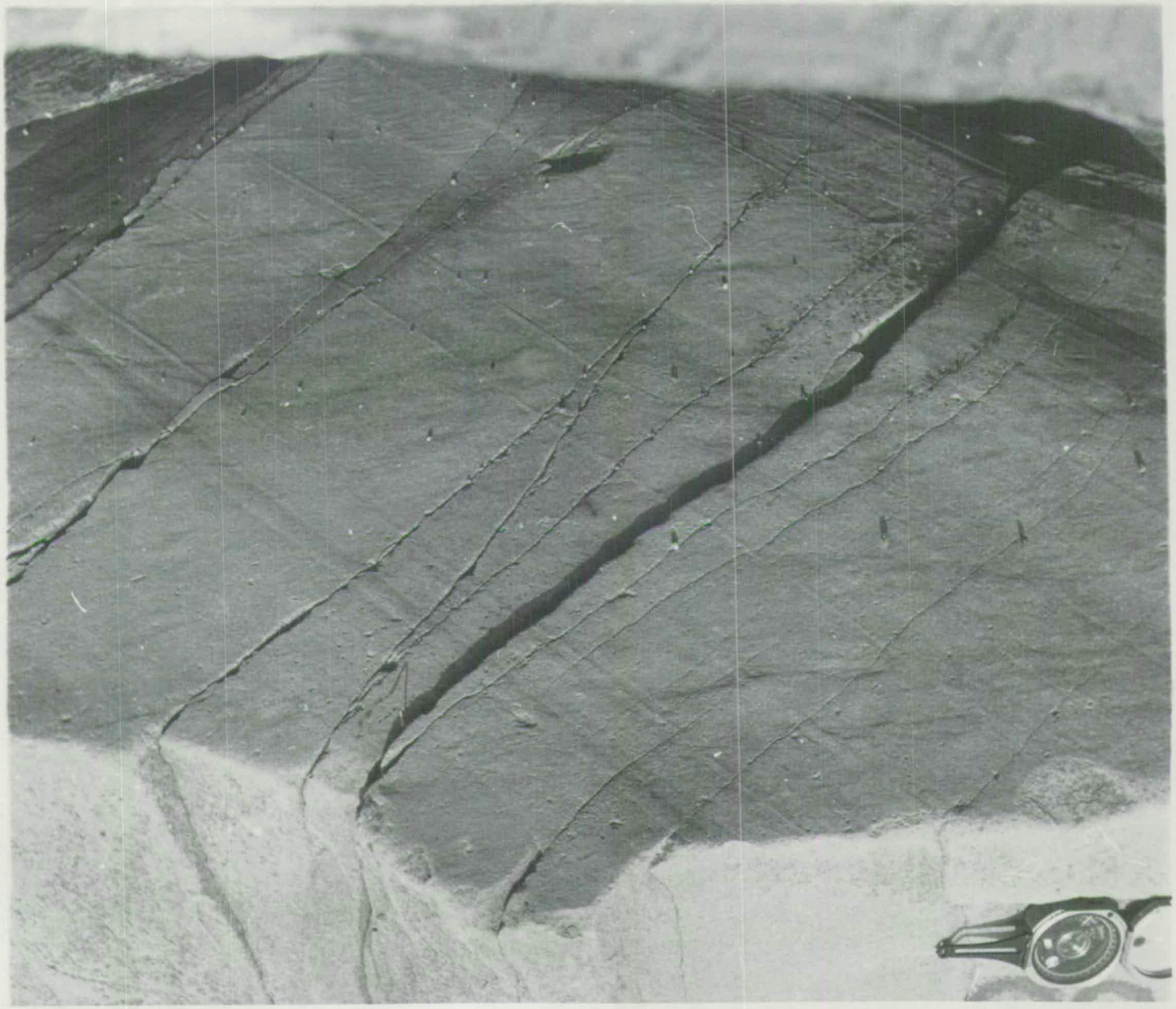

Plate 22. Groove moulds on two parting surfaces in a sandstone bed. The grooves are in places superimposed on scour depressions (internal flutes and channels).

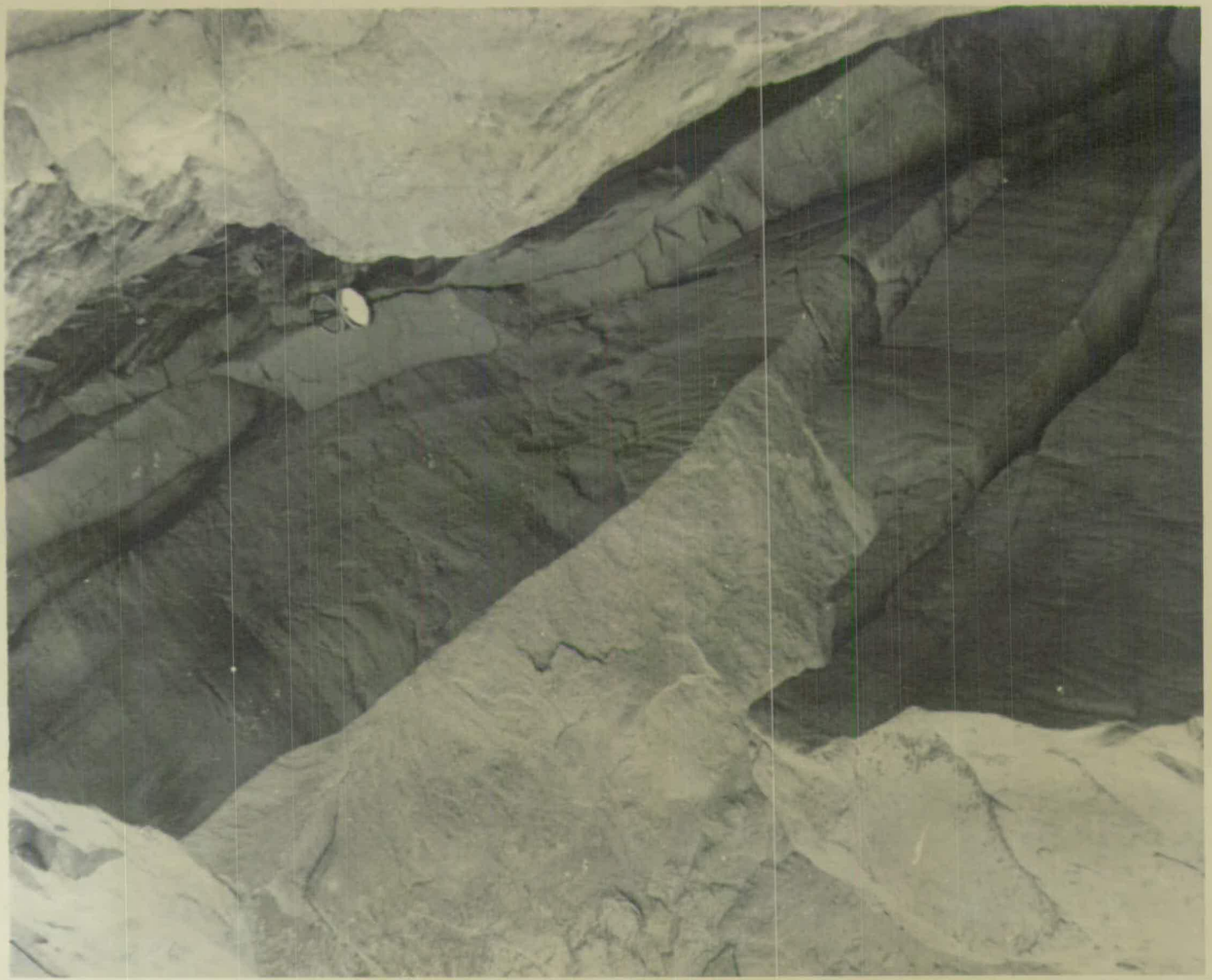

Plate 24. Groove moulds on a parting surface. Incipient tension cracks transverse and oblique to the grooves. Primary current lineation beside hammer-head (hammer length 35 cm.).

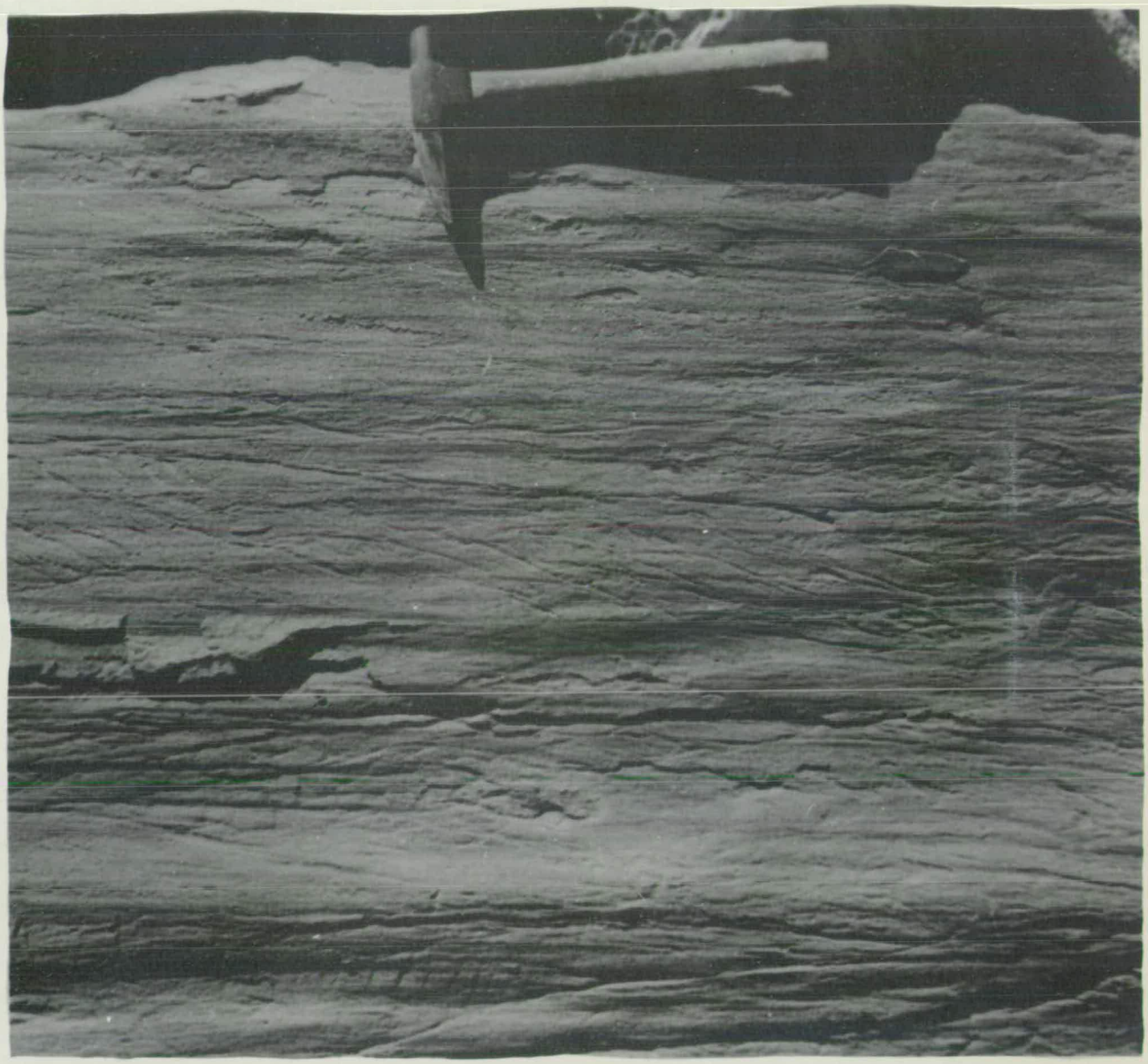

separations oblique to the lineation of the grooves and associated current structures (Plate 24). Primary current lineation (Stokes 1947, Crowell 1955) occurs on some of the intra-bed, grooved surfaces (Plate 24).

Bounce and prod moulds occur on the soles of some sandstone beds, generally in association with groove moulds.

Scour Moulds

(a) Flute Moulds

(i) Sole Flutes and Associated Structures

Flute moulds occur on the soles of approximately 15 percent of the sandstone beds. Shallow, closely spaced flute moulds associated with longitudinal furrow moulds predominate (Plates 25, 26 and 27). This variety of flute moulds tends to be distributed longitudinally on the soles, commonly with a diagonal alignment as well. Other types of under-surface flute moulds are uncommon (e.g., Plates 28 and 29).

Longitudinal furrow moulds and flute moulds commonly pass laterally into zones of scaliform and dimpled, non-oriented structures (Plate 30). Small, reticulate, scour moulds, comparable to forms produced experimentally by Allen (1969, Fig. 2), are rarely present (Plate 31).

(ii) Internal Flutes

Internal flutes (flute markings on parting surfaces) occur in approximately equal abundance to sole flutes. Internal flutes are commonly delineated on outcrop surfaces by trough cross-laminae. Parallel laminae commonly occur in the same beds

Plate 25. Conical, shallow flute moulds and longitudinal furrow moulds. Current from left to right.

Plate 26. Longitudinal furrow moulds, flute moulds, and dimpled structures. Current from left to right.

459

Plate 27. Longitudinal furrow moulds and shallow flute moulds.
Current from lower left to upper right.

Plate 28. Flute moulds exhibiting a variety of shapes (elongate-symmetrical, linguiform, slightly spiralled, cresentic, irregular). The irregular shapes are suggestive of load deformation. Current from left to right (hammer length 35 cm.).

Plate 29. Anastomosing pattern of evenly distributed, elongate-symmetrical flute moulds.

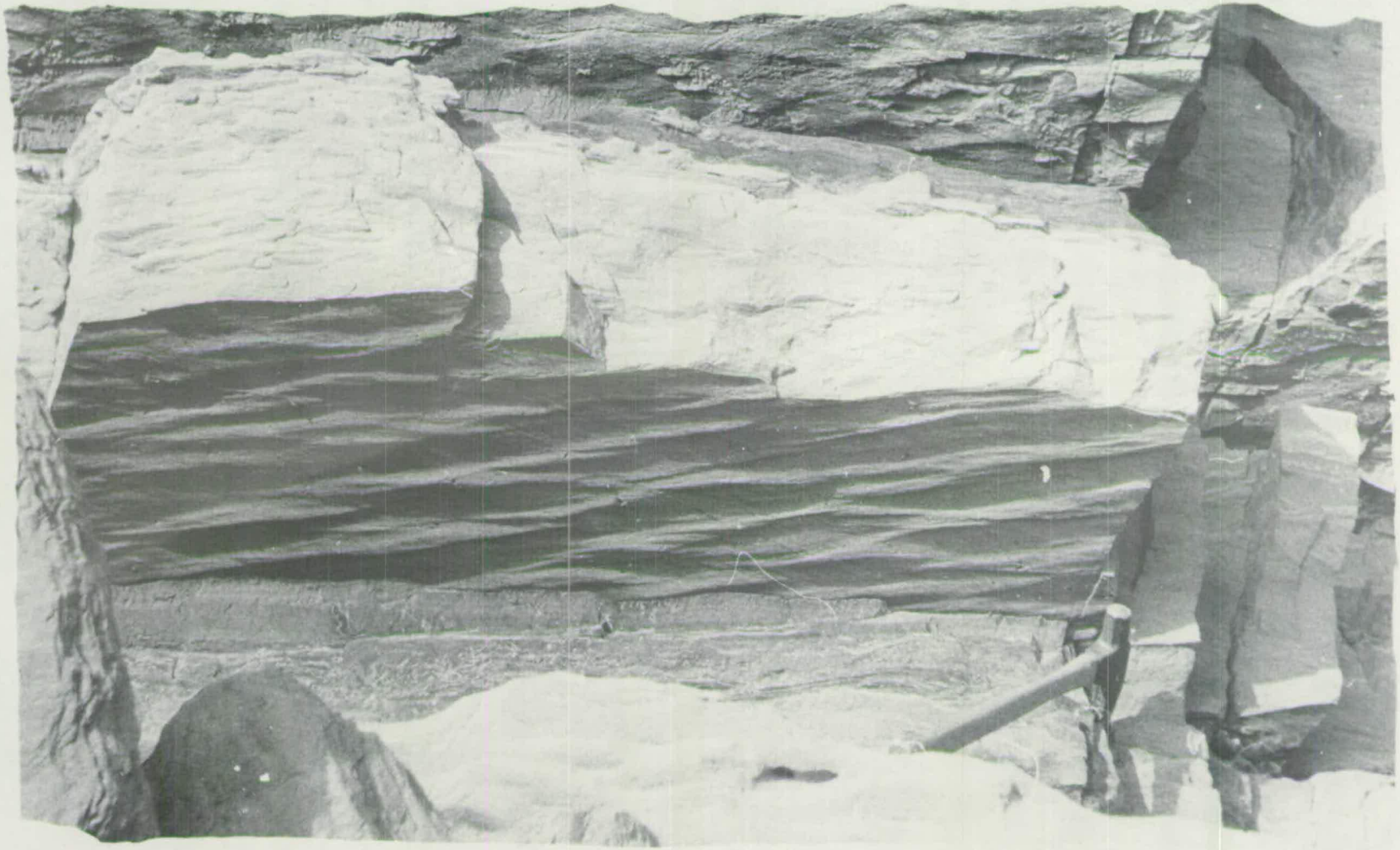

Plate 30. Longitudinal furrow and flute moulds laterally transitional to scaliform, non-oriented structures. Current from left to right (hammer length 35 cm.).

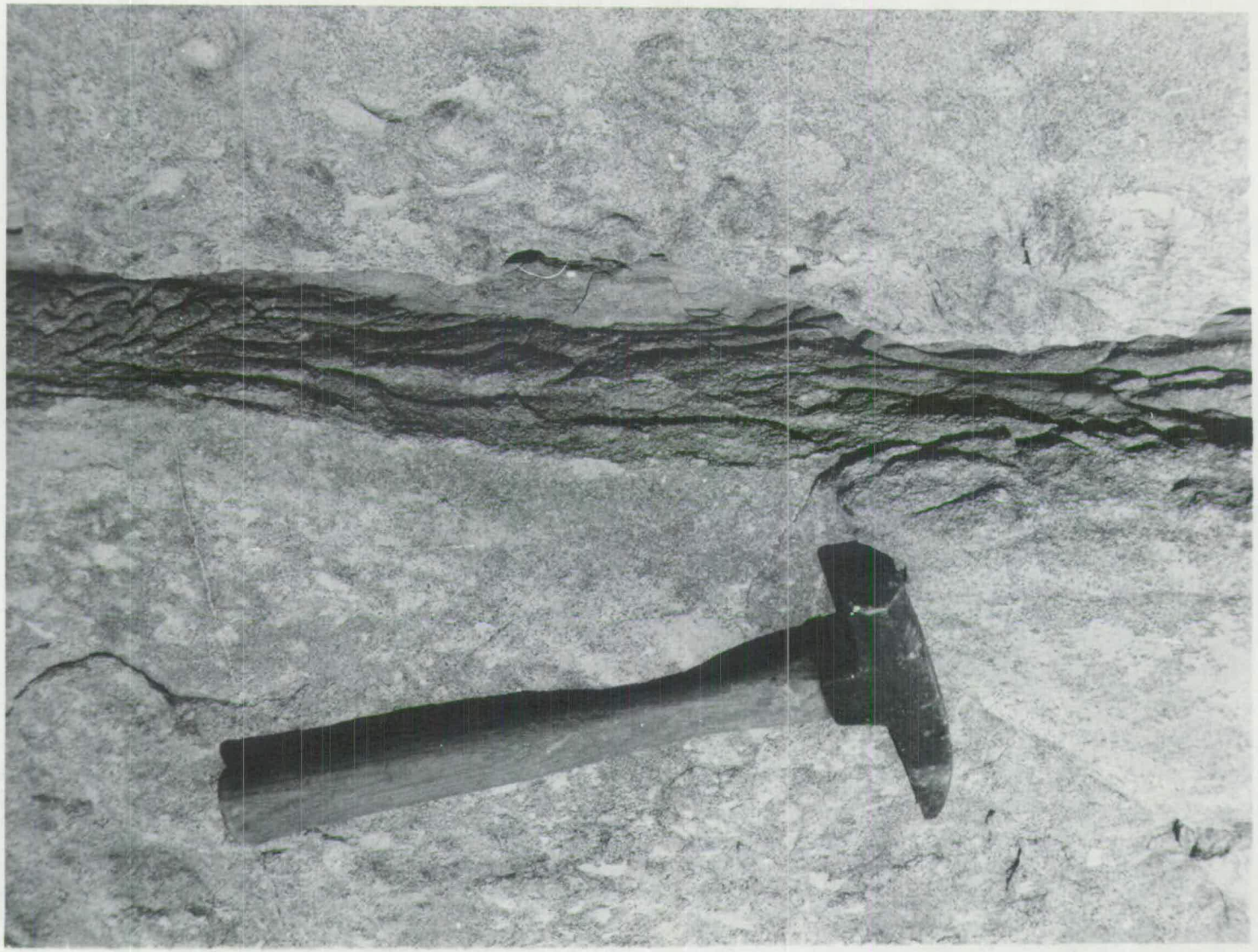

and in close proximity to the cross-laminae.

The internal flutes range from about 10 cm. to more than 100 cm. in length, and generally are notably larger than typical flute moulds on bed soles. Along a given parting surface, the flute marks tend to be approximately equal in size and uniformly distributed over the surface (Plate 32). They generally have tapered and closed down-current ends, in contrast to the flaring shape of many sole flutes.

(c) Channels

Channels (Dzulynski and Walton 1965, p. 87) within and protruding from the base of sandstone beds are evident in many large outcrops (Plates 33 and 34).

Primary Deformation Structures

Load Structures

(a) Description

Load structures, varying from slight bulges several cm. across to large, irregular protruberances several meters in length and depth, occur at the base of many beds (Plates 35 to 39 are representative examples). Flame structures (Walton 1956) generally occur in intimate association with the load structures.

Pseudonodules (ball-and-pillow structures)commonly occur

Plate 33. Cross-section exposure of channel mould. The outcrop consists mainly of sandstone in the upper half and slate in the lower half. The mould extends about 5 meters below the main part of the base of the sandstone bed in which it occurs (west shore of Wolf Island, 1 kilometer southwest of thesis area).

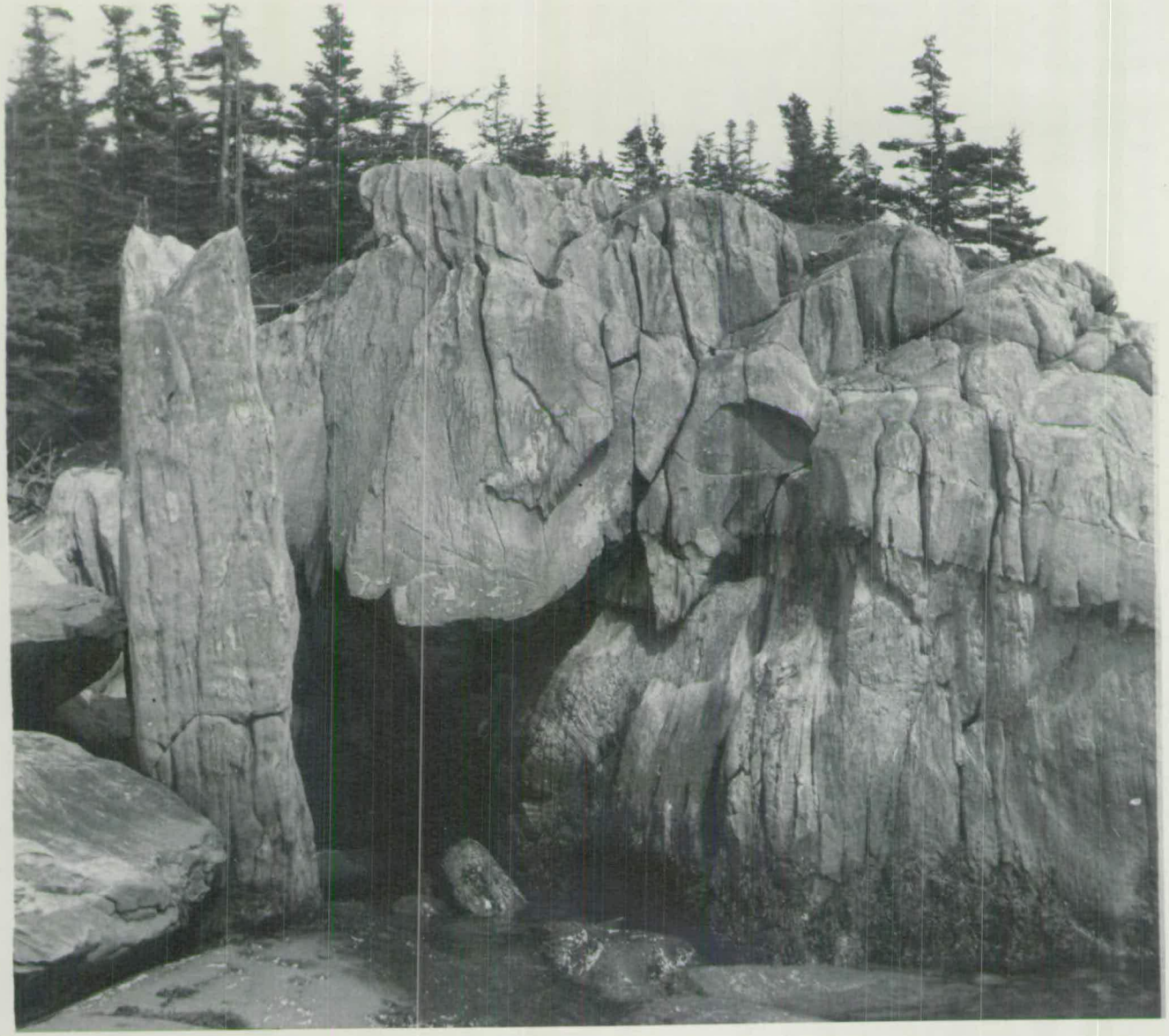

Plate 34. Longitudinal-section exposure of channel mould.
The channel effects amalgamation with the underlying
sandstone bed.

Plate 36. Load mould at base of sandstone bed (hammer length 35 cm.).

Plate 37. Load structures at base of sandstone bed.

Undeformed parallel lamination above load structures.

at the base of very fine sandstone and sandy siltstone beds overlying mudstone (Plate 38). Similar structures rarely occur at the base of very fine sandstone and sandy siltstone beds directly overlying fine sandstone (Plate 39).

(b) Interpretation

Undeformed laminae in beds with load structures at the base (Plate 37) suggest that the load structures formed during deposition of the bed. In other cases, the beds are deformed throughout, and the load-structures may have been formed following deposition.

Pseudonodules at the base of very fine sandstone and sandy siltstone beds directly overlying fine-grained sandstone are unusual features. Pseudonodules develop by virtue of the sediment above being more dense than the sediment into which the pseudonodules sink (Dzulynski and Walton 1965, p. 153). Their development in the case under consideration, therefore, is attributed to the original fine sand becoming temporarily quick due to foundering of the bed, earthquake shocks, or other causes, while the sandy siltstone remained sufficiently cohesive to sink into the quick sand as pseudonodules. Fine-grained sands are particularly susceptible to spontaneous liquefaction (Dzulynski and Walton 1965, p. 162), which may explain why the sandy silt remained sufficiently cohesive to form pseudonodules when the sand became quick.

Plate 38. Pseudonodules formed from thin beds of sandy siltstone overlying mudstone (in central part of photograph) (south end of Wolf Island, 1 kilometer southwest of thesis area).

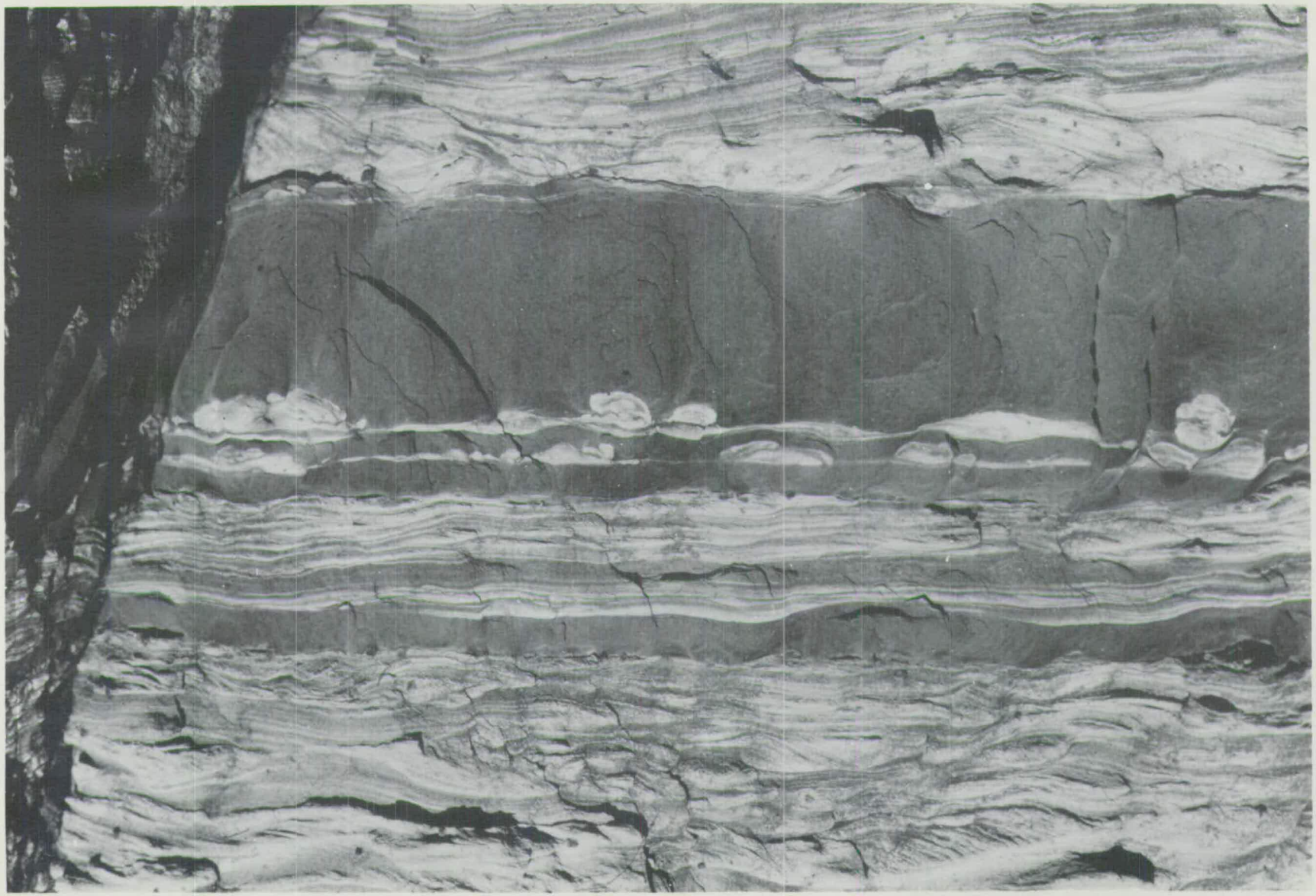

Primary Folds

(a) General Description

Primary folds and contortions occur in about 60 percent of the beds. The most commonly occurring variety is a unique type herein referred to as slurried bedding and described below under a separate heading. Primary folds other than those represented by slurried bedding occur in about 30 percent of the beds. Well developed primary folds, excluding slurried beds, are most prevalent in relatively thick beds (Plates 40 to 43 inclusive)and commonly occur above slide-marked surfaces.

(b) Slurried Bedding

(i) Description

Slurried bedding is characterized by highly contorted and somewhat diffuse laminae and injection dykes of arenaceous material intimately intermixed with argillaceous material (Plates 44 and 45). Wood and Smith (1958a, p. 173) described apparently comparable structures in the Aberystwyth Grits of Wales, which they referred to as 'slurried beds'.

The slurried bedding typically occurs as a graded division transitional from sandstone below to slate above. The grading of slurried divisions is partly obscured by their highly deformed state, but, in general, the proportion of argillaceous material increases upwards and the contorted laminae and injection dykes become more diffuse in the same direction.

The slurried beds shown in Plates 44 and 45 have relatively

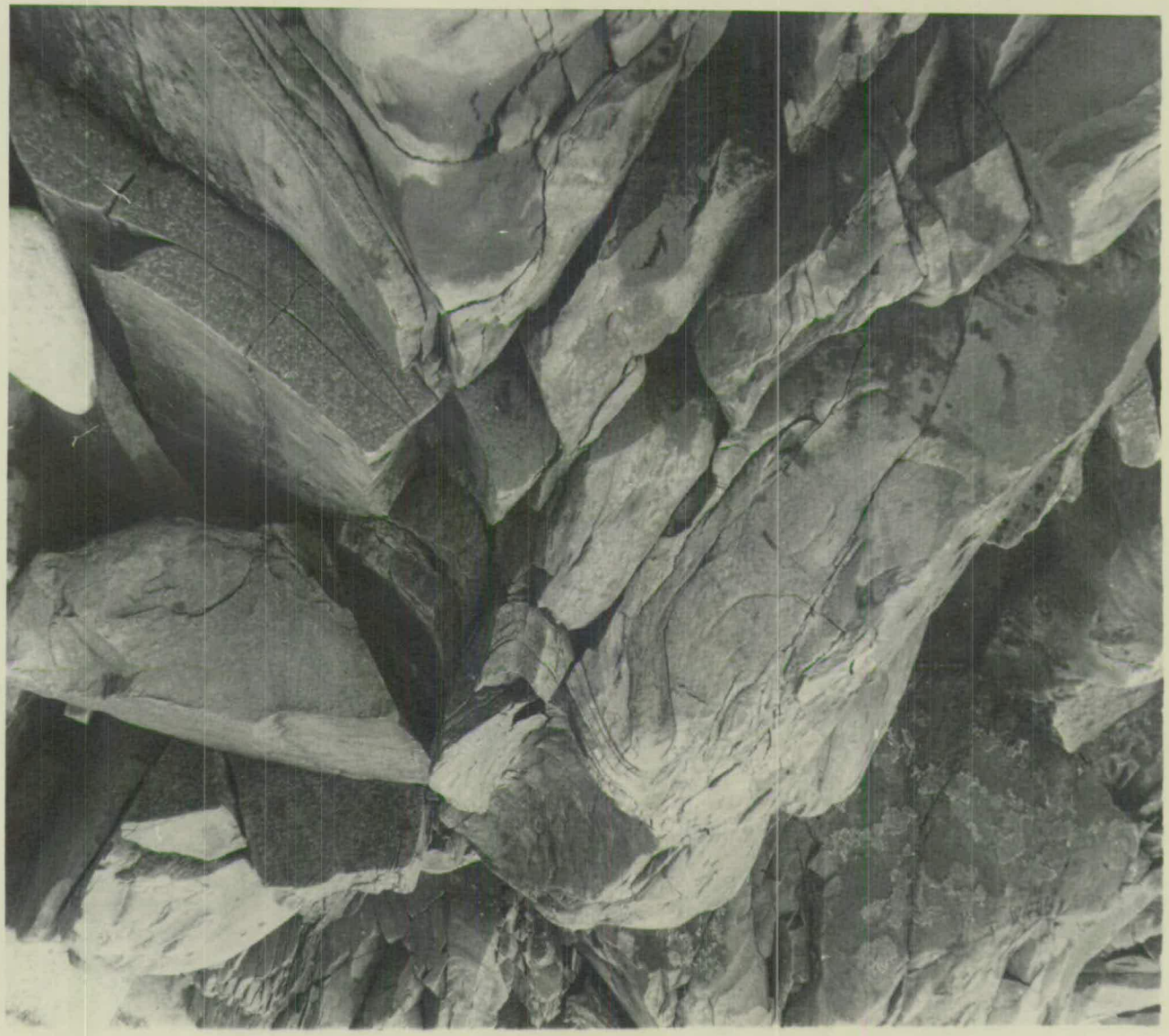

Plate 42. Slump-deformed bed with primary folds throughout. A folded bedding-surface beneath left foot of man.

Plate 44. Slurried bedding, consisting of deformed laminae, detachment bodies and injection dykes of sandstone interspersed in argillaceous material. Base of overlying sandstone bed in upper right of photograph; undeformed slate beneath the slurried bed (south end of Phoenix Island; hammer length 35 cm.).

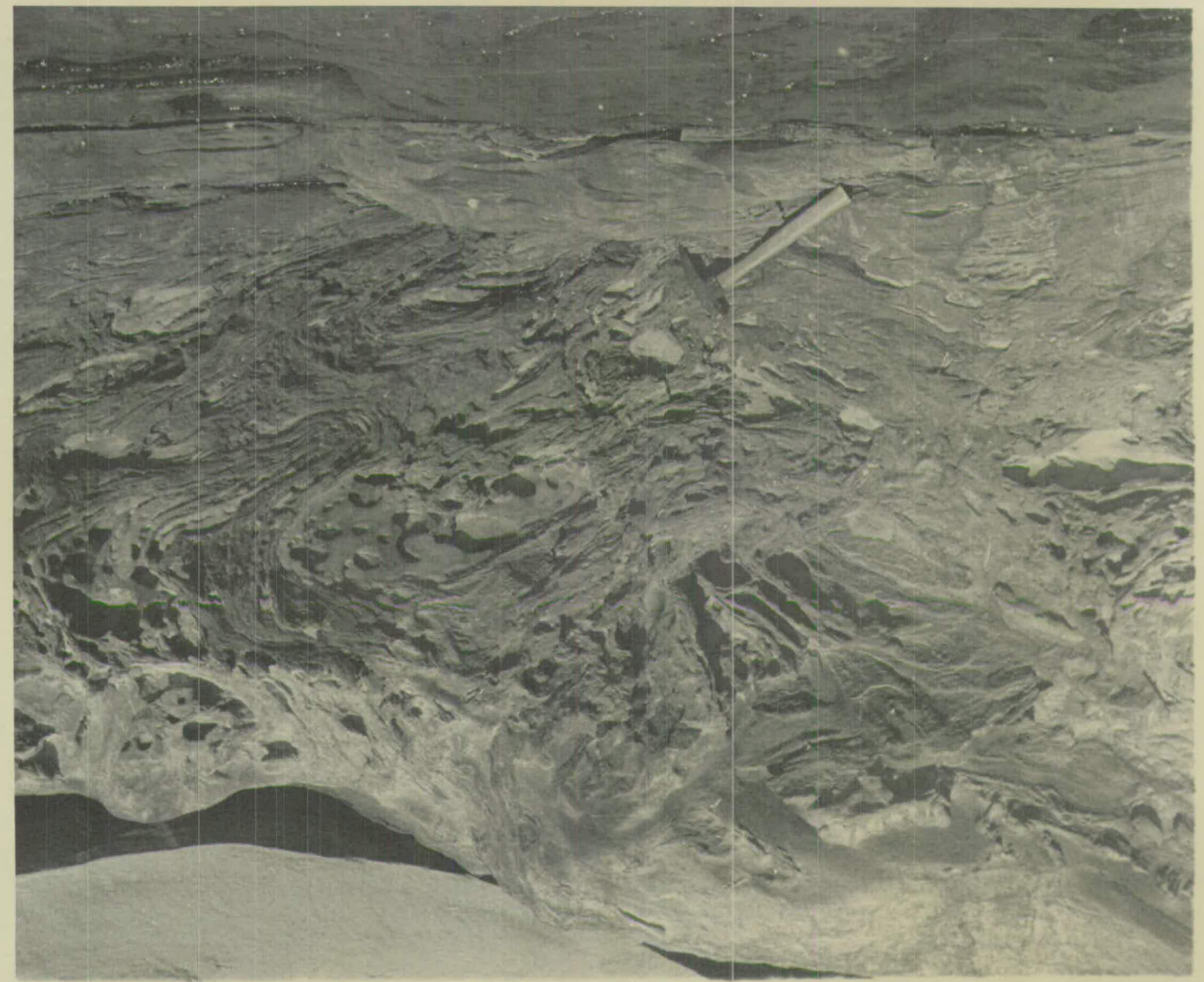

Plate 45. Slurried bed beneath undeformed sandstone and above undeformed slate (hammer length 35 cm.).

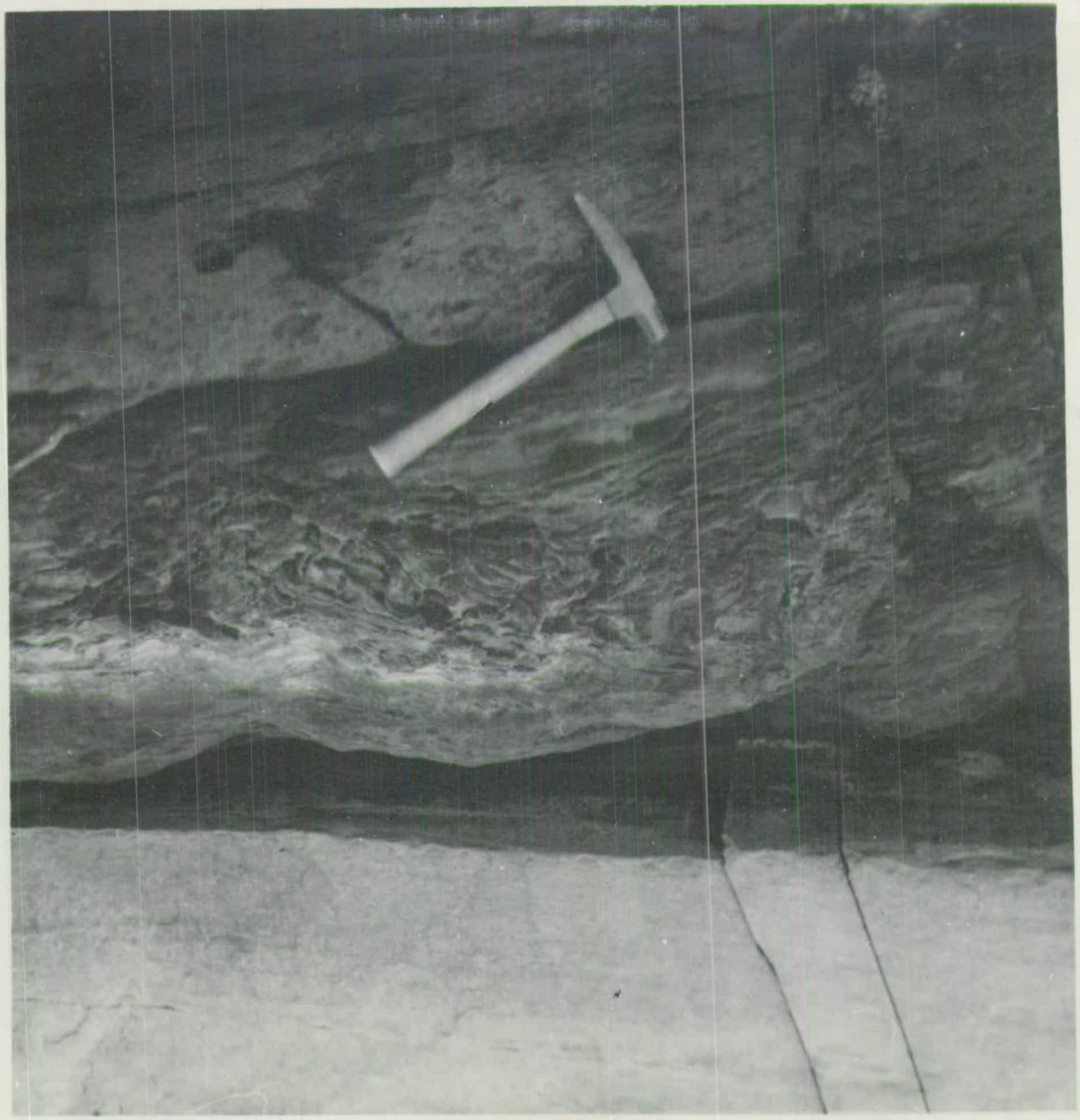

thin, unslurried, basal sandstone portions. In general, however, the basal sandstone portions are much thicker than the slurried divisions. Slurried divisions are rarely as thick as those shown in Plates 44 and 45; the average thickness is about 30 cm. Both the sandstone which occurs beneath slurried divisions and the overlying slate or sandstone are commonly undeformed.

(ii) Interpretation

Slurried bedding is associated with slide-markings on parting surfaces that occur at or near the top of sandstone beds (Plate 46). The slide-marked parting surfaces typically occur near the bottom of the graded part of beds with delayed grading. This suggests that the slurries formed by the slumping of relatively fine sediments over sand, incorporating some of the sand into the slurry during the process of slumping.

Convolute lamination is rare in the thesis area, although present in the Goldenville Formation in other areas (Schenk 1970). The paucity of convolute laminae may be due to a tendency for convolutions to have developed into slurries.

The slurries may have formed during or following deposition. In several observed cases, detached bodies of ripple cross-laminated and parallel-laminated argillaceous sediment are contained in the slurries. This suggests that in these cases the slurries formed after deposition.

Slump Breccia and Pull-Apart Structures

Slump breccia (Plate 47) and pull-apart structures (Plate 48)

Plate 46. Slide markings on upper bedding surface of sandstone bed. Slurried bedding (not shown in photograph) occurs immediately above the slide-marked surface. Transverse ripples with tectonically oversteepened crests (left side of picture) on another bedding surface.

Plate 47. Slump breccia, consisting of detached bodies of conglomeratic sandstone enclosed in an argillaceous (slate) matrix (south side of Outer Island).

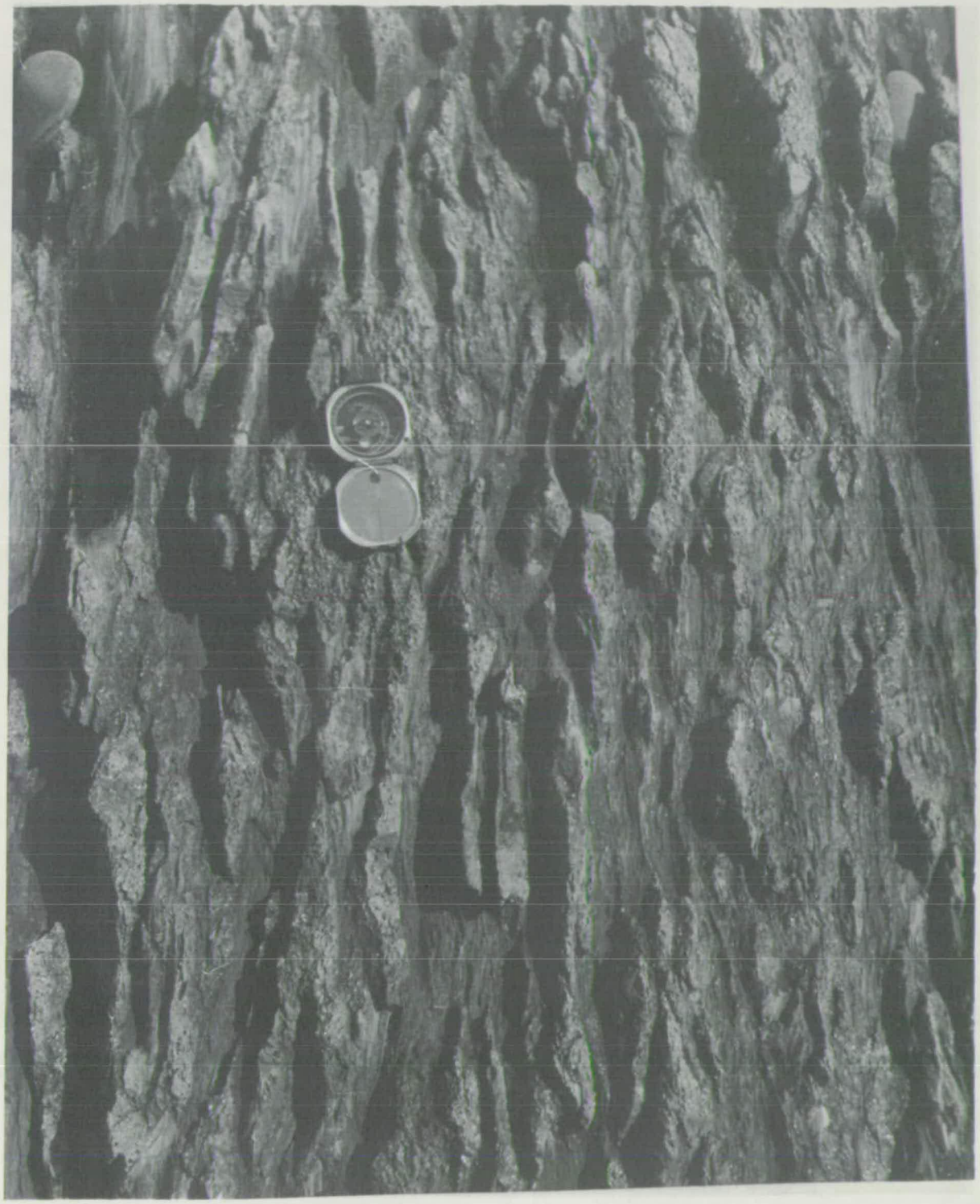

Plate 48. Pull-apart structure represented by discontinuous sandstone bed below hammer (east side of Stony Island; hammer length 35 cm.).

are uncommon (about ten examples of each observed in the thesis area). Slump breccia zones tend to persist laterally parallel to bedding for distances in excess of a kilometer, thereby providing useful marker horizons for detailed correlations.

Liquefaction and Biogenic Structures

Sand Mounds

(a) Description

Sand mounds (Plates 49 and 50) occur on the upper bedding surfaces of approximately 30 percent of the sandstone beds. They have an average diameter of about 10 cm. and a maximum observed diameter of 60 cm. Each sand mound has a central depression which is the surface expression of a vent that extends, generally many centimeters, into the sandstone below. The vents are sub-cylindrical cores or pipes consisting of relatively matrix-free sandstone, commonly impregnated with calcite cement.

External, radial grooves occur on many of the sand mounds (Plate 49), a product of discrete sand flows down the sides of the developing mounds, analagous to lava flows down the sides of volcanic cones.

Tiny sand mounds (Plate 51) dot the upper bedding-surface of some sandstone beds, and rarely occur in the same beds with larger sand mounds.

(b) Origin

The sand mounds may be biogenic structures or they may be

Plate 50. Upper bedding-surface of sandstone bed with abundant sand mounds.

Plate 51. Small sand mounds (? pit and mound structures) on upper bedding-surface of sandstone bed.

sand volcanoes (Rettger 1935; Gill and Kuenen 1957; *Warren 1963) formed by the liquefaction and intrusion of water-laden sand close to the surface of deposition. The matrix-free core-sand suggests the action of upwelling water in the vents during formation of the sand mounds. This is not diagnostic of origin, however, as both biogenic and liquefaction processes are capable of producing vigorous upwelling currents (Kuenen 1968; Shinn 1968).

The small sand mounds shown in Plate 51 may have formed as tiny sand volcanoes, or as pit and mound structures from escaping gas bubbles (Shrock 1948; p. 132-6), or as the discharge heaps of sand-dwelling organisms.

Probable sand mounds in the Goldenville Formation have been described by previous workers as a trace fossil (Astropolithon hindii, Dawson 1890).

(c) Allied Structures

Sub-vertical sand pipes that extend beneath the sand mounds are commonly exposed on outcrop surfaces at large angles to the bedding. These structures are described and interpreted in the following sub-section.

Low mounds with radial plate-like structures extending outwards from a central aperture occur on the upper bedding-surface of a single sandstone bed at Taylor Head (Plate 52). These may represent collapsed sand mounds that developed radial 'fracture'

---

* The examples described by Warren have internal structures suggestive of organic origin (E.K. Walton, pers. commun., 1971).

Plate 52. Oval structures with radial, plate-like grooves about a central aperture.

partings during collapse. On the other hand, they may have been formed by organisms in some manner unrelated to the development of sand mounds, as, for example, by a tube-dwelling animal that probed the sediment round about its tube in a systematic, radial pattern in search of food ('programmed feeding', Seilacher 1967).

Small protrusions dot the base of some sandstone beds (Plate 53). These structures are probably moulds that formed in the apertures of vents developed in the underlying mud either by organisms or by escaping water or gas.

Sand Pipes

(a) Description

Sand pipes (Plates 54 and 55) occur in about 35 percent of the sandstone beds. They are commonly associated with sand mounds, but are also prolific in beds without sand mounds. The sandstone in the pipes generally contains less matrix than the enclosing sandstone. Because of this, welding by pressure solution of the constituent quartz and other framework grains is more advanced than in the enclosing sandstone, with the result that the pipes stand out in outcrop as slightly raised ridges.

The pipes are sub-cylindrical tubes that tend to be straight-sided in their upper portions, but become branched and diffuse downwards. The pipes are about 0·75 cm. in diameter, on average, and generally do not exceed 2 cm. in diameter, although very large pipes (maximum observed diameter 6 cm.) are rarely present. The pipes are commonly associated with slump-deformed bedding.

Plate 53. Small protrusions at base of sandstone bed.
Possibly developed as moulds in the apertures of
vents in the underlying mud.

Plate 54. Sand pipes in dip-section exposure of sandstone bed. Apparent tilting of the pipes towards the bedding is a tectonic effect (hammer length 30 cm.).

(b) Interpretation

Most of the pipes probably formed as a result of liquefaction processes closely allied to those which produced the sand volcanoes. Some may have formed by 'settling convection' in a dense suspension of sediment during the final phase of deposition (Kuenen 1968). Many are post-depositional structures. The pipes illustrated in Plate 55, for example, clearly formed subsequent to slump-deformation of the bedding.

A proportion of the pipes may be biogenic structures, particularly those that are unbranched over their exposed length (up to 75 cm.)(Hallam and Swett 1966). Such pipes have the general appearance of Skolithus (Scolithus, Tigillites) tubes (Lessertisseur 1955, Fig. 34; Häntzschel 1962; Fig. 134), and were so named by Taylor (1967) in the southwestern part of the Meguma region.

Sheet Structures

(a) Description

Vertical and subvertical sheet-like structures (Plate 56) occur in about 15 percent of the sandstone beds. On weathered parting surfaces parallel to bedding, the sheets occur as swarms of slightly raised ridges that individually trace a wavy path over the bedding surface. In section, the sheets are sinuous, sub-parallel features that generally fork into two or more branches in their lower extremities. They vary in width from 1 to 5 cm. and in height from 4 to 50 cm. The sandstone within the sheets contains

Plate 56. Sheet structures displayed in rock slab derived from sandstone bed. The structures occur as undulous, anastomosing and slightly raised ridges on the weathered (upper) parting surface, and as sinuous sub-parallel ridges with commonly branching terminations on the joint surface.

less matrix than that without, and calcite cement is commonly present. In slump-deformed beds, the sheets are deformed along with the bedding, in contrast to the sand pipes which commonly occur as undeformed features in such beds.

(b) Interpretation

Identical structures have been observed in the Aberystwyth Grits of Wales (Wood and Smith 1958b) and in a Silurian turbidite sequence in northeast Galway, Eire (Laird 1970). Wood and Smith considered that the structures were produced by earthquakes or early tectonic movements which disturbed the packing of the grains and caused injection of water-laden sediment from below into relatively water-free sediment above, a process they called 'auto-injection'. Laird found that the sheet structures tend to occur parallel to the sedimentary grain fabric (i.e., the sheets occur parallel to paleocurrent directions), and, by analogy with 'settling convection' structures produced experimentally by Kuenen (1968), he interpreted the sheets as features formed during the last stage of deposition of the sediment, and therefore related to the direction of paleocurrent movement of the sediment as it came to rest. I accept Laird's (1970) interpretation.

In the Goldenville Formation, the sheet structures commonly occur as stratiform layers within a sandstone bed (Plate 57). This characteristic may have resulted from pulsations of the depositional current during one episode of sedimentation, or it may reflect a succession of separate sedimentation episodes.

Plate 57. Sheet structures in sandstone occurring in layers separated by structureless sandstone (hammer length 35 cm.).

In the rocks observed by Laird (1970), the sheet structures are restricted to sediments with an average grain-size greater than 0·5 mm. The minimum average grain-size of sandstone in the Goldenville Formation in which these structures occur is estimated at 0·2 mm.

Sand Injection Dykes and Sills

Sand injection dykes and sills (Dzulynski and Walton 1965, p. 159-162) are developed in about 15 percent of the beds.

Trace Fossils

(a) Description

Trace fossils in the Goldenville Formation, excluding sand mounds and sand pipes, are uncommon. They are represented mainly by the trails of organisms at the base of sandstone beds (Plates 58, 59, 60).

(b) Interpretation

Bottom-surface markings comparable to those shown in Plates 58, 59 and 60 have been interpreted in other flysch sequences as the moulds of trails or burrows that have been buried rapidly by a sudden inrush of sandy sediment, or as burrows of animals that travelled downwards through the sand in quest of organic-rich mud and, having arrived, then foraged more or less horizontally (Crowell 1955; Kuenen 1957; Seilacher 1962).

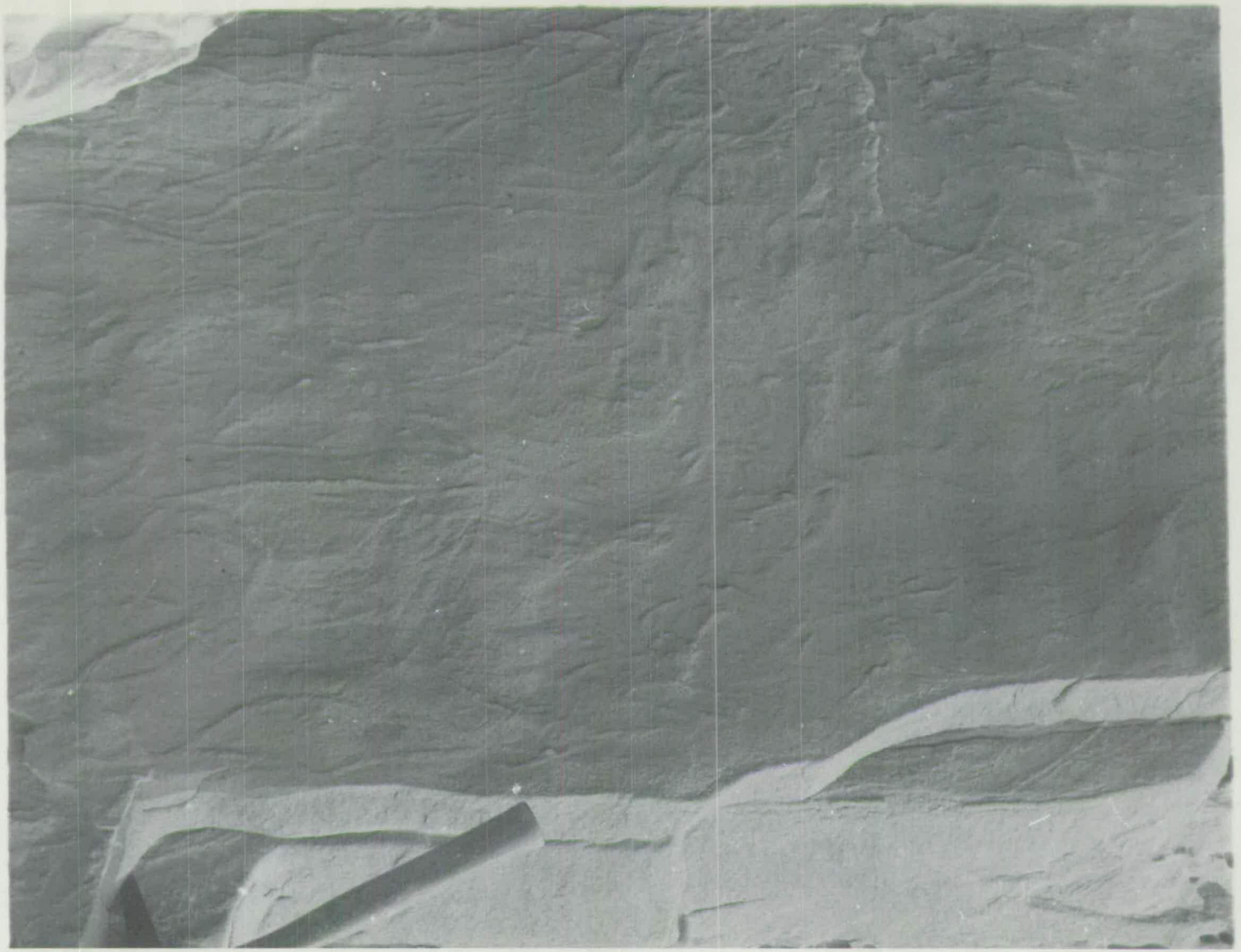

Plate 59. Mould of winding, organic trail on base of sandstone bed.

Plate 60. Organic trails on sandstone sole.

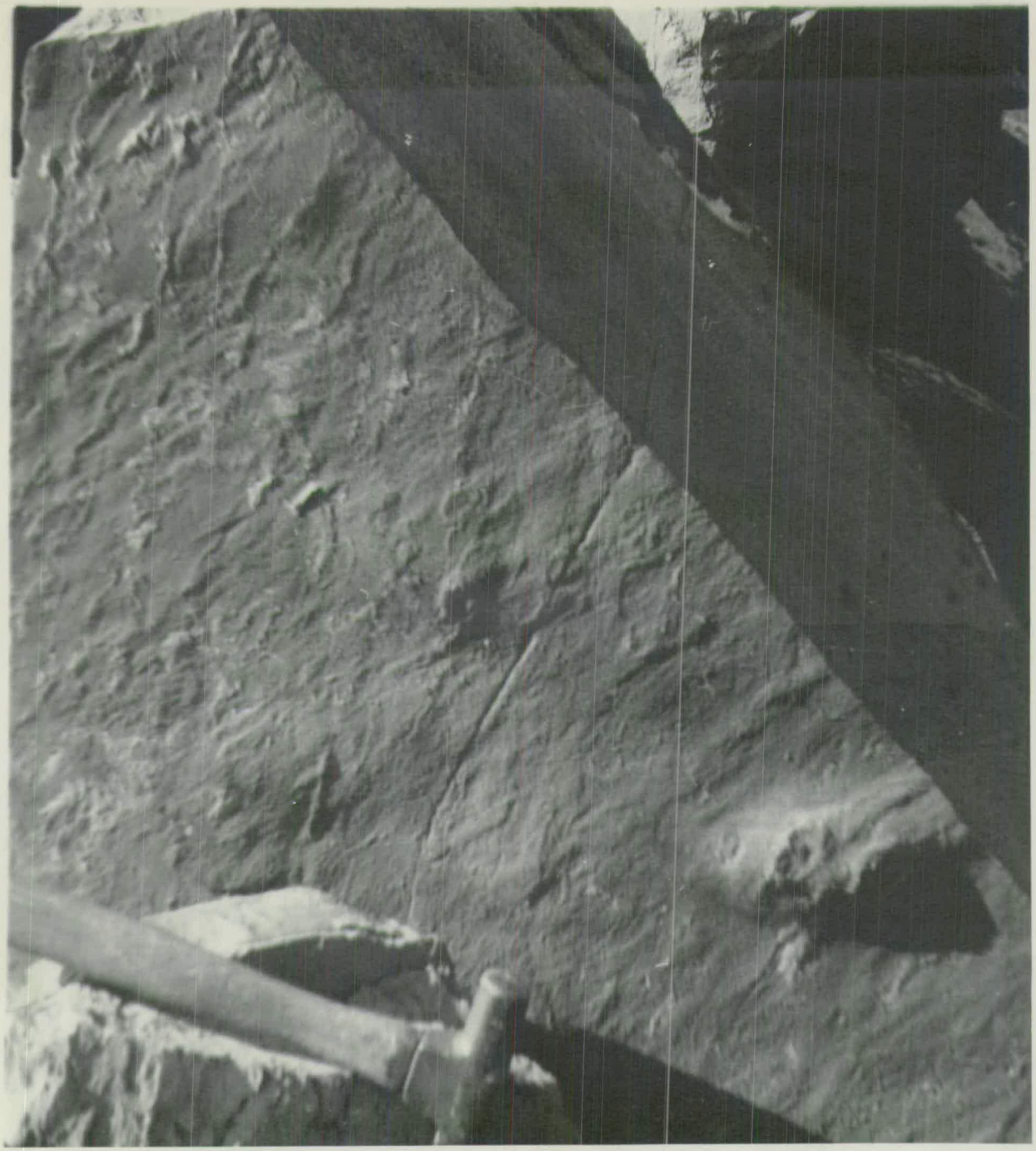

(c) Previous Accounts

Previous workers have provided lengthy and rather unclear descriptions of trace fossils in the Meguma Group. The previous descriptions have centered chiefly on the trace fossil Astropolithon hindii, on which conflicting interpretations have been given. A summary of the previous accounts is provided in Appendix 5.

R-Mode Association Analysis

An R-mode association analysis of sedimentary properties observed in a representative succession of 231 cycles (a cycle consists of a sandstone bed below and a slate band above) is given in Table 6. The observations were taken at Section 3. The analysis is a measure of the degree to which the listed sedimentary properties tend to be associated.

The table is based on a chi-square test of two-by-two contingency tables which were compiled using presence-absence criteria. The chi-square values are converted to probability values by the formulas given by Abramowitz and Stegun (1964, p. 262). The associations are listed in columns headed by these probability values. Positive association is indicated when two species are found to occur together more frequently than expected under an assumption of independence. Negative association is indicated when two species occur together less frequently than expected. A high level of association is signified by probability values close to 1·000. Associations at probability values below 0·95 may be regarded as random, and are not included in the table.

Groove(Int)	=	Internal groove markings
Groove(base)	=	Under-surface groove markings
Flute	=	Under-surface flute moulds
Flute X-bed	=	cross-laminae associated with internal flutes
Slurry	=	slurried bedding
// lams(base)	=	parallel laminations within 25 cm. of base
// lams(mid)	=	parallel lamination more than 25 cm. above base
Rip-up	=	mudflake inclusions
Rip-up(lg)	=	mudflake inclusions longer than 1 meter
Amalgamated	=	amalgamated bedding
Collapse	=	all structures indicative of foundering, other than load structures and slurried bedding
Load	=	load structures
Slide(top)	=	slide markings on upper surface of sandstone bed
Sand Pipes	=	sand pipes
Sand Mounds	=	sand mounds
Sheet Strs	=	sheet structures
Ave(med)	=	average grain-size of framework grains about 0·40 mm.
Ave(med/fi)	=	average grain-size of framework grains about 0·25 mm.
Ave(fi)	=	average grain-size of framework grains about 0·17 mm.
Ave(fi/v.fi)	=	average grain-size of framework grains about 0·12 mm.
Max(v.co)	=	maximum grain-size of framework grains 1·00 mm. or more
Max(med)	=	maximum grain-size of framework grains about 0·40 mm.

TABLE 6. R-Mode Association Analysis of Sedimentary Structures in 231 Sedimentation Cycles (Sandstone bed plus overlying slate band). The degree of association between structures listed in the left-hand column and those in the remaining columns is given by probability values ranging from 1·000 (association at high level of significance) to 0·950 (nearly random associations). Negative associations are underlined, positive associations are not. Bracketed figures indicate the percentage of cycles in which each structure occurs.

	0·999 to 1·000	0·995 to 0·999	0·985 to 0·995	0·950 to 0·985
Groove(Int) (18)		// lams(base)	Sand Mounds	Ave(med/fi) Collapse Sand Pipes Groove(base)
Flute (14)				Ave(med) Max(v.co)
Slurry (43)	Slide(top)		Max(v.co)	Ave(fi) Ave(med) Amalgamated Sand Mounds Sheet Strs
// Lams(base) (32)	// lams(mid)	Groove(base) Groove(int) Collapse Sand Pipes Max(med)	Ave(med/fi) Sand Mounds	Ave(fi/v.fi)
// Lams(mid) (13)	// lams(base) Sheet Strs	Flute X-bed	Ave(med/fi) Max(v.co)	Collapse Max(med)
Flute X-bed (16)	Max(v.co)	Ave(med/fi) // lams(mid)	Rip-up(lg) Collapse Sand Mounds	Ave(med) Sheet Strs // lams(base)
Rip-up(lg) (10)	Rip-up	Sand Mounds	Flute X-bed	Ave(med)
Rip-up (49)	Rip-up(lg)		Sand Pipes	
Amalgamated (14)			Ave(med) Ave(fi)	Max(v.co) Slurry Sand Mounds

Collapse (38)	Load	Ave(med/fi)
		// lams(base)
		Sand Pipes
			Max(v.co)
			Flute X-bed
			Ave(fi/v.fi)
				Groove(Int)
				// lams(mid)
				Max(med)

Load (16)	Collapse			Groove(base)
Slide(top) (26)	Slurry		Max(co)	Ave(fi) Ave(med) Max(v.co)
Sand Pipes (34)	Sand Mounds	Max(v.co) // lams(base) Collapse	Ave(med/fi) Rip-up	Groove(Int) Ave(fi/v.fi) Max(med)
Sand Mounds (29)	Sand Pipes	Ave(med/fi) Rip-up(lg) Sheet Strs Max(med)	Max(v.co) Groove(Int) // lams(base) Flute X-bed	Ave(fi/v.fi) Slurry Amalgamated
Sheet Strs (18)	// lams(mid)	Max(v.co) Ave(med/fi) Collapse Sand Mounds	Max(med)	Flute X-bed Slurry

PART III - GEOLOGICAL HISTORY

CHAPTER 6 - BASIN ANALYSIS

Introduction

The local, detailed study of the Goldenville Formation is part of a larger programme, initiated by Dr. P.E. Schenk, to assess the sedimentology and geological history of the Meguma geosynclinal succession. Schenk (1970) has described and interpreted the results of a reconnaissance to establish regional trends in sedimentary structures, textures and composition in the rocks of the Meguma Group. Schenk's method of study and his conclusions are reviewed below prior to a discussion of the sedimentation of the Goldenville Formation based solely on the present, local study. The limitations of both the regional and local studies are considered. Combining the regional and local findings, an analysis of the sedimentation in the basin is presented.

Interpretation Based on Regional Investigation

(a) Method and Results of Study

Schenk's (1970) interpretation of Meguma sedimentation is based on plots of moving-averages for directional properties (Pelletier 1958) and polynomial trend-surfaces (Krumbein and Graybill 1965) for all other sedimentary properties measured at selected outcrops nearest to intersection points of a five-kilometer grid placed over the entire Meguma region. The moving-average analyses indicate that the paleocurrent trend is axial and arcuate, describing an almost right-angle change in direction from the southwestern to northeastern parts of the Meguma region. Current

elongated approximately parallel to the paleocurrent trend, and the resulting trends may be appreciably distorted because of this.

Schenk's (1970) investigation was concerned only with assessing sedimentary features; an assessment of structural (tectonic) influences was not attempted.

Interpretations Based on Local Study

(a) Nature of Sedimentation

The mean direction of current lineations on the soles of sandstone beds is parallel to the mean direction of slide markings (see Table 1). This indicates that the currents that produced the lineations moved down-slope, and therefore were probably gravity-impelled turbidity currents.*

Ripple-mark on upper bedding-surfaces of sandstone beds indicates current action generally at large angles to the mean direction of turbidity currents. Ripple cross-lamination suggests that the direction of current movement was approximately northwards. This suggests reworking of the fine sediment by transverse, indigenous bottom currents.

Slurried beds, pseudonodules of siltstone in sandstone, sand mounds, sand pipes and vertical sheet structures reflect a tendency for the deposition of loosely packed, water-laden sand which yielded readily to slump and liquefaction. The reason or reasons that these structures are abundant in the rocks of the Goldenville Formation but rare in other flysch sequences is not known. The fact that the Goldenville sandstone is predominantly fine-grained may be part of the answer; sediment of this grain-size is

* This observation is discussed in Appendix 6 in connection with previous, conflicting interpretations on the interrelationship of slopes, slumps and depositional currents in flysch basins.

particularly susceptible to spontaneous liquefaction (Dzulynski and Walton 1965).

Deposition from turbidity currents with high concentrations of suspended sediment may have been a factor as well. High concentration tends to lead to rapid deposition with a consequent development of 'quick' sand (Middleton 1967) in which liquefaction structures might readily form. High concentrations also tend to maintain high velocities in the turbidity currents. Compound stratification, amalgamated bedding, channels, internal flute markings and very large mudflake inclusions indicate that turbidity currents with above-average velocities (relative to turbidity currents in general associated with the deposition of fine-grained sand) may have been common during the sedimentation of the Goldenville Formation. Rapid accumulation of beds may also have contributed to unstable conditions favouring the development of slump and liquefaction structures.

(b) Relationship of Fold Pattern to Sediment Distribution

Folds parallel the mean turbidity paleocurrent trend. In Chapter 3, it is hypothesized that sedimentary structures, particularly the large-scale arrangement of beds, determined the initial orientation of the folds, whereupon both the folds and the paleocurrent trend were rotated into a stable tectonic position. The amount of horizontal rotation involved is not known.

Fig. 8. Hypothetical model of sedimentation in the Meguma Geosyncline.

A. **Initial** accumulation of flysch **sediments** on an early Paleozoic **continental** rise (birth of the **Goldenville** Formation)

B. Turbidity currents travel down submarine canyon, then along fan-channel before spreading out on the slope of principal turbidite deposition. Fine sediments accumulate on either side of the fan-channels (birth of the Halifax Formation). The turbidites prograde seawards

C. Depositional basin fills to shelf edge. Shelf then moves progressively seawards, along with continental rise. Paralic deposits prograde out over the shelf.

D. Persistence of the sedimentation pattern and continued progradation results in a diachronous sequence of **Goldenville** sandstone, Halifax **shale**, and conformably overlying **paralic deposits**.

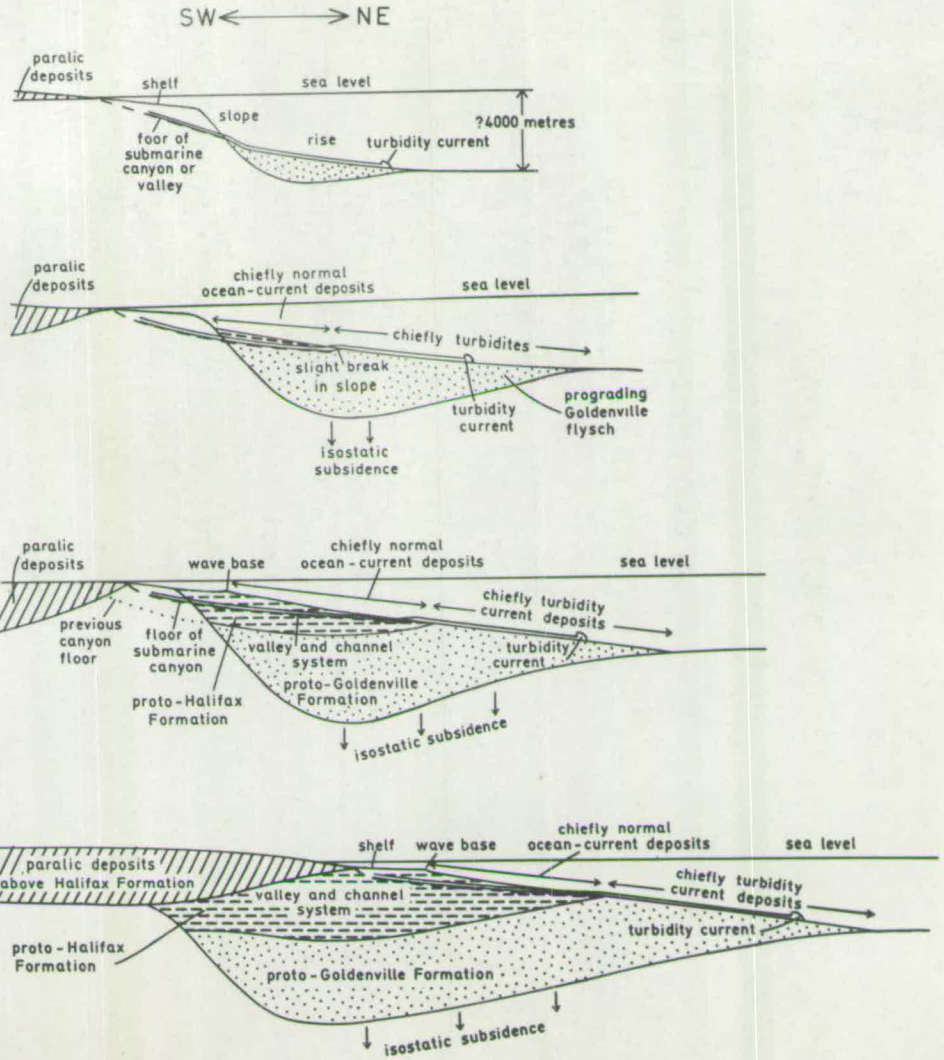

that the change in sedimentation from sandy flysch to predominantly argillaceous deposits and finally paralic deposits may have been tectonically controlled.

(b) Dispersal and Provenance

Moving averages of paleocurrent data indicate that the dispersal of the Goldenville Formation is everywhere longitudinal. Indications of lateral supply by trend-surface analyses are herein discounted for reasons cited above. The longitudinal dispersal pattern is arcuate in trace due to tectonic effects (horizontal rotation of folds).

The dispersal (paleocurrent) trend, together with the fold pattern, is broadly parallel to the southwest/northeast structural trend that pervades the northeastern Appalachian geological province. This suggests that the Meguma basin may have occupied a trough or trench parallel to the geosynclinal axis and the early Paleozoic continental margin. Conversely the lack of paleocurrent evidence of lateral sediment supply suggests possible progradation outwards at a large angle to the continental margin. In this event, the present axial alignment of the Meguma dispersal pattern may be explained by assuming that the early Paleozoic continental margin in the region of the Meguma basin was at a large angle to the axis of the geosyncline, or that horizontal rotation of folds was exceptionally large.

The paleocurrent trend in the southwestern part of the Meguma region suggests that the source of sediment was from the south.

Paleocurrent studies in other areas indicate that the great bulk of sediment which filled the central and northern Appalachian Geosyncline came from the southeast (Pettijohn 1960). Furthermore, the large volume and petrographic character of this sediment, including that of the Meguma Group, makes an island arc derivation rather unlikely. According to recent theories of continental drift and lithosphere-plate tectonics (Wilson 1966, Bird and Dewey 1970) the source of sediment supply for much of the Appalachian Geosyncline was the lower Paleozoic Afro-European landmass.

APPENDIX 1 - Diagrammatic Representation of Internal Strain

Fig. 9 schematically depicts deformed sedimentary structures and quartz and chlorite-filled pressure fringes around pyrite crystals in rocks on the southeast limb of the Sober Island syncline. The diagram is based on observations at Sections 1 to 5 inclusive, where the average dip of the beds is 48 degrees northwest. The axial plane of the Sober Island syncline dips at about 80 degrees towards the northwest, as shown.

The pressure fringes bordering the pyrite crystal at X indicate extension approximately parallel to aa', probably accompanied by an element of rotational strain. The pyrite crystal itself is slightly flattened, suggesting shortening along cc'. The pressure fringes bordering the pyrite crystal pictured in the vent of the sand mound (Y) indicates extension parallel to bb', to a lesser extent than the extension along aa' indicated at X. The pyrite crystal at Z has larger pressure fringes than the crystal at X. This is explained by the observation that the cleavage is not parallel to the axial plane; rotation of the cleavage away from the axial surface, due chiefly to differential compression of the slate relative to the sandstone, probably accounts for the apparent additional extension.

The sand mound, flute cast, channel cast and ripple cross-laminations are deformed as described in the text (see above). The sand mound forms an ellipse in the bedding plane with a short axis/long axis ratio of 0·67. The trace of the sand

Fig. 9. Schematic representation of tectonically deformed sedimentary structures in rocks in the southeast limb of the Sober Island syncline. Notations and meaning of the diagram explained in text.

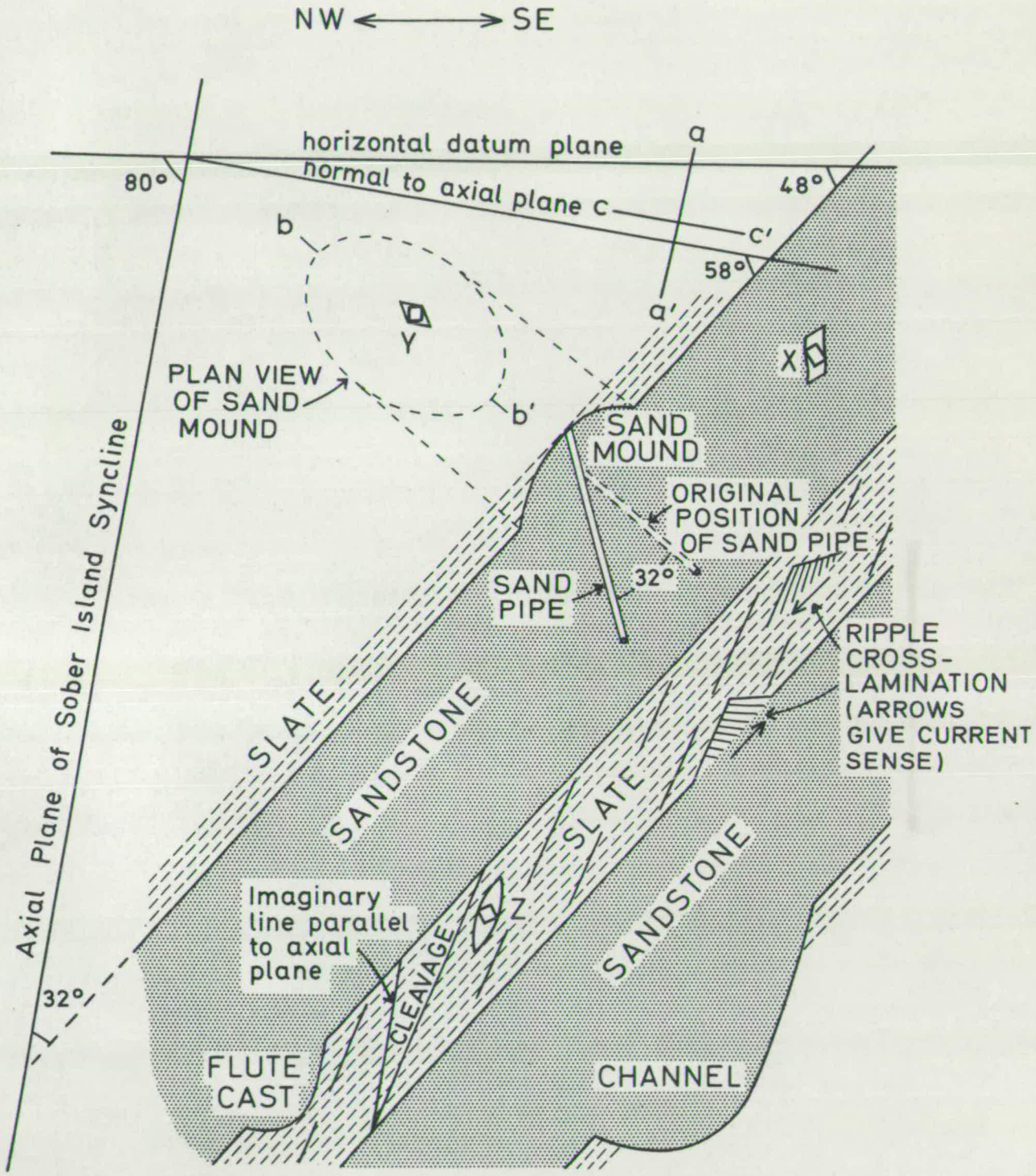
NW ⟷ SE
horizontal datum plane
normal to axial plane c
a
a'
b
b'
c'
80°
48°
58°
32°
32°
Y
X
Z
PLAN VIEW OF SAND MOUND
SAND MOUND
ORIGINAL POSITION OF SAND PIPE
SAND PIPE
RIPPLE CROSS-LAMINATION (ARROWS GIVE CURRENT SENSE)
Axial Plane of Sober Island Syncline
SLATE
SANDSTONE
SLATE
SANDSTONE
Imaginary line parallel to axial plane
CLEAVAGE
FLUTE CAST
CHANNEL

mound in the plane of maximum and intermediate principal strains (the bc plane) is an ellipse with a short axis/long axis ratio of 0·36 (this ellipse not shown in the diagram). The Scolithus-like sand pipe beneath the sand mound has been rotated approximately 32 degrees from its original position, relative to the bedding.

APPENDIX 2 - Vector Summation

Vector summation was used to estimate the mean and dispersion of ten sets of orientation data (Chapter 3, Table 1). The method of calculation employed is as follows: Each set of data indicated by columns 1 and 2 in Table 1 were first grouped into 9 class intervals of 20° each, extending from 0° to 180° (Fig. 8A). Krumbein's (1939) method of "doubling the angles" was followed in the calculation of the trigonometric moments listed in columns 3, 4 and 5 of Table 1. These calculations, for grouped data and doubled azimuth angles, are

$$X = \sum_{i=1}^{n} n_i \cos 2\theta_i$$

$$Y = \sum_{i=1}^{n} n_i \sin 2\theta_i$$

$$\bar{\theta} = \tfrac{1}{2} \arctan \frac{Y}{X}$$

$$r = \frac{\sqrt{X^2 + Y^2}}{n}$$

$$r_c = 1{\cdot}021r$$

$$s = \frac{\sqrt{2(1 - r_c)}}{2} \text{ radians}$$

$$= \frac{57{\cdot}296 \sqrt{2(1 - r_c)}}{2} \text{ degrees}$$

where θ_i is the mid-point azimuth of the $i^{\underline{th}}$ class interval, $\bar{\theta}$ is the azimuth of the resultant vector, n_i is the number of observations in each class, n is the total number of observations,

r is the magnitude of the resultant vector, r_c is a corrected value of r, and s is the mean angular deviation. The limits of r are 0 and 1. The former represents a perfectly uniform distribution of data points, and the latter represents an absolute concentration of data points (zero dispersion). The correction factor involved in recalculating r to r_c depends on the size of the class intervals (20° in the present case) and may be drawn from tables (Batschelet 1965, Table 12-1). It compensates for the distortion effect caused by grouping the data into classes. The mean angular deviation is approximately comparable to the familiar standard deviation. Approximately 67 percent of the measured values fall in the interval from $(\overline{\theta} - s)$ to $(\overline{\theta} + s)$, providing s is not greater than 50° (as s increases beyond 50°, the percentage of values contained in this interval decreases gradually from 67 to 45 percent). When r equals 1, s equals 0, and when r equals 0, s equals 81·029°, which is its maximum possible value (Batschelet 1965).

APPENDIX 3 - Methods of Petrographic Examination

The petrographic descriptions in Chapter 4 and Appendix 4 are based on the examination of 86 thin-sections (78 of sandstone and 8 of slate). A number of thin-sections and polished-surfaces of sandstone were treated with cobaltinitrate in order to stain potassium feldspars yellow and with amaranth dye to stain plagioclase feldspars red, following the procedure outlined by Laniz et al. (1964). None of the staining tests gave any indication of potassium feldspar, which is therefore assumed to be absent from most of the rocks. To ensure that the apparent absence of potassium feldspar was not due to error in staining technique, a polished surface of granite was treated in the usual manner with cobaltinitrite, giving, as expected, a yellow stain to the orthoclase grains.

The composition of plagioclase in the sandstone is calcic albite/sodic oligoclase, with remarkably little variation. This was ascertained by microscope examination using a Universal stage, supplemented by a determination of the plagioclase composition by X-ray diffraction analyses of two representative samples of arenaceous rocks, using the computer program developed by Evans et al.(1963) for determining unit-cell parameters from measured and corrected 2θ values. In utilizing this program, initial unit cell parameters were taken from Orville's (1967) paper and all 2θ values were given unit weight; a combination of pre-indexed 2θ values and computer indexed values was used until at

least six 2θ values deviated less than the approximate error of measurement ($0{\cdot}05^{\circ}2\theta$). Finally, the composition of the plagioclase was determined by comparing the calculated unit cell parameters with data and diagrams given by Wright and Stewart (1968).

APPENDIX 4 - Mineralogy of the Sandstone of the Goldenville Formation

Framework Components

Quartz

Nearly all quartz grains have strained extinction. Many possess a network of curved and straight fractures. A small number have deformation lamellae comparable to that described in high-grade metamorphic quartz (Fairbairn 1949).

The majority of grains possess a few small inclusions, but are otherwise quite clear. Some grains have minute, globular and irregular inclusions aligned in straight or slightly curved trains. Where several trains occur together, they may be parallel or at various angles to one another. Needle-like (?)rutile inclusions are common, generally in otherwise clear grains. A minority of quartz grains contain relatively large, euhedral to anhedral inclusions of magnetite, epidote, and other minerals.

Overgrowths, suturing, and replacement by chlorite, white mica and other minerals have affected the grain margins. Where quartz grains are in mutual contact, the grain margins are highly sutured and interpenetrating (Plate 3). The margins are much less modified where quartz borders on matrix chlorite and mica.

In this account and in the modal analyses (see above), polycrystalline quartz grains are included with quartz rather than with rock fragments, following the recommendation of Dickinson (1970). Polycrystalline grains constitute between 10 and 20 percent

of the framework quartz. The majority of these are mosaics of interlocking, roughly equant, straight-sided crystals with distinct triple-point junctions (Plate 4), forming a granoblastic-polygonal texture (Spry 1969).

Plagioclase

About half the plagioclase grains show characteristic albite twinning. Carlsbad and pericline twins are commonly combined with albite twins. Twin lamellae are commonly bent or fractured (Plate 3). Characteristic feldspar cleavage is well developed.

The grains commonly have a turbid interior portion surrounded by a clear outer rim, characteristic of plagioclase overgrowths in many sandstones with graywacke affinities (Carozzi 1960). Some grains are brilliantly clear throughout, and a proportion of these have fractured or rounded margins characteristic of detrital particles.

Inclusions of zircon and (?)sphene are relatively common, and generally take the form of irregular-shaped masses (Plate 6). Anhedral to euhedral inclusions of epidote and magnetite are present but not abundant. Replacement bodies of feldspar, quartz and carbonate are prominent in some grains, and tend to be developed preferentially along twin lamellae and cleavage fractures.

The majority of feldspar grains contain small replacement bodies of white mica and quartz that tend to be aligned along cleavages and other fractures and twin lamellae. This alignment

is commonly preserved in highly altered grains even though the actual fractures and twin lamellae may no longer be present. The proportion of the white mica and other replacement minerals relative to the feldspar varies greatly from grain to grain. Some grains are totally unaffected, whereas others have much more white mica than feldspar. Some grains consisting of finely intermixed white mica, quartz and other minerals, and having the general appearance of metamorphic rock fragments, may have been original feldspar grains that have been altered to such an extent that little or none of the original feldspar remains (Carozzi 1960).

Detrital Mica

Detrital particles of white mica and biotite in the original sediment have been recrystallized to white mica and intergrown white mica and chlorite. When intergrown with chlorite, the white mica tends to occur in even bands bounded by its own cleavage, whereas the chlorite generally adopts a more uneven distribution (Plate 61). These micaceous flakes tend to lie parallel to the bedding.

Rock Fragments

Rock fragments are herein regarded as any polycrystalline particles consisting of two or more mineral species, plus distinctive chlorite mosaics recrystallized from intraformational mud and shale fragments. Quartz and feldspar with intergrown carbonate and varying proportions of other minerals comprise the most abundant variety of rock fragments.

Plate 61. Photomicrograph showing flake of white mica and chlorite recrystallized from biotite(?) detrital particle (x 100).

The above-mentioned chlorite mosaics are generally large relative to the other allogenic constituents. Quartz and other minerals may be intermixed in varying amounts; particles with appreciable quartz represent fragments of siltstone.

Fragments of schist and phyllite (particles consisting of finely intermixed white mica, quartz and chlorite with an overall schistose fabric) are present but not common. Some of these fragments may have been altered from feldspar grains, as noted above. Rare fragments of fine-grained chlorite, white mica, quartz, feldspar and magnetite have an intergranular texture suggestive of volcanic rock fragments.

Fragments of intraformational sandstone may be abundant, particularly in the coarsest of the arenaceous rocks, but they generally are not easily recognized. The finer components of such fragments merge imperceptibly with the fine-grained matrix in the main body of the rock, and the sand and silt grains within the fragments are identical to all but the largest of the grains without. Because of the difficulty in recognizing them, the proportions of rock fragments listed in Table 3 may not be truly representative of the Goldenville sandstone.

Non-Opaque Heavy Minerals

The non-opaque heavy minerals recognized in thin-section are, in decreasing order of abundance, epidote/clinozoisite, zircon, sphene, tourmaline, apatite, zoisite, staurolite and rutile. The epidote group minerals (epidote, clinozoisite, zoisite) are grouped together as epidote, for the purpose of this description.

Epidote constitutes about 1·5% of the average sandstone, of which roughly 50% is allogenic and 50% authigenic. Zircon constitutes slightly less than one percent, and the remaining non-opaque heavy minerals about 0·5%. Staurolite and rutile are rare. Marginal overgrowths are developed on most grains; generally very small on zircon, slightly larger on sphene and apatite, larger still, in general, on epidote, and very large (commonly over 50% of the grain) on tourmaline.

Relatively large (up to 0·5 mm.), fractured, commonly inequant, and clean particles of epidote, zircon and sphene, many with well-developed cleavage and crystal faces, are common. Perfectly rounded grains, both large and small, of the same mineral species are also present.

Epidote and zircon are common constituents of rock fragments, generally in association with quartz and feldspar.

Tourmaline and apatite are relatively consistent in size and, excluding marginal overgrowths, are generally well rounded. Tourmaline grains typically have large overgrowths with straight sides and uneven terminations.

Aggregate masses with high refractive indices and consisting chiefly of sub-microscopic crystals are scattered throughout the sandstone. The aggregates are generally semi-opaque and clouded with leucoxene, and commonly occur as coherent bodies of equi-dimensional shape. Finely crystalline material of identical appearance occurs in zones on the margins and within grains of sphene, zircon and, occasionally, epidote. Sphene in particular commonly displays this type of replacement.

Secondary Components

For the purpose of this discussion, secondary components include any post-depositional crystal growth, other than overgrowths on or replacements within recognizable detrital grains. In many cases, the designation of rock components as secondary is a matter of subjective deduction. In view of this, points of interpretation are included, where necessary, to facilitate the description.

Non-Opaque Minerals

Finely intermixed chlorite and white mica constitute the major part of the matrix. Metamorphic porphyroblasts of chlorite and biotite, the latter generally present in relatively small proportions, are dispersed throughout the sandstone.

Many small grains of quartz and feldspar in the sandstone may be secondary (Deer, et al., 1965; Dapples 1967).

Carbonate is present in some rocks and is absent in others. It occurs as relatively large, irregular growths (up to 1 mm. in maximum diameter) interstitial to and partly enclosing adjacent detrital particles. It tends to be concentrated in patches, as observed in thin-section, and is commonly associated with small-scale penecontemporaneous deformation structures (produced either by bioturbation or liquefaction processes).

Small, roughly equant grains of epidote, generally with diffuse margins, are widely and more or less uniformly dispersed throughout the matrix. Most of these are probably diagenetic

or metamorphic growths, although some may be recrystallized detrital grains. Minute grains having the high refractive index and general appearance of zircon and/or sphene are also widely dispersed and also may be chiefly secondary growths (Poldervaart 1955).

Opaque Minerals

(a) Magnetite

(i) Description

Magnetite is much the most abundant (over 90 percent) of the opaque minerals. A proportion of the grains identified as magnetite may be ilmenite. It occurs as approximately equant, euhedral to anhedral crystals, often bordered with quartz- and chlorite-filled pressure fringes (Spry 1969). The crystals roughly correspond in size to the framework grains.

Magnetite crystals are commonly thinly coated with brick-red or deep reddish-brown hematite or hydrous iron oxides. Rare, oval or irregular and generally small grains of magnetite or ilmenite are enveloped in irregular masses of white leucoxene and deep red or orange iron hydroxides. These secondary envelopes are notably larger than the thin hematite or iron hydroxide coatings that surround many euhedral magnetite grains.

(ii) Origin

The above description suggests that two or more generations of magnetite (and (?)ilmenite) may be present; an early, possibly detrital phase that suffered appreciable marginal replacement, and

a later and much more abundant secondary phase that has been relatively little altered.

Although common to the sandstone, magnetite occurs very sparingly in the slate. The magnetite, therefore, may have been derived largely through the breakdown of iron-bearing particles common to the coarse-grained fraction but uncommon to the fine-grained fraction.

(b) Pyrite

(i) Description

Authigenic pyrite is very widespread and much more noticeable in outcrop than magnetite because it tends to occur as large crystals, commonly in zones and clusters within the rock. The pyrite crystals are invariably bordered with quartz- and chlorite-filled pressure fringes.

All pyrite crystals show some degree of alteration to hydrous iron oxides; noticeably more so than most magnetite crystals in the same rocks.

(ii) Replacement

Pyrite appears never to occur as small (less than 0·1 mm.) crystals. Therefore, the smallest of the pyrite crystals may have been entirely replaced with iron hydroxides. Bodies of iron hydroxide with square, rectangular and other outlines suggestive of replaced pyrite crystals are common.

APPENDIX 5 - Previous Reports of Trace Fossils in the Meguma Group

In the first published account of trace fossils in the Meguma Group, Hind (1869, p. 62) reported "fossils resembling Palaeotrochus major and minor (Emmons)" in the rocks at Waverley, 40 km. north of Halifax. He described these as "concretionary forms [which] vary from half an inch to 4 inches in diameter. They are generally oval in shape, but sometimes round, with a depression in the centre. Attached to some of them are numerous arms, all symmetrically arranged".

Dawson (1878, p. 82-3) examined Hind's specimens and assigned to them the name Astropolithon hindii. He originally described these forms as "fucoids with radiating fronds" but later (Dawson 1890, p.604-5) as "mouths of large burrows with radiating trails, the radiating trails in this case seem to be of the nature of vertical plates rather than grooves".

Woodman (1908, p. 103) favoured an inorganic origin for Astropolithon, and suggested that radiating fractures and discoidal joints resulting from the weathering (oxidation and expansion) of pyrite crystals might account for the radial markings and circular to elliptical outlines.

Bailey (1898, p. 55) mentioned mound-like structures which he called Astropolithon on upper bedding surfaces in the Goldenville Formation at Loche Island, 210 km. southwest of Halifax. Taylor (1967, p. 14) examined this locality and "identified the form as

Scolithus. The tube portion is about one-half inch in diameter and is separated from the matrix by a thin layer of muscovite, which lies normal to the bedding plane. Inside the tube is rock indistinguishable from that without. Each Scolithus stands out on the surface of the bed so that the surface is now a series of small circular hummocks, the largest 8 inches in diameter". The last part of the above quote probably is in reference to sand mounds, in which context the term Scolithus is not applicable (cf., Häntzschel 1962).

Phinney (1961, p. 1451) reported trace fossils in Goldenville sandstone at Beaver Point, 30 km. northeast of Taylor Head. He described "U-shaped tubes approximately half an inch in diameter and several inches long in many of the quartzite beds. The two limbs of the U emerge at the surface of the bed. At the end of one limb there is a tentacular pattern radiating from a central hole. At the end of the other limb there is an ellipsoidal mound with a hole in the centre. There are hundreds of mounds and tentacular patterns on certain dip slopes, and they seem to have been caused by boring animals of some sort".

I was unable to find the structures described by Phinney (1961) either in the rocks of the thesis area or in outcrops that I visited at Beaver Point, and I therefore surmise that Phinney may have misinterpreted the structures he reported. Truncated, small-scale folds in sandstone beds commonly have an appearance suggestive of spreiten (laminae resulting from biogenic activity and commonly developed between the limbs of U-tubes, Seilacher 1967,

p. 418-9). Such folds and commonly occurring grooved and ungrooved sand mounds may be the "trace fossils" which Phinney (1961) observed.

Campbell (1966, p. 17-20; Figs. 4, 5, 6) figured specimens comparable to Dawson's (1890, p. 606; Fig. 10) type specimen of Astropolithon hindii. Campbell described "eighteen major ridges ... on each of the best-preserved specimens. These ridges radiate from a central depression which is divided into two parts. In plan view the organism is ellipsoidal, but with one end wider than the other; in section it is hemispherical, but with one end higher than the other. The 'base' is flat and featureless". Campbell's description of Astropolithon is incorrect in regard to it being a body fossil.

APPENDIX 6 - A Summary Discussion of the Controversy on the Interrelationships of Slopes, Slumps, Turbidity Currents and Depositional Patterns in Flysch Basins

Previous studies indicate that in some turbidite sequences the paleoslope direction inferred from slump structures is perpendicular to the paleocurrent trend inferred from directional sole markings and other current structures (Murphy and Schlanger 1962; Marschalko 1963; McBride and Kimberley 1963; Hubert 1966; Scott 1966). This anomalous relationship is regarded by some authors as evidence that normal ocean currents, rather than turbidity currents, are the principal agent of flysch sedimentation (Murphy and Schlanger 1962; Hubert 1966, 1968; Scott 1966). Proponents of the turbidity current hypothesis, however, point out that slump movement perpendicular to the predominant direction of turbidity current flow might be induced by longitudinal faults and flexures in a tectonically active trench and borderland (Marschalko 1963; McBride and Kimberley 1963; Bailey 1967; Kuenen 1967; Walker 1970). In an elongate trough, turbidity currents might be funnelled axially along a gently inclined or flat floor, whereas slumps would originate mainly on and move out from the lateral slopes (Bailey 1967).

Klein (1966) cited an example of a flysch sequence in which the paleocurrent trend inferred from directional sole markings is dissimilar to the direction of sediment transport inferred from a

study of the sandstone petrology. Klein concluded from this that the sole markings were formed chiefly by normal ocean currents that reworked the sediment carried into the depositional basin by turbidity currents, sand flows and slumps from marginal sources. Briggs and Cline (1967) and Cline (1970) implied, on the other hand, that much of the sediment transport took place during an early, mainly erosional phase of turbidity current flow and that the preserved sole structures and depositional structures generally reflect a relatively late phase of turbidity current flow when the currents had become deflected along the axis of the depositional trough.

A predominant slump direction coincident with the mean current direction deduced from sole marks is documented by Crowell (1957), Ksiazkiewicz (1958), ten Haaf (1959), Allen (1960), Marschalko (1963), Ballance (1964), Marschalko and Pulec (1967), and the present writer (Table 1). Sole markings in the Goldenville Formation indicate a longitudinal paleocurrent trend over the entire region of Meguma outcrop (Schenk 1970). The Meguma basin was large (i.e., not a restricted trough), and therefore the direction of sole and slide markings probably reflects the regional paleoslope. This relationship is possibly characteristic of unrestricted flysch basins.

REFERENCES

Abramowitz, M. and Stegun, I.A. (eds) 1964. Handbook of mathematical functions. National Bureau of Standards, Washington.

Allen, J.R.L. 1960. The Mam Tor sandstones: a 'turbidite' facies of the Namurian deltas of Derbyshire, England. Jour. Sed.Pet., V.30, p.193-208.

_____. 1969. Erosional current marks of weakly cohesive mud beds. Jour.Sed.Pet., v.39, p.607-623.

Ami, H.M. 1900. Synopsis of the geology of Canada. Proc. and Trans.Roy.Soc.Can., new series, v.6, p.187-226.

Audley-Charles, M.G. 1967. Greywackes with a primary matrix from the Viqueque Formation (Upper Miocene-Pliocene), Timor. Jour. Sed. Pet., v.37, p.1-11.

Bailey, E.H., Irwin, W.P., Jones, D.L. 1964. Franciscan and related rocks, and their significance in the geology of Western California. Calif.Div.Mines and Geology, Bull.183.

Bailey, L.W. 1898. Report on the geology of southwest Nova Scotia, in Annual Report for 1896. Geol.Surv.Can., new series, v.9, part M.

Bailey, R.J. 1967. Paleocurrents and paleoslopes: a discussion. Jour.Sed.Pet., v.37, p.1252-1255.

Ballance, P.F. 1964. The sedimentology of the Waitema Group in the Takapuna section, Auckland. New Zealand Jour.Geol. Geophys., v.7, p.466-499.

Batschelet, E. 1965. Statistical methods for the analysis of problems in animal orientation and certain biological rhythms. Amer.Inst.Biol.Sciences, Monograph, p.57.

Bird, J.M. and Dewey, J.M. 1970. Lithosphere plate-continental margin tectonics and the evolution of the Appalachian orogen. Bull.Geol.Soc.Amer., v.81, p.1031-1060.

Bokman, J. 1953. Lithology and petrology of the Stanley and Jackfork formations. Jour.Geology, v.61, p.152-170.

Bouma, A.H. 1962. Sedimentology of some flysch deposits: a graphic approach to facies interpretation. Elsevier Pub.Co., Amsterdam.

Brenchley, P.J. 1969. Origin of matrix in Ordovician graywackes, Berwyn Hills, North Wales. Jour.Sed.Pet., v.39, p.1297-1301.

Briggs, G. and Cline, L.M. 1967. Paleocurrents and source areas of late Paleozoic sediments of the Ouachita Mountains, southeastern Oklahoma. Jour.Sed.Pet., v.37, p.985-1000.

Campbell, F.H.A. 1966. Paleocurrents and sedimentation of part of the Meguma Group (Lower Paleozoic) of Nova Scotia, Canada. M.Sc. Thesis, Dalhousie University.

Campbell, F.H.A. and Schenk, P.E. 1967. Paleocurrent and basin analysis of the Meguma Group, Nova Scotia, Maritime Sediments, v.3, p.27-30.

Carozzi, A.V. 1960. Microscopic sedimentary petrography. John Wiley & Sons, New York.

Cayeux, Lucien. 1929. Les Roches sédimentares de France: roches siliceuses. Imprimerie Nationale, Paris.

Clarke, F.W. 1924. The data of geochemistry (5th ed.). U.S. Geol.Surv., Bull.770.

Cline, L.M. 1960. Stratigraphy of the Late Paleozoic rocks of the Ouachita Mountains, Oklahoma. Oklahoma Geol.Surv., Bull.85.

_____. 1970. Sedimentary features of Late Paleozoic flysch, Ouachita Mountains, Oklahoma. Geol.Assoc.Can., Special Paper 7, p.85-101.

Craig, G.Y. and Walton, E.K. 1962. Sedimentary structures and paleocurrent directions from the Silurian rocks of Kirkcudbrightshire. Trans.Edinburgh Geol.Soc., v.19, p.100-119.

Crosby, D.G. 1962. Wolfville map-area, Nova Scotia. Geol.Surv. Can., Mem.325.

Crowell, J.C. 1955. Directional-current structures from the Pre-alpine flysch, Switzerland. Bull.Geol.Soc.Amer., v.66, p.1351-1384.

_____. 1957. Origin of pebbly mudstones. Bull.Geol.Soc. Amer., v.68, p.993-1010.

Cummins, W.A. 1962. The greywacke problem. Geol.Jour., v.3, p.51-72.

Curray, J.R. 1956. The analysis of two-dimensional orientation data. Jour.Geology, v.64, p.117-131.

Dapples, E.C. 1967. Diagenesis of sandstones, in G.Larsen and G.V.Chilingar (eds.), Diagenesis in sediments. Elsevier Pub.Co., Amsterdam, p.91-127.

Dawson, J.W. 1850. On the metamorphic and metalliferous rocks of eastern Nova Scotia. Quart.Jour.Geol.Soc.London, p.347-364.

_____. 1878. Acadian geology (3rd ed.). MacMillan and Co., London.

_____. 1890. On burrows and tracks of invertebrate animals in Paleozoic rocks, and other markings. Quart.Jour.Geol.Soc.London, v.46, p.595-618.

Deer, W.A., Howie, R.A. and Zussman, J. 1965. Rock-forming minerals: Vol.4, Framework silicates. Longmans, Green and Co., London.

Dickinson, W.R. 1970. Interpreting detrital modes of graywacke and arkose. Jour.Sed.Pet., v.40, p.695-707.

Dott, R.H. 1964. Wacke, graywacke and matrix. Jour.Sed.Pet., v.34, p.625-632.

Douglas, G.C., Milner, R.L. and MacLean, J. 1938. The deposition of the Halifax series. Nova Scotia Dept.Public Works and Mines, Ann.Rept. for 1937, pt.2, p.34-45.

Doveton, J.H. and Parsley, A.J. 1970. Experimental evaluation of trend surface distortions induced by inadequate data-point distributions. Trans., Sec.B., Inst.Mining Metall., v.79, p.197-207.

Dzulynski, S. 1965. New data on experimental production of sedimentary structures. Jour.Sed.Pet., v.35, p.196-212.

Dzulynski, S., Ksiazkiewicz, M. and Kuenen, Ph.H. 1959. Turbidites in flysch of the Polish Carpathian Mountains. Bull.Geol.Soc.Amer., v.70, p.1089-1118.

Dzulynski, S. and Walton, E.K. 1963. Experimental production of sole markings. Trans.Edinburgh Geol.Soc., v.19, p.279-305.

Dzulynski, S. and Walton, E.K. 1965. Sedimentary features of flysch and greywackes. Elsevier Pub.Co., Amsterdam.

Eckel, E.C. 1904. On the chemical composition of American shales and roofing slates. Jour.Geol., v.12, p.25-29.

Einsele, G. 1963. Uber Art und Richtung der Sedimentation im klastichen rheinischen Oberdevon (Famenne). Abhandl. Hess.Landesamtes Bodenforsch., v.43, p.1-60.

Enos, P. 1969. Anatomy of a flysch. Jour.Sed.Pet., v.39, p.680-723.

Evans, H.T., Appleman, D.E. and Handwerker, D.S. 1963. The least squares refinement of crystal unit cells with powder diffraction data by an automatic computer indexing method (abst.). Amer.Crystallogr.Assoc., Ann.Meeting, Program, p.42-43.

Fairbairn, H.W. 1949. Structural petrology of deformed rocks (2nd ed.). Addison-Wesley Pub.Co., Reading, Mass.

Fairbairn, H.W., Harley, P.M., Pinson, W.H. and Cormier, R.F. 1960. Age of granitic rocks of Nova Scotia. Bull.Geol.Soc.Amer., v.71, p.399-414.

Faribault, E.R. 1896. Tangier sheet. Geol.Surv.Can.Map Series, Map-sheet 39.

_____. 1897. Sheet Harbour sheet. Geol.Surv.Can.Map Series, Map-sheet 40.

_____. 1909. Southern part of Kings and eastern part of Lunenburg counties, Nova Scotia. Geol.Surv.Can., Summ.Rept. for 1908, p.150-158.

_____. 1913. The Goldbearing series of Nova Scotia. Geol. Surv.Can., Guidebook 1, p.158-192.

_____. 1914. Greenfield and Liverpool Town map-areas, Nova Scotia. Geol.Surv.Can., Summ.Rept. 1912, p.334-340.

Fleuty, M.J. 1964. The description of folds. Proc.Geol.Assoc., v.75, p.461-492.

Fyson, W.K. 1966. Structures in the Lower Paleozoic Meguma Group, Nova Scotia. Bull.Geol.Soc.Amer., v.77, p.931-944.

Garland, G.D. 1953. Gravity measurements in the Maritime Provinces. Can.Dom.Obs., Publ., v.16, p.185-275.

Gill, W.D. and Kuenen, P.H. 1957. Sand volcanoes on slumps in the Carboniferous of County Clare, Ireland. Quart.Jour.Geol.Soc.London, v.113, p.441-460.

Hallam, A. and Swett, K. 1966. Trace fossils from the Lower Cambrian Pipe Rock of the northwest Highlands. Scott.Jour.Geology, v.2, p.101-106.

Häntzschel, W. 1962. Trace fossils and problematica, in R.C.Moore (ed.), Treatise on Invertebrate Paleontology, Part W, Miscellania. Univ.Kansas Press, Lawrence, Kansas, p.177-249.

Harris, I.M. and Schenk, P.E. 1968. A study of sedimentary structures in the Goldenville Formation, eastern Nova Scotia. Maritime Sediments, v.4, p.1-3.

Hind, H.Y. 1869. Report on the Waverley gold district, with geological maps and sections. Halifax, N.S.

Hsu, K.J. 1964. Cross-laminations in graded bed sequences. Jour.Sed.Pet., v.34, p.379-388.

Hubert, J.F. 1966. Sedimentary history of Upper Ordovician geosynclinal rocks, Girvan, Scotland. Jour.Sed.Pet., v.36, p.677-699.

_____. 1968. Currents and slopes in flysch basins: a discussion. Jour.Sed.Pet., v.38, p.1390-1393.

Hubert, J.F., Scott, K.M. and Walton, E.K. 1966. Composite nature of Silurian flysch sandstones shown by groove moulds on intra-bed surfaces, Peeblesshire, Scotland. Jour.Sed.Pet., v.36, p.237-241.

Kay, M. and Colbert, E.H. 1965. Stratigraphy and life history. John Wiley and Sons, New York.

Kelling, G. 1958. Ripple-mark in the Rhinns of Galloway. Trans.Edinburgh Geol.Soc., v.17, p.117-132.

_____. 1964. The trubidite concept in Britain, in Turbidites, A.H.Bouma and A.Brouwer (eds.). Elsevier Pub.Co., Amsterdam, p.75-92.

Klein, G.de V. 1963. Analysis and review of sandstone classifications in the North American geological literature, 1940-1960. Bull.Geol.Soc.Amer., v.74, p.555-576.

Klein, G.de V. 1966. Dispersal and petrology of sandstones of the Stanley-Jackfork boundary, Ouachita fold belt, Arkansas and Oklahoma. Bull.Amer.Assoc.Pet.Geol., v.50, p.308-326.

Krumbein, W.C. 1939. Preferred orientation of pebbles in sedimentary deposits. Jour.Geology, v.47, p.673-706.

Krumbein, W.C. and Graybill, F.A. 1965. An introduction to statistical models in geology. McGraw-Hill Book Co., New York.

Ksiazkiewicz, M. 1954. Graded and laminated bedding in the Carpathian flysch. Ann.Soc.Géol.Pologne, v.22, p.399-449.

_____. 1958. Submarine slumping in the Carpathian flysch. Ann.Soc.Géol.Pologne, V.28, p.123-150.

_____. 1960. Pre-orogenic sedimentation in the Carpathian geosyncline. Geol.Rundschau, v.50, p.8-31.

Kuenen, Ph.H. 1953. Significant features of graded bedding. Bull.Amer.Assoc.Petrol.Geol., v.37, p.1044-1066.

_____. 1957. Sole markings of graded greywacke beds. Jour.Geology, v.65, p.231-258.

_____. 1966. Matrix of turbidites, experimental approach. Sedimentology, v.7, p.267-297.

_____. 1967. Emplacement of flysch-type sand beds. Sedimentology, v.9, p.203-243.

_____. 1968. Settling convection and grain-size analysis. Jour.Sed.Pet., v.38, p.818-831.

Laird, M.G. 1970. Vertical sheet structures - a new indicator of sedimentary fabric. Jour.Sed.Pet., v.70,p.428-434.

Laniz, R.V., Stevens, R.E. and Norman, M.B. 1964. Staining plagioclase feldspar and other minerals with F.D. and C.Red No.2. U.S. Geol.Survey Prof.Paper 501-B, p.152-153.

Lessertisseur, Jacques, 1955. Traces fossiles d'activité animale et leur signification paleobiologique. Soc.Géol.France, Mém.74, p.148.

Lombard, A. 1963. Stratonomie des séries du flysch. Geologica Helv., v.56, p.482-511.

Lovell, J.P.B. 1969. Tyee Formation: a study of proximality in turbidites. Jour.Sed.Pet., v.39, p.935-953.

Mackie, W. 1896. The sands and sandstones of Eastern Moray. Trans. Edinburgh Geol. Soc., v.7, p.148-172.

Malcolm, W. 1929. Gold fields of Nova Scotia. Geol.Surv.Can., Mem.156.

Marschalko, R. 1963. Sedimentary slump folds and the depositional slope. Geologické Prace, v.28, p. 161-168.

Marschalko, R. and Pulec, M. 1967. Sedimentology of the Lunz beds. Geol.Sbornik, v.18, p.331-344.

Mattiat, B. 1960. Beitrag zur Petrographic der Oberharzer Kulm grauwacke. Beitr.Mineralogie u. Petrog., v.7, p.242-280.

McBride, E.F. 1962. Flysch and associated beds of the Martinsburg Formation (Ordovician), central Appalachians. Jour. Sed.Pet., v.32, p.39-91.

_____. 1963. A classification of common sandstones. Jour.Sed.Pet., v.33, p.664-669.

McBride, E.F. and Kimberley, J.E. 1963. Sedimentology of Smithwick Shale (Pennsylvanian), eastern Llano region, Texas. Bull.Amer.Assoc.Petrol.Geol., v.37, p.1840-1854.

Middleton, G.V. 1960. Chemical composition of sandstones. Bull. Geol.Soc.Amer., v.71, p.1011-1026.

_____. 1967. Experiments on density and turbidity currents. III: deposition of sediment. Can.Jour. Earth Sci., v.4, p.475-505.

Murphy, M.A. and Schlanger, S.O. 1962. Sedimentary structures in Ilhas and Sao Sebastiao Formations, (Cretaceous), Reconcavo Basin, Brazil.Bull.Amer.Assoc.Petrol. Geol., v.46, p.457-477.

Orville, P.M. 1967. Unit cell parameters of the microcline-low albite and the sanadine-high albite solid solution series. Amer. Mineralogist, v.52, p.55-86.

Pelletier, B.R. 1958. Pocono paleocurrents in Pennsylvania and Maryland. Bull.Geol.Soc.Amer., v. 69, p.1033-1064.

Pettijohn, F.J. 1943. Archean sedimentation. Bull.Geol.Soc. Amer., v. 54, p.925-972.

Pettijohn, F.J. 1957. Sedimentary rocks (2nd ed.). Harper and Bros., New York.

_____. 1960. Some contributions of sedimentology to tectonic analysis. Report 21st Session Norden, Part 18, p. 446-454.

_____. 1963. Chemical composition of sandstones - excluding carbonate and volcanic sand. U.S. Geol. Surv., Paper 440-S.

Phinney, W.C. 1961. Possible turbidity-current deposits in Nova Scotia (abst.). Bull.Geol.Soc.Amer., v.72, p.1453-1454.

Pincus, H.J. 1953. The analysis of aggregates of orientation data in the earth sciences. Jour. Geology, v.61, p.482-509.

Poldervaart, A. 1955. Zircon in rocks: 1. sedimentary rocks. Amer.Jour.Sci., v.253, p.433-461.

Poole, W.H. 1967. Tectonic evolution of Appalachian region of Canada. Geol.Assoc.Can., Special Paper 4, p.9-51.

Poole, W.H., Kelley, D.G. and Neale, E.R.W. 1964. Age and correlation problems in the Appalachian region of Canada. Roy.Soc.Can., Special Pub. No. 8, p. 61-84.

Potter, P.E. and Pettijohn, F.J. 1963. Paleocurrents and basin analysis. Springer-Verlag, Berlin.

Prentice, J.E. 1956. The interpretation of flow markings and load-casts. Geol.Mag., v.93, p.393-400.

Ramsay, J.G. 1961. The effects of folding upon the orientation of sedimentation structures. Jour. Geology, v. 69, p.84-100.

Rettger, R.E. 1935. Experiments on soft-rock deformation. Bull. Geol.Soc.Amer., v.72, p.1453-1454.

Schenk, P.E. 1970. Regional variation of the flysch-like Meguma Group (Lower Paleozoic) of Nova Scotia, compared to Recent sedimentation off the Scotian Shelf. Geol. Assoc.Can., Special Paper 7, p.127-153.

Scott, K.M. 1966. Sedimentology and dispersal pattern of a Cretaceous flysch sequence, Patagonian Andes, Southern Chile. Bull.Amer.Assoc.Petrol.Geol., v.50, p.72-107.

Seilacher, A. 1962. Paleontological studies of turbidite sedimentation and erosion. Jour.Geology, v.70, p.227-234.

_____. 1967. Fossil behavior. Scientific American, v.217, p.72-80.

Shepard, F.P. 1965. Importance of submarine valleys in funnelling sediments to the deep sea in M. Sears (ed.), Progress in oceanography, Vol.3, Pergamon Press, Oxford, p.321-332.

Shinn, E.A. 1968. Burrowing in recent lime sediments of Florida and the Bahamas. Jour.Paleont., v.42, p.879-894.

Shrock, R.R. 1948. Sequence in layered rocks. McGraw-Hill Book Co., New York.

Smitheringale, W.G. 1960. Geology of the Nictaux-Torbrook map-area, Annapolis and Kings Counties, Nova Scotia. Geol. Surv.Can., Paper 60-13.

Sorby, H.C.S. 1908. On the application of quantitative methods to the study of the structure and history of rocks. Quart. Jour.Geol.Soc.London, v. 64, p.171-233.

Spry, A. 1969. Metamorphic textures. Pergamon Press, Oxford.

Stevenson, I.M. 1959. Shubenacadie and Kennetcook map areas, Colchester, Hants and Halifax counties, Nova Scotia. Geol.Surv.Can., Mem.302.

Stokes, W.L. 1947. Primary lineation in fluvial sandstones: a criterion of current directions. Jour. Geology, v.55, p.52-54.

Sujkowski, Zb.L. 1957. Flysch sedimentation. Bull.Geol.Soc.Amer., v.68, p.543-554.

Taylor, F.C. 1965. Silurian stratigraphy and Ordovician-Silurian relationships in southwestern Nova Scotia. Geol.Surv. Can., Paper 64-13.

_____. 1967. Reconnaissance geology of Shelburne map-area; Queens, Shelburne and Yarmouth Counties, Nova Scotia. Geol.Surv.Can., Mem.349.

_____. 1969. Geology of the Annapolis-St. Marys Bay map-area, Nova Scotia. Geol.Surv.Can., Mem.358.

Taylor, F.C. and Schiller, E.A. 1966. Metamorphism of the Meguma Group of Nova Scotia. Can.Jour.Earth Sci., v.3, p.959-974.

Ten Haaf, Ernst 1959. Graded beds of the Northern Apennines. Ph.D. Thesis, Rijks University of Groningen.

Tercier, J. 1947. Le flysch dans la sédimentation alpine. Ecologae Geol.Helv., v.40, p.163-198.

Turner, F.J. and Verhoogen, J. 1960. Igneous and metamorphic petrology. McGraw-Hill Book Co., New York.

Van Straaten, L.M.J.U. 1951. Longitudinal ripple marks in mud and sand. Jour.Sed.Pet., v.21, p.47-54.

Walker, R.G. 1965. The origin and significance of the internal sedimentary structures of turbidites. Proc. Yorkshire Geol.Soc., v.35, p.1-32.

_____. 1970. Review of the geometry and facies organization of turbidites and turbidite-bearing basins. Geol.Assoc. of Can., Special Paper 7, p.219-251.

Walker, R.G. and Sutton, R.G. 1967. Quantitative analysis of turbidites in the Upper Devonian Sonyea Group, New York. Jour.Sed.Pet., v.37, p.1012-1022.

Walton, E.K. 1956. Limitations of graded bedding and alternative criteria of upward sequence in the rocks of the Southern Uplands. Trans.Edinburgh Geol.Soc., v.16, p.262-271.

_____. 1967. The sequence of internal structures in turbidites. Scott.Jour.Geology, v.3, p.306-317.

Warren, P.T. 1963. The petrology, sedimentation and provenance of the Wenlock rocks near Hawick, Roxburghshire. Trans. Edinburgh Geol.Soc., v.19, p.225-255.

Wilson, J.T. 1966. Did the Atlantic close and then re-open? Nature, v.211, p.676-681.

Wood, A. and Smith, A.J. 1958a. The sedimentation and sedimentary history of the Aberystwyth Grits. Quart.Jour.Geol.Soc. London, v.114, p.163-165.

_____. 1958b. Two undescribed structures in a greywacke series. Jour.Sed.Pet., v.28, p.97-101.

Woodman, J.E. 1904. Nomenclature of the gold-bearing metamorphic series of Nova Scotia. Amer.Geol., v.33, p. 363-370.

Woodman, J.E. 1908. Probable age of the Meguma (gold-bearing series) of Nova Scotia. Bull.Geol.Soc.Amer., v.19, p.99-112.

Wright, T.L. and Stewart, D.B. 1968. X-ray and optical study of alkali feldspar: I. Determination of composition and structural state from refined unit-cell parameters and 2V. Amer. Mineralogist, v.53, p.38-87.

LEGEND FOR (C)

- Sandstone (average grain-size >0.1mm.)
- Very fine sandstone, siltstone and mudstone transitional above a sandstone bed
- Interbedded very fine sandstone, siltstone and mudstone
- Slurried bedding

Maximum Grain Size (Field Estimate)

- C — coarse (½ to 1 mm.)
- V — very coarse (1 to 2 mm.)
- G — granules, rarely small pebbles (>2 mm.)
- Sharp contact between sandstone above and fine-grained rocks (slate) below
- Transitional contact between sandstone below and fine-grained rocks (slate) above
- Amalgamated bedding
- Channelled, amalgamated bedding
- Discontinuous, erosionally truncated sandstone bed, in sharp contact with fine-grained rocks above and below
- Flat intra-bed surface in compound sandstone bed
- Channelled intra-bed surface in compound sandstone bed
- Discontinuous layer in compound sandstone bed, marked by joined intra-bed surfaces
- Intra-bed surface marked by abrupt change in grain-size
- Parallel lamination in sandstone (parallel, wavy)
- NE — Cross-lamination in sandstone (associated with internal flutes, associated with channels - inferred current direction toward the northeast)
- NE — Ripple cross-lamination (in very fine sandstone and siltstone interbedded with mudstone, in sediment at the top of and transitionally above sandstone beds - inferred current direction toward the northeast)
- >NE — Ripple-mark on upper bedding-surface of sandstone bed, inferred current direction toward the northeast
- Intra-bed slump folds and associated primary deformation structures (strongly developed, weakly developed)
- Erosionally truncated, intra-bed slump folds in compound sandstone beds
- Load structures (on under-surfaces of sandstone beds, in slate bands - pseudo-nodules of very fine sandstone and siltstone sunk into siltstone and mudstone)
- NE — Flame structures (symmetrical and randomly assymetrical, preferentially assymetrical - leaning towards the northeast)
- LG — Mudflake inclusions (maximum observed length < 1 meter, maximum observed length > 1 meter)
- CH — Channels
- GV45 GV45> GV70+120 — Grooves (tilt-corrected orientation is 45° azimuth, orientation is 45° azimuth - inferred northeastward current direction, two sets of grooves - at 70° and 120° azimuth)
- FL — Flutes, azimuths and current directions indicated as in the case of grooves
- LF — Longitudinal furrows, azimuths and current directions indicated as in the case of grooves
- GV+FL+LF135> — Grooves, flutes and longitudinal furrows, inferred southeastward current direction
- SL90 — Slide markings, tilt-corrected orientation is 90° azimuth
- PD — Prod markings
- Sand pipes
- Sheet structures
- Sand mounds
- Biogenic structures on sole of bed
- Sole of bed not exposed

VERTICAL SCALE IN METERS: 5, 4, 3, 2, 1, 0

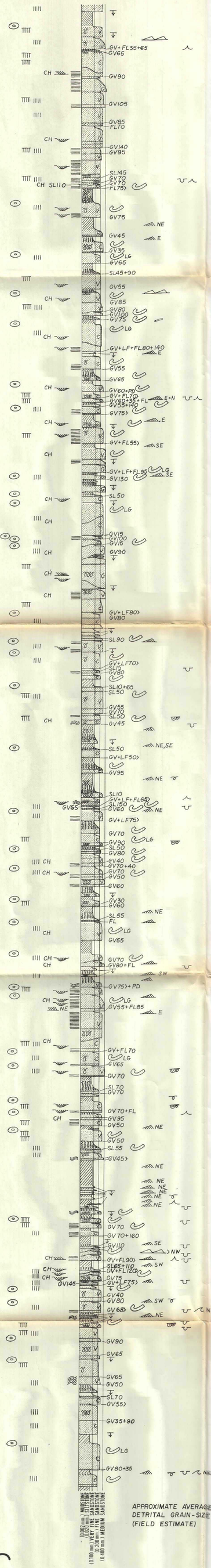

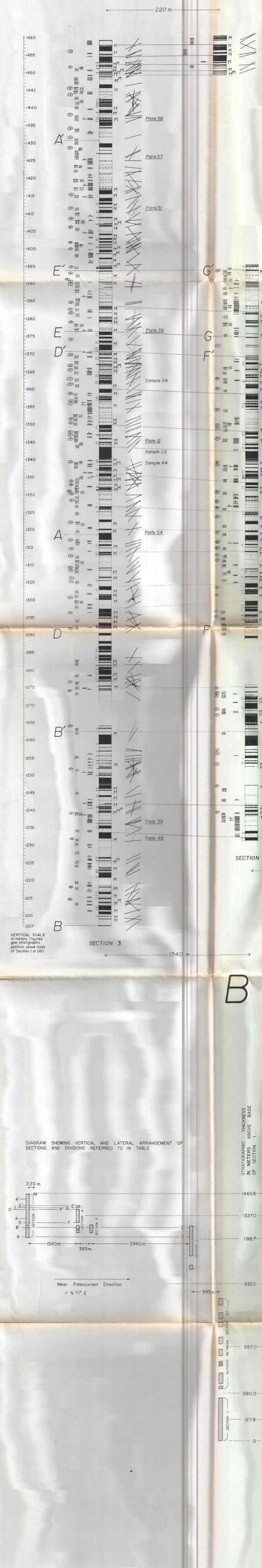

LEGEND FOR (A) AND (B)

- Sandstone (estimated average, detrital grain-size greater than 0.1 mm.)
- Slate (estimated average, detrital grain-size less than 0.1 mm.)
- Amalgamated bedding
- Channelled, amalgamated bedding
- Flat intra-bed surface in compound sandstone bed
- Channelled intra-bed surface in compound sandstone bed
- Uneven intra-bed surface in compound sandstone bed, generally associated with slump structures
- Slump breccia
- Sand injection structures
- Linear tool and scour markings. The azimuth for each tilt-corrected lineation is indicated by the orientation of the symbol; a vertical line represents 0 degrees azimuth, a horizontal line represents 90 degrees azimuth, etc.
- Slide markings. Azimuths indicated as in the case of linear tool and scour markings
- Parallel lamination in sandstone
- Cross-lamination in sandstone associated with flutes and channels
- Zone of slurried bedding
- Sand pipes
- Sheet structures
- Sand mounds
- M — Mudflake inclusions
- A — Marker referred to in caption
- 1310 — Stratigraphic thickness in meters above the base of Section 1
- Sample C2 — Sample C in table 2 of text
- Sample B3 & C4 — Sample B in table 3 and sample C in table 4 (one sample referred to in two tables)
- Plate 25 — Plate 25 in text
- m. — Meters

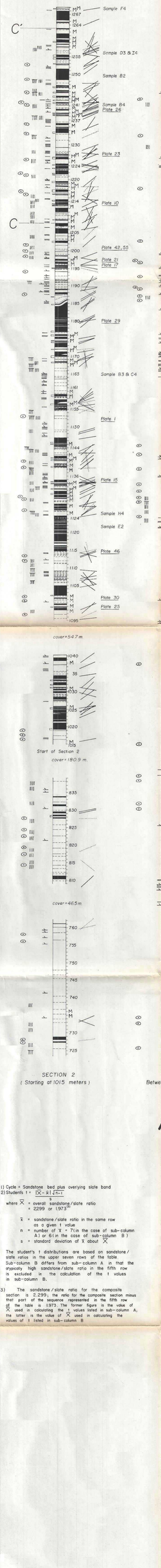

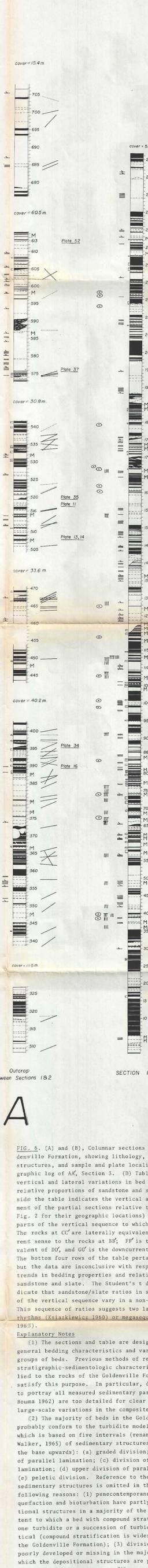

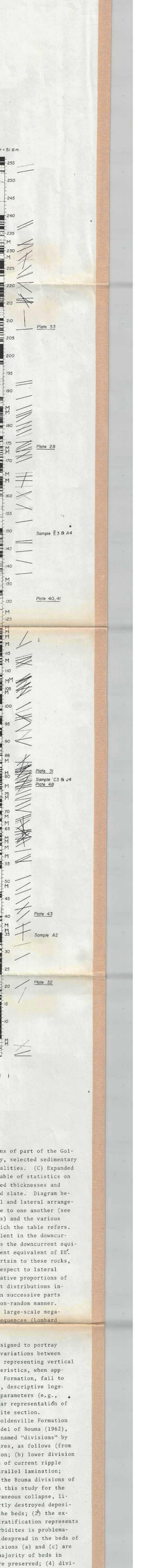

DIAGRAM SHOWING VERTICAL AND LATERAL ARRANGEMENT OF SECTIONS AND DIVISIONS REFERRED TO IN TABLE

STRATIGRAPHIC THICKNESS IN METERS ABOVE BASE OF SECTION 1

BEDDING CHARACTERISTICS & DISTRIBUTION OF SANDSTONE & SLATE

Stratigraphic Interval	Number of Cycles(1)	Aggregate Thickness in Meters: Cycles(1)	Aggregate Thickness in Meters: Sandstone Beds	Aggregate Thickness in Meters: Slate Bands	Average Thickness in Centimeters: Cycles(1)	Average Thickness in Centimeters: Sandstone Beds	Average Thickness in Centimeters: Slate Bands	Percent Slate	Sandstone/Slate Ratio	Student's t(2) Distributions Based on Sandstone/Slate Ratios: A	Student's t(2) Distributions Based on Sandstone/Slate Ratios: B
Total Sequence (from base of Section 1 to top of Section 3.)	759	902.1	629.2	273.7	119	83	36	30.3	2.2/99 (1.973)(3)		
From 1337.0 to 1460.6 meters (upper part of Section 3.)	141	129.6	91.9	37.7	92	65	27	29.0	2.4/38	0.146	2.910
From 1198.7 to 1337.0 m (lower part Section 3, upper part Section 2.)	114	128.8	84.7	44.1	113	74	39	34.3	1.9/17	0.404	0.350
From 932.0 to 1198.7 meters (lower part of Section 2.)	117	129.1	80.1	49.0	110	68	41	37.8	1.6/36	0.701	2.109
From 557.0 to 932.0 meters (Outcrop between Sections 1 and 2.)	53	128.8	115.8	13.5	243	218	25	10.5	8.5/65	6.631	—
From 280.0 to 557.0 meters (Outcrop between Sections 1 and 2.)	106	129.0	91.4	37.6	122	86	35	29.0	2.4/32	0.140	2.873
From 127.8 to 280.0 meters (upper part of Section 1.)	116	129.0	88.0	41.1	111	75	35	31.8	2.1/42	0.165	1.056
From 0 to 127.8 meters (lower part of Section 1.)	112	127.8	77.3	50.5	114	69	45	39.4	1.5/31	0.812	2.768
B to B', Section 3 (1307.3 to 1362.6.)	42	55.3	36.5	18.8	132	87	45	34.1	1.9/42		
C to C', Section 2 (1307.8 to 1362.9.)	53	55.2	34.6	20.6	104	65	39	37.6	1.6/80		
D to D'+ E to E' Section 3, (1390.5 to 1470.7 + 1476.3 to 1499.7.)	102	98.2	71.3	26.9	96	70	26	27.4	2.6/51		
F to F'+ G to G' Section 4 (1392.0 to 1469.1 + 1474.8 to 1499.6.)	92	96.5	74.7	21.9	105	81	24	22.6	3.4/10		

(1) Cycle = Sandstone bed plus overlying slate band

(2) Students $t = \frac{|\bar{X} - \bar{x}|\sqrt{n-1}}{s}$

where $\bar{X}$ = overall sandstone/slate ratio = 2.299 or 1.973(3)

$\bar{x}$ = sandstone/slate ratio in the same row as a given t value

n = number of $\bar{x}$ = 7 (in the case of sub-column A) or 6 (in the case of sub-column B)

s = standard deviation of $\bar{x}$ about $\bar{X}$

The student's t distributions are based on sandstone/slate ratios in the upper seven rows of the table. Sub-column B differs from sub-column A in that the atypically high sandstone/slate ratio in the fifth row is excluded in the calculation of the t values in sub-column B.

(3) The sandstone/slate ratio for the composite section is 2.299; the ratio for the composite section minus that part of the sequence represented in the fifth row of the table is 1.973. The former figure is the value of $\bar{X}$ used in calculating the t values listed in sub-column A; the latter is the value of $\bar{X}$ used in calculating the values of t listed in sub-column B.

FIG. 6. (A) and (B), Columnar sections of part of the Goldenville Formation, showing lithology, selected sedimentary structures, and sample and plate localities. (C) Expanded graphic log of AA', Section 3. (D) Table of statistics on vertical and lateral variations in bed thicknesses and relative proportions of sandstone and slate. Diagram beside the table indicates the vertical and lateral arrangement of the partial sections relative to one another (see Fig. 2 for their geographic locations) and the various parts of the vertical sequence to which the table refers. The rocks at CC' are laterally equivalent in the downcurrent sense to the rocks at BB'; FF' is the downcurrent equivalent of DD', and GG' is the downcurrent equivalent of EE'. The bottom four rows of the table pertain to these rocks, but the data are inconclusive with respect to lateral trends in bedding properties and relative proportions of sandstone and slate. The Student's t distributions indicate that sandstone/slate ratios in successive parts of the vertical sequence vary in a non-random manner. This sequence of ratios suggests two large-scale megarhythms (Ksiazkiewicz 1960) or megasequences (Lombard 1963).

Explanatory Notes

(1) The sections and table are designed to portray general bedding characteristics and variations between groups of beds. Previous methods of representing vertical stratigraphic-sedimentologic characteristics, when applied to the rocks of the Goldenville Formation, fail to satisfy this purpose. In particular, descriptive logs to portray all measured sedimentary parameters (e.g., Bouma 1962) are too detailed for clear representation of large-scale variations in the composite section.

(2) The majority of beds in the Goldenville Formation probably conform to the turbidite model of Bouma (1962), which is based on five intervals (renamed "divisions" by Walker, 1965) of sedimentary structures, as follows (from the base upwards): (a) graded division; (b) lower division of parallel lamination; (c) division of current ripple lamination; (d) upper division of parallel lamination; (e) peletic division. Reference to the Bouma divisions of sedimentary structures is omitted in this study for the following reasons: (1) penecontemporaneous collapse, liquefaction and bioturbation have partly destroyed depositional structures in a majority of the beds; (2) the extent to which a bed with compound stratification represents one turbidite or a succession of turbidites is problematical (compound stratification is widespread in the beds of the Goldenville Formation); (3) divisions (a) and (c) are poorly developed or missing in the majority of beds in which the depositional structures are preserved; (4) divisions (d) and (e) are not readily separated because depositional structures in the fine-grained rocks are typically indistinct due to slaty cleavage, internal strain, weathering effects, and the destruction of the sedimentary texture by diagenesis and metamorphism.

Liscomb Harbour Syncline

CARTER COVE

TANGIER HARBOUR

Sober Island Syncline

MUSHABOOM HARBOUR

SHEET HARBOUR

CHARLES ISLAND

OUTER ISLAND

PHOENIX ISLAND

STONY IS.

Section 1

Section 2

Section 3

Section 4

Section 5

40% Outcrop (Included in fig 6)

SOBER ISLAND

A

A'

LEGEND

- GRANITE
- HALIFAX FOMATION
- GOLDENVILLE FORMATION
- Bedding, (horizontal, inclined, vertical, overturned)
- Slaty Cleavage, (inclined, vertical)
- Bedding, (general trend & local dip)
- Syncline
- Anticline
- Fault, (defined, inferred)
- Road

N

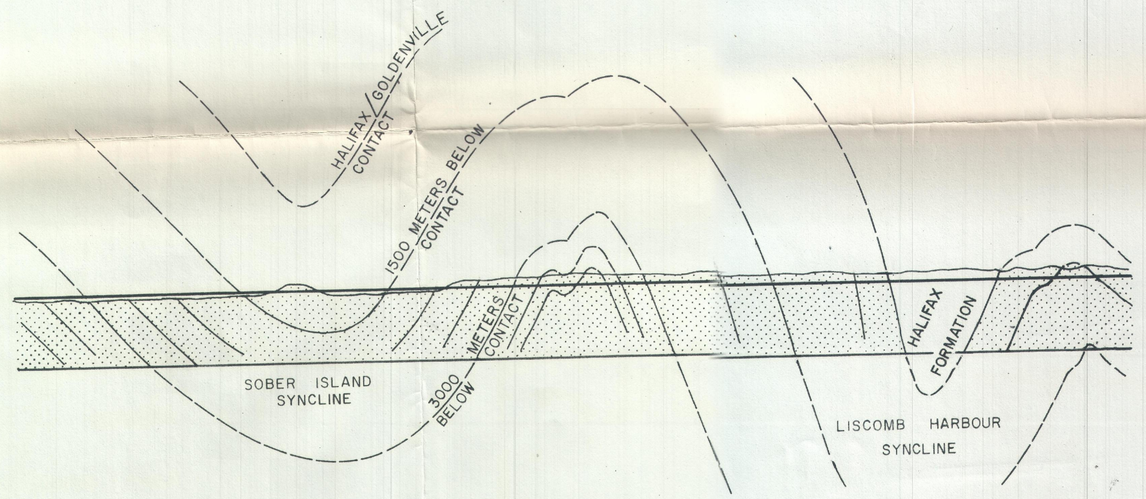

SECTION A'–A

HORIZONTAL & VERTICAL SCALES 1: 50,000

DASHED LINES INDICATE STRATIGRAPHIC INTERVALS OF APPROX. 1500 METERS

FIG. 2 GEOLOGICAL MAP OF THESIS AREA

SCALE = 1: 50,000

1000 500 0 1000 2000 3000 4000 Meters